MOLECULAR FUNCTION OF MAMMALIAN TRANSLOCATOR PROTEIN (TSPO)

A Dissertation

Presented to the Faculty of the Graduate School

of Cornell University

In Partial Fulfillment of the Requirements for the Degree of

Doctor of Philosophy

by

Lan Ngoc Ly Tu

August 2017

MOLECULAR FUNCTION OF MAMMALIAN TRANSLOCATOR PROTEIN (TSPO)

Lan Ngoc Ly Tu, Ph. D.

Cornell University 2017

Translocator protein (TSPO), previously known as the peripheral benzodiazepine receptor (PBR), is a mitochondrial outer membrane protein highly conserved from bacteria to humans. TSPO is found to be upregulated in many pathological conditions, making it an attractive target for both diagnostic and therapeutic purposes in human medicine. However, the exact molecular function of TSPO remained unclear. For the past 25 years, TSPO was depicted to transport cholesterol from the cytosol to the inner mitochondrial membrane, the rate-limiting step in steroid hormone biosynthesis. Its critical role in survival and development was reinforced by a report that claimed TSPO knockout (*Tspo*$^{-/-}$) mice were embryonic lethal. Therefore, there had been no genetic models to study the function of TSPO and all functional interpretations of TSPO were based on *in vitro* experiments using pharmacological tools. Our lab generated the first global *Tspo*$^{-/-}$ mice which surprisingly were healthy with no apparent abnormalities. Deletion of TSPO in different steroidogenic cell lines also did not affect cell viability. Furthermore, steroid hormone production was not affected in *Tspo*$^{-/-}$ mice or in steroidogenic cells lacking TSPO compared to the controls, indicating that TSPO is not involved in steroidogenesis. The stimulating effect of some TSPO binding chemicals on steroid hormone production that formed the early basis for linking TSPO and steroidogenesis was also found to be inaccurate. Using the TSPO knock out MA-10 Leydig cancer cells, I demonstrated that PK11195, the prototypical ligand of TSPO, could modestly induce steroid hormone production to the same extent regardless of the presence or absence of TSPO. This result indicated that the effect of PK11195 is nonspecific and not mediated by TSPO.

My studies subsequently made the first correlation that TSPO is enriched in all tissues rich in

lipid droplets including adipose tissues, suggesting a role of TSPO in lipid metabolism. Using both TSPO knockout MA-10 cells and *Tspo*$^{-/-}$ mice as the models, I demonstrated that deletion of TSPO increased mitochondrial fatty acid oxidation (FAO). However, co-immunoprecipitation result showed that TSPO did not have any interacting partners involved in FAO but formed a dimer, which could be induced by protoporphyrin IX (PPIX), the endogenous ligand of TSPO. Levels of free PPIX were found to be high in tissues rich in lipid droplets and directly regulated by TSPO. I also provided the first evidence for a novel function of PPIX in inhibiting FAO, which forms the basis for TSPO in regulation of FAO.

Overall, my studies helped amend the current model of steroidogenesis by removing TSPO from its core machinery, and paving the way for the precise cholesterol transport mechanism to be identified. The function of TSPO in PPIX sequestering instead of steroidogenesis urges careful reinterpretation of previous studies using TSPO binding chemicals, and rigorous reevaluation of their applications in human medicine. Studying biological functions of PPIX is poised to uncover potentially new pathways with broad implications in biology, and remains a core topic for future investigation.

BIOGRAPHICAL SKETCH

Lan Tu was born in Nov 4, 1988 in Hanoi, Vietnam. She attended kindergarten, primary school and secondary school that were all 15-min walk from home. Her mother went overseas to do a dermatology residency for the entire year when she was in the first grade. Upon return, her mother dedicated a lot of time and money to providing Lan with well-rounded education despite financial hardships at that time. After enrolling in various classes from painting, singing, ballet, martial arts, and music (playing the organ), Lan found her biggest interest in reading and writing stories. She also enjoyed learning knitting and sewing from her mother and had a small collection of products on her own.

In secondary school, Lan won several prizes every year in mathematics, English and chemistry in district- and city-wide competitions. In 2003, she ranked the 1st in the national entrance exam to enroll in the High school for Gifted students, Hanoi University of Science and majored in chemistry. For 3 years of high school, she totally immersed in science, especially chemistry and mathematics. That was the time when reading textbooks was as fun as comic books and she was proud to have read almost all chemistry textbooks up to college level available in the bookstore. In 2006, Lan and 3 other students represented Vietnam to compete in the 38th International Chemistry Olympiad held in South Korea. She won a Gold Medal and was ranked 15 over 254 participants from 64 countries.

Lan enrolled in the Hanoi Medical University to study general medicine in 2006. However, she dropped out after 1 semester as she realized medicine is not her passion. In 2007, she received a full scholarship to study pharmacy in the National University of Singapore as the only Vietnamese student in the department. It was a life-changing experience for her to go abroad and learn to develop independence, perseverance and various survival and social skills. The highlight of her undergraduate years was the research attachment in Dr. Chew Eng Hui's lab where she was first exposed to science outside textbook and classroom. This experience cultivated her interest in science and research later. After graduation in 2011, Lan fulfilled her pharmacist pre-registration training in the Mount Elizabeth hospital in Singapore and obtained her pharmacist license in May 2012. However, she decided not to continue her clinical

practice but pursue research as her career.

In 2012, Lan received the pre-doctoral fellowship from the Vietnam Education Foundation to study in Cornell University. After 3 lab rotations, she decided to join Dr. Selvaraj's lab to embark on a long but fulfilling journey to decode the molecular function of the translocator protein (TSPO). Lan has received the Cornell Center for Vertebrate Genomics Fellowship and the Graduate Student Award for Teaching Excellence. Upon completion of her Ph.D., Lan will pursue her post-doctoral training in University of Pittsburgh, Pennsylvania.

To my mother Nguyen Thi Hai Van

ACKNOWLEDGMENTS

First of all, I express my deepest gratitude to my advisor, Dr. Vimal Selvaraj, for his incredible support and guidance throughout my Ph.D. He is a great mentor who is always available to provide constructive feedbacks and advice on every matter I encounter. With his optimism and constant encouragement, Dr. Selvaraj has walked me through numerous challenges and failures in my Ph.D., nurtured my interest in science and helped shape my positive attitude in life. Not only does he teach me science, he inspires me to be a good scientist.

I also thank other members of my committee, Dr. Robert Weiss, Dr. John Schimenti and Dr. Margaret Bynoe for being involved in my work and providing expert opinions for my experiments. I would also like to thank Dr. Chew Eng-Hui, my first research mentor in college, for introducing me to the world of molecular biology, teaching me the very first laboratory skills and critical thinking, all of which have formed a strong foundation for my future research.

I also express my gratitude to Dr. Eric Clay, my landlord for the 4 years and a half in Ithaca. Eric has provided me not just a room for safe and comfortable stay but also a home to experience American culture and traditions. He has been a friend and a teacher whom I turn to for various questions in life.

I would not have been able to survive long winters in Ithaca and stressful times in the graduate school without support from friends. I thank Kanako Morohaku, Viju Vijayan, Amy Zhao, Hong Bui, Tam Tran, Chou Shao-Pei for great hangouts, fun cooking sessions, and stimulating conversations.

Above all, I dedicate all my academic accomplishments to my mother, who has worked tirelessly and sacrificed a lot to raise me up and nurture me to become whom I am today. She is forever my role model. I also cannot be more grateful to my husband, Phuong Pham, who has driven hundreds of thousands of miles from Pittsburgh to Ithaca to multi-task as a driver, a cook, a friend and a soulmate. His endless support has given me strength to overcome all hardships in life.

Finally, I would like to thank everyone in the Department of Animal Science for giving me such friendly and supportive work environment. I thank the Vietnam Education Foundation and the Cornell Vertebrate Genomics Center for my fundings.

TABLE OF CONTENTS

LIST OF FIGURES

LIST OF TABLES

CHAPTER 1

Introduction and Literature Review

Selvaraj, V., Stocco, D. M., & Tu, L. N. (2015). Minireview: translocator protein (TSPO) and steroidogenesis: a reappraisal. *Molecular endocrinology, 29*(4), 490-501.

Selvaraj, V., & Tu, L. N. (2016). Current status and future perspectives: TSPO in steroid neuroendocrinology. *J Endocrinol, 231*(1), R1-R30.

OVERVIEW OF THE TRANSLOCATOR PROTEIN

Translocator protein (TSPO), also known as the peripheral benzodiazepine receptor (PBR), was first identified in 1977 based on its distinct pharmacology with high affinity binding to benzodiazepines in peripheral tissues (Braestrup et al., 1977; Braestrup and Squires, 1977; Davies and Huston, 1981; Regan et al., 1981). The term 'peripheral' was used to distinguish it from the plasma membrane 'central' benzodiazepine receptor, a complex together with the γ-aminobutyric acid type A ($GABA_A$) receptor that is important for inhibitory neurotransmission in the central nervous system (Macdonald and Barker, 1978; Takahashi et al., 1958). In comparison, TSPO/PBR is present in the mitochondria and its structural and functional properties have been a topic of active research for the past 25 years (Gatliff and Campanella, 2012; Gavish et al., 1999; Rupprecht et al., 2010).

Comparisons of TSPO/PBR amino acid sequence show a high degree of conservation throughout evolution (Yeliseev and Kaplan, 1995). Both human and mouse *Tspo* genes translate to a 169 amino acid protein with 81% sequence homology (Bucan et al., 1993; Riond et al., 1991). Sequence examination of the *Tspo* promoter region revealed a GC-rich region that binds specific protein transcription factors (Sp1/Sp3/Sp4) (Batarseh et al., 2012). Sequences in the promoter region that bind the v-ets erythroblastosis virus E26 oncogene homolog (Ets), and activator protein 1 (AP1) have also been reported (Giatzakis et al., 2007; Giatzakis and Papadopoulos, 2004). In addition, a recent study showed the existence of a non-transcription factor-mediated gene regulation for TSPO via an intron-based short interspersed repetitive element (SINE) B2 natural antisense transcript (Fan and Papadopoulos, 2012). It appears that signaling via protein kinase C ε (PKCε) could induce TSPO expression (Batarseh et al., 2008; Batarseh and Papadopoulos, 2010), however, the precise mechanisms that control *Tspo* gene regulation remain unclear (Batarseh and Papadopoulos, 2010). Expression of TSPO has been reported in different tissues including heart, brain, lung, spleen, testis, ovary, adrenal, kidney, bone marrow, salivary gland, platelets, adipose tissue, skin and liver (Anholt et al., 1985b; Tu et al., 2014; Wang et al., 2012); and within these tissues, TSPO expression is regional and/or cell type specific (Morohaku et al., 2013).

In eukaryotic cells, sub-cellular fractionation and detection using TSPO-binding chemicals showed that TSPO/PBR was enriched in outer mitochondrial membrane (OMM) (Anholt et al., 1985b; Anholt et al., 1986;

Basile and Skolnick, 1986). To a lesser extent, binding sites were also detected in the plasma membrane of erythrocytes (Olson et al., 1988). Antibody-based labeling also confirmed the predominant presence of TSPO in the mitochondria, but also indicated localization in plasma membrane of adrenocortical cells (Oke et al., 1992), and nuclear labeling was observed in adult male germ cells (Manku et al., 2012) and in some cancer cells (Hardwick et al., 1999; Venturini et al., 1998). However, a rabbit monoclonal antibody against TSPO recently released in the market (Cat# ab109497; Abcam, Cambridge, MA) allowed for TSPO detection with high specificity; using this antibody, TSPO expression in adult male germ cells was not detected (Morohaku et al., 2013). Therefore, studies using polyclonal antisera against TSPO for immunolocalization may need to be interpreted with caution. In addition, non-specific signal from TSPO binding chemicals have been detected *in vivo* (Owen and Matthews, 2011), and several non-TSPO mediated effects have been recorded *in vitro* (Gonzalez-Polo et al., 2005; Hans et al., 2005; Walter et al., 2005). Therefore, the existence of non-mitochondrial forms of TSPO remains to be definitively established.

TSPO structure

The structure of murine TSPO was initially described as a five transmembrane alpha helix (Murail et al., 2008). This was followed by a low-resolution structure of *Rhodobacter sphaeroides* TSPO constructed using electron cryo-microscopy, showing the possibility of a channel-like structure with an interior surface for potential substrate translocation (Korkhov et al., 2010). However, it was not possible to assign amino acid sequences to this low-resolution TSPO structure (Korkhov et al., 2010) and any functional prediction was largely speculative. In 1998, a putative cholesterol recognition amino acid consensus (CRAC) sequence was identified at the C terminal region of TSPO, suggesting cholesterol binding property (Li and Papadopoulos, 1998). These structural features contributed to the modeling of TSPO as a membrane-associated cholesterol transport protein (Lacapere et al., 2001; Rupprecht et al., 2010). A more recent high-resolution NMR structure of murine TSPO confirmed the structure of a five alpha helix fold but showed that side chains of the CRAC motif essential for cholesterol binding are located on the outside of the TSPO pointing towards the membrane environment (Jaremko et al., 2014) (Figure 1.1), suggesting that previous model of TSPO transporting cholesterol through the interior core was not accurate. Instead, the CRAC motif could function in associating TSPO with raft microdomains in the membrane (Morohaku

et al., 2014). Binding of PK11195, a prototypical ligand of TSPO, does not involve the CRAC motif (Figure 1.1) and appeared to stabilize its 3D structure (Jaremko et al., 2014).

TSPO has been reported to exist in several forms of oligomers as multiple bands were detected in a western blot using TSPO polyclonal antisera (Delavoie et al., 2003). However, these extra bands are likely nonspecific as they have not been reported in studies using the rabbit monoclonal antibody recognizing the last amino acids at the C-terminus of TSPO (Morohaku et al., 2013). Crystallographic studies of bacterial TSPO concluded that purified TSPO formed a highly stable dimer (Guo et al., 2015; Li et al., 2015) but the NMR structure of murine TSPO was found to be a monomer (Jaremko et al., 2014). Moreover, the dimerization interface was described completely different between *Bacillus cereus* and *Rhodobacter sphaeroides* TSPO (Guo et al., 2015; Li et al., 2015), raising questions why the dimerization sites are not conserved and whether the dimerization itself is an artifact due to hydrophobic aggregation of TSPO during purification and/or crystallization. Therefore, the conclusion of TSPO oligomerization still needs further investigation for more definitive experimental evidence.

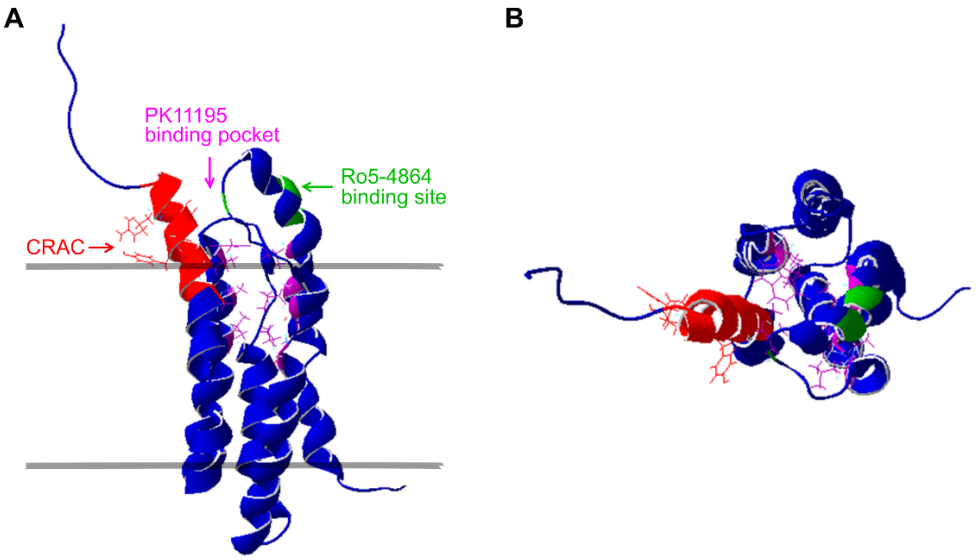

Figure 1.1. Structure of TSPO in outer mitochondrial membrane. **(A)** Side view: TSPO has a five α-helix transmembrane structure. The CRAC motif (in red) is at the C terminus (residues 147 to 159). Side chains of Tyr^{152}, Tyr^{153} and Arg^{156}, essential for cholesterol binding are located on the outside of the TSPO structure and point toward the membrane environment. PK11195 binding pocket (in purple) is formed by residues Ala^{23}, Val^{26}, Leu^{49}, Ala^{50}, Ile^{52}, Trp^{107}, Ala^{110}, Leu^{114}, Ala^{147} and Leu^{150}, that do not involve side chains of CRAC motif amino acids. Binding site for Ro5-4864 (in green) is distinct from that of PK11195 and was identified to include residues Glu^{29}, Arg^{32}, Lys^{39} and Val^{154} (Farges et al., 1994). **(B)** Top view: Cholesterol binding side chains of the CRAC motif pointing outside of the TSPO structure and do not interfere with internal PK11195 binding site. From high-resolution NMR structure PDB ID: 2MGY (Jaremko et al., 2014).

TSPO pharmacology

Pharmacology of benzodiazepines provided most of the early information about TSPO. Benzodiazepine Ro5-4864 (4'-chlorodiazepam), and a non-benzodiazepine PK11195 (an isoquinoline carboxamide derivative) were initially established as prototypical TSPO binding chemicals (Le Fur et al., 1983a; Le Fur et al., 1983b), as they bind to TSPO but not to $GABA_A$ (Benavides et al., 1983a; Benavides et al., 1983b). This ability to detect TSPO using binding chemicals with reasonable accuracy, and the pathological TSPO upregulation seen at sites of inflammation led to the development of TSPO as a diagnostic target (Chen and Guilarte, 2008). TSPO-binding chemicals linked to tracers could be used to detect inflammatory lesions *in vivo* in a variety of human diseases using positron emission tomography (Banati et al., 2000; Chauveau et al., 2008). Therefore, many classes of TSPO binding chemicals have been developed and used in both basic and clinical research across multiple fields of human medicine (reviewed in (Kim and Pae, 2016)). Clinical trials for different TSPO binding drugs for this application are either in progress or have been recently completed (clinicaltrials.gov; Identifiers: NCT02181582, NCT01547780, NCT01527695, NCT01428505, NCT02086240, NCT02062099, NCT01613703), and this remains an area of active research.

Beyond this use as a diagnostic tool, several functional interpretations of TSPO based on responses to chemical binding have been documented. These implicated a primary role for TSPO in steroid hormone production (Mukhin et al., 1989; Papadopoulos et al., 1990), and additional roles in mitochondrial respiration (Larcher et al., 1989; Rosenberg et al., 2013), cell proliferation (Takai et al., 2012; Wu and Gallo, 2013), production of reactive oxygen species (Lehtonen et al., 2012; Zeno et al., 2012) and execution of apoptosis via modulating the mitochondrial permeability transition pore (MPTP) (Sileikyte et al., 2011; Zulian et al., 2011). Moreover, beneficial pharmacological effects were observed in treatments using TSPO binding chemicals in preclinical models across a variety of diseases/disorders. As a result, there has been immense interest in promoting different TSPO binding chemicals as drugs for treatment of a variety of conditions that include: neurological disorders (Rupprecht et al., 2010), neurotrauma (Papadopoulos and Lecanu, 2009), multiple sclerosis (Daugherty et al., 2013), cancer chemotherapy (Austin et al., 2013), cardiovascular disease (Qi et al., 2012), and Alzheimer's disease (Barron et al., 2013). Therapeutic benefits from use of TSPO binding chemicals were explained by their putative

ability to induce steroid hormone production in these different conditions (Rone et al., 2009). This link was made due to the prevailing model at the time that proposed an indispensable role for TSPO in steroid hormone production (Papadopoulos and Miller, 2012).

It is important to note that there are reports in the literature of TSPO-independent actions of several putative binding chemicals, although specific cellular targets other than TSPO have not been characterized. TSPO ligands like PK11195 can insert themselves into lipid bilayers affecting membrane properties (Hatty et al., 2014), a phenomenon that could modulate cholesterol availability to the steroidogenic machinery. PK11195 has also been demonstrated to target the F1F0-ATPsynthase and inhibit mitophagy without the involvement of TSPO (Seneviratne et al., 2012). In another study, an apoptosis-sensitizing effect for PK11195 was observed even after TSPO was completely knocked down (Gonzalez-Polo et al., 2005). The anti-tumor effect of TSPO binding chemicals Ro5-4864 and FGIN-1-27 was identical irrespective of the presence or absence of TSPO in different tumors (Hans et al., 2005). In hematologic cancers, PK11195 showed broad inhibition of adenosine triphosphate (ATP)-binding cassette transporters by binding to plasma membrane sites without involvement of TSPO (Walter et al., 2005). In cells of mesenchymal origin, PK11195 and Ro5-4864 could inhibit cell proliferation through decreases in activation of ERK and c-Jun independent of TSPO (Kletsas et al., 2004). Therefore, interpretations of biological effects mediated by TSPO binding chemicals require caution as they might not translate to the true function of TSPO.

Human TSPO polymorphism

Mutations/polymorphisms for TSPO were previously sought and excluded in lipoid congenital adrenal hyperplasia patients (Lin et al., 1993). However, a common human polymorphism in TSPO (*rs6971*, leading to amino acid change Ala147Thr) has been demonstrated to cause differences in affinity of TSPO binding chemicals used for diagnostic imaging (Mizrahi et al., 2012; Owen et al., 2012). Ala147 is considered part of the TSPO PK11195 binding pocket (Jaremko et al., 2014), suggesting that a change to Thr147 could affect binding properties of PK11195 and other chemicals that bind to this region. Functionally, this *rs6971* polymorphism was linked to adult separation anxiety in patients with depression (Costa et al., 2009b). This same polymorphism was

subsequently associated with decreased pregnenolone production by immune cells in both Thr147 homozygous and heterozygous individuals (Costa et al., 2009a).

TSPO homolog

Due to *Tspo* sequence conservation from bacteria to humans, there has been some interest in studying the functional evolution of this gene (Fan et al., 2012). *Tspo2* (PBRL/Peripheral benzodiazepam-like) was identified as a gene that emerged from a duplication event preceding speciation of reptiles, birds and mammals (Nakazawa et al., 2009). TSPO2 expression appears restricted to the bone marrow (Fan et al., 2009; Nakazawa et al., 2009), and has not been detected in steroidogenic tissues [confirmed in (Morohaku et al., 2014; Tu et al., 2014)]. Subcellular localization of TSPO2 using specific antibodies has not been performed; localization based on overexpression studies using C-terminal GFP/DsRed-TSPO2 fusion proteins (chicken, mouse and human) in cell lines have led to conflicting proposals. The group who studied chicken TSPO2 demonstrated mitochondrial localization (Nakazawa et al., 2009), and the group who studied mouse and human TSPO2 proposed that TSPO2 is localized to the endoplasmic reticulum and the nuclear membrane (Fan et al., 2009). These studies have demonstrated functional disparities as well. Based on the study in the chicken, a strict co-regulation of TSPO2 expression but not TSPO expression with genes involved in hematopoiesis was demonstrated (Nakazawa et al., 2009). This led to the conclusion that TSPO2 may be involved in heme availability for the assembly of hemoglobin (Nakazawa et al., 2009). In contrast, the study with mouse and human TSPO2 was an extrapolation of previous work on TSPO and steroidogenesis from the same authors, and suggested that TSPO2 is involved in cholesterol uptake and trafficking in erythroid cell types (Fan et al., 2009). At the present time, there are no gene knockout models to study loss-of-function resulting from TSPO2 deletion, and understanding of its function remains rudimentary. Nevertheless, what we do know is that distinct tissue localization patterns and regulation between TSPO and TSPO2 negates concerns of potential functional redundancy in studies that use *Tspo* gene-deleted models.

TSPO AND STEROIDOGENESIS

Establishment of the model

The first observation that chemicals that bind to TSPO could stimulate steroid biosynthesis was made in adrenal tumor cells in 1989 (Mukhin et al., 1989). Subsequent experiments in a variety of steroidogenic cells reinforced that synthetic small molecule drugs that bind TSPO could increase steroid hormone production (Krueger and Papadopoulos, 1990; Papadopoulos et al., 1990; Papadopoulos et al., 1991c). In support of these xenobiotic effects, a naturally occurring intracellular protein, the Acyl-CoA-binding protein (ACBP/ACBD1), previously known as the diazepam binding inhibitor (DBI) that binds TSPO, increased steroid synthesis in steroidogenic cells (Garnier et al., 1993; Papadopoulos et al., 1991a; Papadopoulos et al., 1991b; Papadopoulos et al., 1992). Subsequent experiments using knockdown technology to inhibit TSPO expression also indicated that the presence of TSPO was essential for steroid synthesis (Boujrad et al., 1993; Papadopoulos et al., 1997b). Further, it was reported that the presence of a higher affinity ligand-binding site on TSPO was responsible for the constitutive biosynthesis of steroids observed in the R2C rat Leydig tumor cell line (Garnier et al., 1994). Supporting this mechanism, targeted disruption of TSPO in these R2C cells was shown to obliterate their ability to produce steroid hormones (Papadopoulos et al., 1997b). TSPO sequence also showed the existence of a cholesterol-binding amino acid consensus (CRAC) motif suggesting a molecular mechanism in place for cholesterol binding and/or transport (Li et al., 2001). All these points of evidence led to a conclusion that TSPO played an indispensable role in the process of cholesterol transfer to the mitochondrial inner membrane and steroidogenesis.

The steroidogenic acute regulatory protein (STAR) was modeled to deliver cholesterol to the OMM and TSPO carried out the mitochondrial cholesterol import process. Expression of STAR in steroidogenic cells in the absence of hormone stimulation resulted in an increase in steroid biosynthesis (Clark et al., 1994). Mutations in the *Star* gene were responsible for the potentially fatal lipoid congenital adrenal hyperplasia (lipoid CAH), a disease in which severely afflicted individuals are unable to synthesize steroids (Lin et al., 1995). Mitochondrial cholesterol transport mediated by StAR was proposed as a shuttling event in that either StAR transfers cholesterol molecules, one at a time, to the IMM; or the START domain of StAR may alter the mitochondrial membrane to

allow for the passage of cholesterol, before reaching its final resting place in the mitochondrial matrix (Stocco, 2001). But these models for StAR required modifications because deletion of 62 amino acids at the N-terminus of StAR without affecting the START domain prevented mitochondrial import, but did not affect cholesterol transfer and steroid production (Arakane et al., 1996; Wang et al., 1998). Moreover, Tom20-StAR fusion protein affixed to the OMM could induce steroidogenesis suggesting that StAR entry into the mitochondrion was not necessary, and that functional effects mediated by StAR are completed at the level of the OMM (Bose et al., 2002). Using this same model expressing OMM-affixed StAR-TOM20 fusion protein, it was demonstrated that TSPO knockdown using antisense oligonucleotides could reduce steroidogenic capacity (Hauet et al., 2005). These findings ultimately led to the conclusion that there was a functional cooperation between StAR and TSPO to mediate mitochondrial cholesterol transport required for steroid hormone biosynthesis. Therefore, a model in which StAR is considered the 'initiator' of cholesterol transport and TSPO is considered the 'gate' for cholesterol entry into mitochondria was established (Papadopoulos and Miller, 2012) and prevailed for the past 25 years.

Limitations of studies linking TSPO to steroidogenic function

Examination of previous literature on TSPO suggests that the proposed link to steroidogenesis was based on a complex combination of multiple interdependent indicators from a variety of methodologies, most of which were inconclusive, and in several cases may have been over-interpreted.

There were two key elements that initially made a function for TSPO in steroidogenesis plausible; they were its localization to the OMM, and its high level of expression noted in steroidogenic cells (Anholt et al., 1986). However, these were just interesting associations and not direct indications. As another layer of support, often presented was the demonstration that hypophysectomy could decrease TSPO expression in the adrenal and testes (Anholt et al., 1985a). If we dissect their study, rats were examined 23 days after hypophysectomy, during which body weights had decreased significantly (to 55% of the control rats), and the adrenal was in a severe state of involution (only 28% the weight of control adrenals) (Anholt et al., 1985a). It should be noted that loss of adrenal weight after hypophysectomy is mainly due to shrinkage of the adrenal cortex (Deane and Greep, 1946), however depletion of Ro5-4864 binding (used as a measure of TSPO) in their study was calculated based on whole adrenal weight (Anholt et al., 1985a). It should also be noted that depletion of mitochondrial CYP11A1 activity after

hypophysectomy shows an almost linear drop to just 10% of control values in just 7 days, a time point when the adrenal weight was still 65% compared to control adrenals (Kimura, 1969). A subsequent study by another group demonstrated that the decrease in Ro5-4864 binding in the adrenal after hypophysectomy in rats was associated with mitochondrial depletion, and that changes to TSPO expression after ACTH restoration was not temporally related to the induction of steroidogenesis (Cavallaro et al., 1993). Although this study by Cavallaro *et al.* provided an early indication that previous evidence for TSPO was simply circumstantial, it was rarely referenced (14 citations to date), whereas mention of previous work by Anholt *et al.* was very common (113 citations to date).

Pharmacology of TSPO binding chemicals was often presented as direct evidence for the role of TSPO in steroid hormone production (Mukhin et al., 1989; Papadopoulos et al., 1990). Among the different TSPO binding chemicals tested, PK11195 was the most potent inducer of steroidogenesis followed by Ro5-4864. However, the response itself was very modest (maximal levels were 80-fold lower than a response seen with hCG), and transient (progesterone production reached maximal levels within 40 minutes, with no progressive accumulation, and levels remained unchanged for the next 4 hours of this experiment). Although these observations suggested a physical response to treatment rather than a sustained physiological response (as seen with hCG), this possibility was not investigated. Moreover, effects of TSPO binding chemicals were not always consistent. PK11195 and Ro5-4864 were shown to have different thermodynamic properties, and predicted to be antagonistic and agonistic respectively (Le Fur et al., 1983b), even before studies linking TSPO and steroidogenesis. In agreement with this prediction and contrary to a stimulatory effect on steroidogenesis, it was demonstrated that treatment with PK11195 completely inhibited adrenal steroidogenesis stimulated by ACTH in hypophysectomized rats (Cavallaro et al., 1992). In another study, PK11195 was shown to inhibit brain pregnenolone synthesis in adrenalectomized-castrated rats, whereas another TSPO-binding chemical FGIN-1-27 was shown to increase pregnenolone production under similar conditions (Romeo et al., 1993). Effects consistent with an inhibitory role for PK11195 in steroidogenesis and other effects were reported in several other studies (Auta et al., 1993; Frye et al., 2009; Korneyev et al., 1993; Tsuda et al., 1998). Also, when placental explants were exposed to Ro5-4864, Ro5-4864 stimulated a 2.4-fold increase in progesterone levels at a low dose, but caused a significant decrease

compared to baseline at high doses (Barnea et al., 1989). In another study, Ro5-4864 was found to suppress estradiol production *in vivo*, whereas PK11195 had no effect on ovarian steroidogenesis (Weizman et al., 1997).

Binding of the Acyl-CoA-binding protein (ACBP) and its processed peptides to TSPO stimulated steroid hormone production in isolated mitochondria (Papadopoulos et al., 1991b). In hypophysectomized rats, ACTH failed to acutely increase the amount of adrenal ACBP or TSPO, but increased the rate of ACBP processing and hormone production (Cavallaro et al., 1992). This ACTH-induced increase in ACBP processed peptides was interpreted as playing an important role in steroidogenesis. In support, knockdown of ACBP expression using a cholesterol-linked phosphorothioate oligodeoxynucleotide antisense, demonstrated decreased steroid hormone production in cultured Leydig tumor cells (Boujrad et al., 1993). ACBP is present in eukaryotes ranging from yeast to mammals (Knudsen et al., 1999), and was demonstrated to play a role in maintaining the intracellular Acyl-CoA ester pool size (Mandrup et al., 1993), and synthesis of very long chain fatty acids and sphingolipids (Gaigg et al., 2001). A spontaneous mutant mouse *nm1054* cataloged at the Jackson Laboratory (Ohgami et al., 2005a; Ohgami et al., 2005b), was subsequently identified to also contain a mutation in the ACBP gene locus (Lee et al., 2007). Loss of ACBP in these *nm1054* mice was linked to fatty acid metabolism abnormalities in skin and hair (Lee et al., 2007). The subsequent generation of ACBP knockout mice ($ACBP^{-/-}$) resulted in a finding that they were early embryonic lethal at the blastocyst stage of development (Landrock et al., 2010). However, a second independent $ACBP^{-/-}$ mouse generated showed that they were viable and fertile, and developed normally but with delayed metabolic adaptation to weaning (Neess et al., 2011). Further studies on this latter mouse (Bloksgaard et al., 2012; Neess et al., 2013) showed that metabolic abnormalities seen in skin and hair matched observations previously reported for the *nm1054* mutation. There was no phenotypic evidence that indicated defects in steroid hormone production in these $ACBP^{-/-}$ mice. But why was there such a discrepancy between the two ACBP knockout mice? One explanation is that abnormal random insertional mutagenesis in embryonic stem cell clones could have resulted in lethality unrelated to ACBP deletion in the first $ACBP^{-/-}$ mouse line; validation to rule out this possibility was not presented (Landrock et al., 2010). Nevertheless, more recent understanding of ACBP function does not indicate a link to steroidogenic function as previously concluded.

Cholesterol is considered a natural ligand for TSPO. The CRAC motif that binds cholesterol was identified at the TSPO C-terminal region (Li and Papadopoulos, 1998). The CRAC motif is a sequence pattern – L/V-X_{1-5}-Y-X_{1-5}-R/K – with an extremely loose definition with only one unique residue and two large variable segments. It was pointed out that the genome of *Streptococcus agalactiae* that encodes 2094 known and hypothetical proteins, almost all of which will have no association with cholesterol, have 5737 CRAC motifs (2.7/protein and 1/122 amino acids) (Palmer, 2004); something that is probably true for all organisms. Therefore, predictive value of the CRAC motif is poor, and cannot be considered an indicator of cholesterol binding or transport function in a protein. For example, the CRAC motif in the nicotinic acetylcholine receptor was found in an energetically unfavorable location to bind cholesterol, and an alternative region of cholesterol binding was ultimately identified (Baier et al., 2011). But for TSPO, there is certainly evidence in the literature that cholesterol can interact with the CRAC motif (Li and Papadopoulos, 1998; Li et al., 2001). Most functional CRAC motifs have been described in proteins that associate with cholesterol-rich membrane regions called raft microdomains, for example: myelin P0 (Luo et al., 2007) and caveolin-1 (Yang et al., 2014). Given the new findings that TSPO is not involved in steroid hormone production, it is necessary to ask the question whether there is enough functional evidence for TSPO in mitochondrial cholesterol transport? As suggested previously (Morohaku et al., 2014), it is possible that the CRAC motif of TSPO could merely function in associating with cholesterol-rich raft microdomains. A proposed TSPO-interacting protein, voltage dependent anion channel 1 (VDAC1) on the OMM is a resident protein in raft microdomains (Herrera et al., 2011). Therefore, TSPO membrane raft association via the CRAC motif could be the basis for proximity and interaction with VDAC1.

For demonstrating cholesterol transport, *Escherichia coli* DE3 bacteria that do not have TSPO or cholesterol were shown to gain the ability to accept cholesterol when TSPO was overexpressed (Li and Papadopoulos, 1998); mutations to the CRAC motif, Y153S and R156L completely abolished this cholesterol absorption. In this heterologous system, it was possible to demonstrate that TSPO cholesterol binding was reproducible. However, ^{3}H-cholesterol acceptance by bacteria over a 120-minute period at 37˚C did not show saturation. This failure to saturate was considered as evidence that TSPO was a channel rather than cholesterol-binding protein. But it was not examined if there was a pool of cholesterol that was not bound to TSPO in the

bacterial plasma membrane. In addition, the cholesterol-loaded bacteria were not tested for the presence of any inclusion bodies to suggest uptake and storage. It should be noted that the bacterial cytoplasm does not have any membrane-bound organelles or mechanisms to store excessive cholesterol. Moreover, bacterial proliferation and continued TSPO expression that could have occurred during the 120-minute incubation period was not considered. Therefore, this prediction of a function for TSPO in cholesterol translocation can be considered premature.

Another piece of genetic evidence was the report that global TSPO knockout mice were early embryonic lethal (Papadopoulos et al., 1997a), which has been repeatedly referenced (286 citations to date). This was frequently presented as evidence for TSPO being important for basic cellular functions that included steroidogenesis. However, this review article failed to explain experimental methods covering the recombination strategy used and the exact stage of embryonic mortality; these specific methods/results were never published.

ALTERNATIVE PERSPECTIVES FOR TSPO ACTION IN CELLS

As TSPO research spans multiple fields/disciplines, attempts to explain its function has resulted in rather divergent yet unique perspectives. Some of these perspectives lack coherence in that they do not describe a unifying function for TSPO that is applicable to all cell types and/or the organism as a whole. Nevertheless, we present evidence published in support of the different perspectives (Figure 1.2), and when appropriate, indicate limitations and areas that require further exploration to refine and accelerate understanding towards the precise function of TSPO.

TSPO is not part of the mitochondrial permeability transition pore

Distinct from the purported role for TSPO in steroidogenesis, it was also thought that TSPO might play a role in the mitochondria-mediated cell death process called the mitochondrial permeability transition (MPT). The MPT refers to the opening of a non-specific pore that permits any molecule <1.5 kDa through the inner mitochondrial membrane allowing equilibration of the mitochondrial matrix and the cytosol leading to loss of mitochondrial function and cell death (Haworth and Hunter, 1979; Hunter and Haworth, 1979a; Hunter and Haworth, 1979b). Effects observed using TSPO binding drugs (Kinnally et al., 1993), and copurification of TSPO with other proteins

thought to be involved in MPT (McEnery et al., 1992), initially linked TSPO to this process. However, through development of conditional *Tspo*$^{c\Delta/\Delta}$ genetic models, it was recently demonstrated that TSPO plays no role in the regulation or structure of the MPT pore (Sileikyte et al., 2014). Implications from this recent understanding of TSPO and advances towards explaining the MPT process, have been critically assessed elsewhere [see review (Bernardi et al., 2015)].

TSPO as a regulator of redox homeostasis

There are seemingly disparate mechanisms that have been proposed for TSPO in redox homeostasis. First, a putative association of TSPO and the voltage-dependent anion channel protein (VDAC) is believed to induce ROS production. It was demonstrated that TSPO overexpression in cells induces mitochondrial ROS production, with a reverse trend observed after TSPO knockdown (Gatliff et al., 2014). However, there exists contrasting evidence that TSPO overexpression could dampen mitochondrial ROS production through an identical VDAC-dependent mechanism (Joo et al., 2015; Joo et al., 2012). Second, without the need for any protein interactions, it has been suggested that TSPO could act to neutralize ROS. According to this hypothesis, the abundance of tryptophans in TSPO might react with ROS to generate tryptophan radicals (Guo et al., 2015). Third, a putative TSPO-NADPH oxidase 2 (NOX2) association has been proposed to play a role in ROS generation. In this postulate, TSPO is surmised to behave as a carrier or transporter for both cholesterol and heme (Guilarte et al., 2016).

Although all the above mechanisms are conceivable, they are attempts to explain TSPO function in cells based on effects that were initially observed using TSPO binding drugs. Distinct from cells that consistently show high levels of TSPO expression (such as in the adrenal cortex and brown adipose tissue), these explanations almost always deal with cells that upregulate TSPO in response to different forms of stress. Therefore, it is possible that these interpretations may be confounded with cellular effects associated with the obvious link between stress and ROS production. The TSPO-VDAC relationship to ROS production has had contrasting results in similar TSPO overexpression studies (Gatliff et al., 2014; Joo et al., 2015; Joo et al., 2012). The TSPO-NOX2 association (Guilarte et al., 2016), remains a hypothesis. The finding that cardiac-specific *Tspo*$^{c\Delta/\Delta}$ mice did not show any difference in the extent of ischemia reperfusion injury (Sileikyte et al., 2014), a pathology that is partly directed by myocardial NOX2 (Braunersreuther et al., 2013), seems to suggest that TSPO and NOX2 may not have a

functional connection. Perhaps via an interaction of multiple pathways, it is not too surprising that pharmacological evidence have linked TSPO to a variety of mechanisms related to cardioprotection after ischemia reperfusion injury: preventing mitochondrial permeability (Obame et al., 2007), increasing activities of mitochondrial oxidative enzymes (Xiao et al., 2010), or by reducing mitochondrial cholesterol transport (Paradis et al., 2013). In TSPO deficient MA-10$^{Tspo\Delta/\Delta}$ Leydig cells, loss of TSPO resulted in modest increases in ROS production (Tu et al., 2016), an observation that was linked to a shift in cellular metabolism (discussed below). Therefore, future studies carefully examining *Tspo*$^{-/-}$ models to observe loss-of-function are absolutely essential before an effect for TSPO in redox homeostasis can be confirmed.

TSPO as an enzyme for protoporphyrin IX degradation

Distinct from studies involving steroid production, porphyrins, a group of cyclic tetrapyrroles involved in heme synthesis, are considered endogenous ligands that bind TSPO (Verma et al., 1987). This porphyrin binding property of TSPO appears highly conserved from bacteria to humans, but the function of this association continues to remain unclear. It was initially proposed that TSPO binds and transports protoporphyrin IX (PPIX), the precursor of heme, into the mitochondria (Wendler et al., 2003), a concept that emerged based on TSPO ligands being able to partially rescue cells from porphyrin-induced phototoxicity (Ratcliffe and Matthews, 1995), and high levels of TSPO expression seen in the bone marrow (Rampon et al., 2009; Taketani et al., 1994). Although the property of PPIX binding to TSPO remains true, recent studies using *Tspo*$^{-/-}$ mice and cell lines have established that TSPO is not a porphyrin transporter for heme synthesis (Banati et al., 2014; Zhao et al., 2016). Using the bacterial *Chlorobium tepidum* TSPO purified in detergent, it was demonstrated that TSPO could induce rapid spectral changes to added PPIX indicative of chemical catalysis (Ginter et al., 2013). A similar observation has been reported for *Bacillus cereus* TSPO (Guo et al., 2015). However, the reaction rate was not proportional to TSPO concentration, but dependent on the availability of light and oxygen. Although this photo-oxidative PPIX degradation mediated by purified C. *tepidum* and B. *cereus* TSPO have been discussed in broad terms, there is no functional evidence that this occurs in any intact biological model systems. Moreover, the relevance of this light-dependent activity in deeper organs like the adrenal and brain remains questionable. Analysis of PPIX degradation/elimination as a time course in *Tspo*$^{-/-}$ mouse tissues and plasma suggests that this putative TSPO-

mediated degradation, at least in mammalian systems is not a critical regulator of PPIX levels (Zhao et al., 2016). Although this observation does not validate a role for TSPO in PPIX degradation, it certainly does not discount a physiological function for the highly conserved TSPO-PPIX association. Use of *Tspo*$^{-/-}$ models across different biological systems for investigating conserved properties in future studies may offer clues to uncovering specific functions for this association.

TSPO as a regulator of oxygen consumption

Evidence from lower organisms has indicated an oxygen-sensing function for TSPO (Yeliseev et al., 1997). In isolated primary microglia from *Tspo*$^{fl/fl}$ and *Tspo*$^{-/-}$ mice, measurement of oxygen consumption rate (OCR) indicated that basal OCR was significantly lower in *Tspo*$^{-/-}$ microglia (Banati et al., 2014). In an independent study, OCR compared between *Tspo*-deficient mitochondria isolated from liver-specific *Tspo*$^{c\Delta/\Delta}$ mice and control *Tspo*$^{fl/fl}$ mice showed no differences in OCR (Sileikyte et al., 2014). Although this contrast has been a topic of speculation with respect to the need for an intact cellular environment, and changes to metabolic demand in cells [reviewed in (Gut, 2015)], it subsequently became clear that there was also no correlation between TSPO expression levels and OCR deficits observed in different cell types. Measurements of OCR in embryonic fibroblasts that express low levels of TSPO from *Tspo*$^{-/-}$ mice showed significantly diminished values compared to embryonic fibroblasts from *Tspo*$^{fl/fl}$ mice (Zhao et al., 2016). In contrast, measurements of OCR in steroidogenic MA-10 cells that express very high levels of TSPO showed no difference when compared to TSPO-deleted MA-10 cells (Tu et al., 2016). All these studies indicate that the change in OCR is a cell-type dependent indirect effect, inconsistent with TSPO expression levels, perhaps reflecting on the diversity of mitochondrial types, metabolism and energetic status of cells, and therefore does not reveal a direct mechanism for TSPO in regulating OCR.

Tspo-knockout studies in another *in vivo* model, *Drosophila melanogaster*, indicated that *Tspo*$^{-/-}$ flies are without any abnormalities (Lin et al., 2014), similar to reports in mice (Banati et al., 2014; Tu et al., 2014). Interestingly, cells in *Tspo*$^{-/-}$ flies showed increased survival after hydrogen peroxide exposure or γ-irradiation (Lin et al., 2014). In only male *Tspo*$^{-/-}$ flies, an extended lifespan was observed compared to male wild type flies (Lin et al., 2014). Isolated *Tspo*-deficient mitochondria from these flies, irrespective of sex, showed a decreased rate of oxidative phosphorylation compared to *Tspo*$^{+/+}$ mitochondria (Lin et al., 2014). Continued studies in

Tspo$^{-/-}$ *D. melanogaster* have linked TSPO function to ethanol-sensitivity and tolerance (Lin et al., 2015). These seemingly disparate effects point to general mechanisms that surround mitochondrial function and do not pinpoint a specific indication for TSPO function.

Along the lines of cellular energy metabolism, a drug screen for identifying small molecules that induce expression of the gluconeogenic gene, phosphoenolpyruvate carboxykinase 1 (*Pck1*), using a transgenic zebrafish reporter line, PK11195 was identified as an agent that activates a state akin to fasting metabolism (Gut et al., 2013). Although this seems to be an exciting observation, it is unclear if the major effects observed are mediated through TSPO. This is because PK11195 is also known to bind the constitutive androstane receptor (CAR) (Anderson et al., 2011; Li et al., 2008), which can affect *Pck1* transcription, together with other genes that affect energy metabolism (Ueda et al., 2002). The overall functions of CAR could also be linked to fasting metabolism (Ding et al., 2006; Maglich et al., 2004). Therefore, interpretation of PK11195 or other drug effects in the context of TSPO needs further affirmation using genetic models that can delineate off target effects from specific effects.

TSPO as a regulator of lipid metabolism

Two independent exploratory studies identified *Tspo* as a candidate gene that could influence lipid metabolism. First, *Tspo* was identified as one of six novel transcripts that showed robust positive correlation with adipocyte differentiation in a differential display RT-PCR screen (Wade et al., 2005). Second, *Tspo* was identified as one of five genes that could influence triglyceride metabolism in an examination of quantitative trait loci between inbred mouse strains (Leduc et al., 2011). In agreement, recent examination of TSPO expression levels in different murine tissues indicated that high TSPO expression correlated with tissues active in lipid storage/metabolism, and was not specific for steroidogenic cells (Tu et al., 2016). As support for this correlation, it must be noted that steroidogenic cells also have substantial presence of lipid droplets. Measurement of energy metabolism in TSPO deficient MA-10$^{Tspo\Delta/\Delta}$ Leydig cells that do not show any deficits in steroid biosynthesis revealed a metabolic shift in substrate utilization from glucose to fatty acids compared to TSPO expressing MA-10 cells. The MA-10$^{Tspo\Delta/\Delta}$ Leydig cells had higher levels of fatty acid oxidation, and modest increases in ROS production compared to MA-10 controls (Tu et al., 2016).

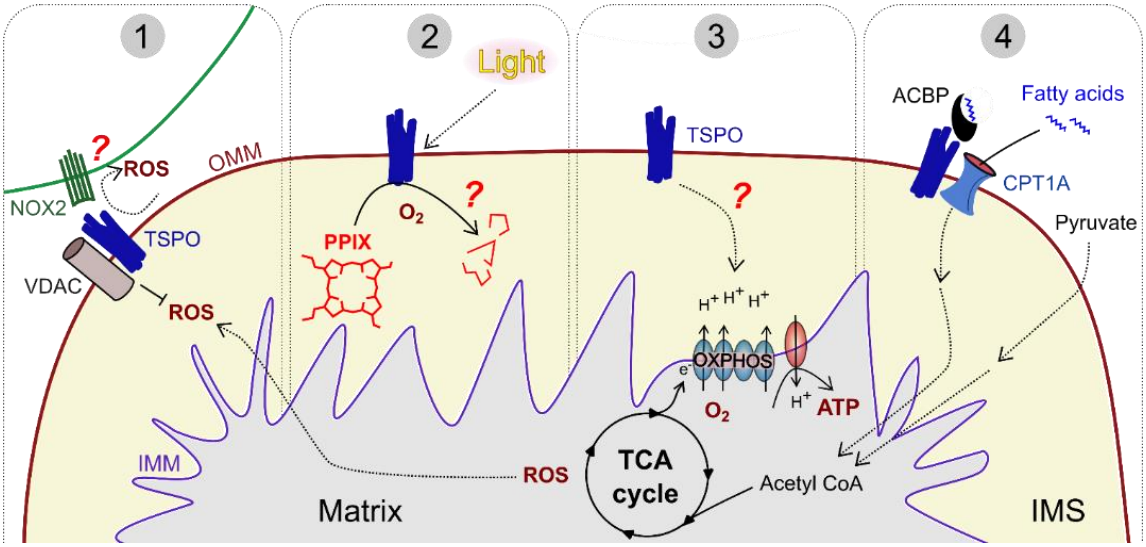

Figure 1.2. Alternative perspectives for TSPO action in cells. **(1) TSPO as a regulator of redox homeostasis.** It has been suggested that TSPO could interact with VDAC1 or NOX2 to induce production of ROS (Gatliff et al., 2014; Guilarte et al., 2016). On the contrary, the association of TSPO with VDAC1 (Joo et al., 2015; Joo et al., 2012), or TSPO by itself (Guo et al., 2015), could facilitate ROS neutralization. Although TSPO regulation of ROS is conceivable, at least as a secondary effect, functional evidence for the interactions and specific role of TSPO remains to be demonstrated. **(2) TSPO as an enzyme for protoporphyrin IX degradation.** Chemical catalysis of PPIX degradation by bacterial TSPO has been proposed as a function for TSPO (Ginter et al., 2013; Guo et al., 2015). The reaction rate was dependent on availability of light and oxygen. Lack of light in mammalian tissues that express high levels of TSPO like the adrenal glands raises question for the functional relevance and significance of this action. Nevertheless, conserved binding of TSPO to PPIX suggests a yet to be determined action in cells. **(3) TSPO as a regulator of oxygen consumption.** Loss of TSPO had different effects in oxygen consumption rate in different cell types. Decreased oxygen consumption was observed in TSPO deficient microglia and fibroblasts (Banati et al., 2014; Zhao et al., 2016), but no effects were observed in hepatocytes and Leydig cells (Sileikyte et al., 2014; Tu et al., 2016). These inconsistent effects are probably attributed to the diversity of mitochondrial types and energetic status of cells. Therefore, the direct mechanism remains unclear. **(4) TSPO as a regulator of lipid metabolism.** Several studies have correlated TSPO expression to functional changes in lipid metabolism (Leduc et al., 2011; Wade et al., 2005). It was identified that TSPO deletion could increase fatty acid oxidation in steroidogenic cells (Tu et al., 2016). Potential interaction of TSPO with ACBP or CPT1A could affects import of fatty acids into mitochondria for β-oxidation. All the above perspectives require additional investigation.

In summary, the exact molecular function of TSPO remains unclear despite the great interest in targeting TSPO in human medicine. The prevalent model of TSPO and steroidogenesis appears to be inaccurate and will be systematically re-evaluated in my studies using both genetic and pharmacological tools. Using TSPO knockout mice and MA-10 cell line as the models, I will investigate the effects of TSPO loss on various cellular processes in order to elucidate the true function of the mammalian TSPO.

REFERENCES

Anderson, L.E., A.M. Dring, L.D. Hamel, and M.A. Stoner. 2011. Modulation of constitutive androstane receptor (CAR) and pregnane X receptor (PXR) by 6-arylpyrrolo[2,1-d][1,5]benzothiazepine derivatives, ligands of peripheral benzodiazepine receptor (PBR). *Toxicol Lett*. 202:148-154.

Anholt, R.R., E.B. De Souza, M.J. Kuhar, and S.H. Snyder. 1985a. Depletion of peripheral-type benzodiazepine receptors after hypophysectomy in rat adrenal gland and testis. *Eur J Pharmacol*. 110:41-46.

Anholt, R.R., E.B. De Souza, M.L. Oster-Granite, and S.H. Snyder. 1985b. Peripheral-type benzodiazepine receptors: autoradiographic localization in whole-body sections of neonatal rats. *J Pharmacol Exp Ther*. 233:517-526.

Anholt, R.R., P.L. Pedersen, E.B. De Souza, and S.H. Snyder. 1986. The peripheral-type benzodiazepine receptor. Localization to the mitochondrial outer membrane. *J Biol Chem*. 261:576-583.

Arakane, F., T. Sugawara, H. Nishino, Z. Liu, J.A. Holt, D. Pain, D.M. Stocco, W.L. Miller, and J.F. Strauss, 3rd. 1996. Steroidogenic acute regulatory protein (StAR) retains activity in the absence of its mitochondrial import sequence: implications for the mechanism of StAR action. *Proc Natl Acad Sci U S A*. 93:13731-13736.

Austin, C.J., J. Kahlert, M. Kassiou, and L.M. Rendina. 2013. The translocator protein (TSPO): a novel target for cancer chemotherapy. *Int J Biochem Cell Biol*. 45:1212-1216.

Auta, J., E. Romeo, A. Kozikowski, D. Ma, E. Costa, and A. Guidotti. 1993. Participation of mitochondrial diazepam binding inhibitor receptors in the anticonflict, antineophobic and anticonvulsant action of 2-aryl-3-indoleacetamide and imidazopyridine derivatives. *J Pharmacol Exp Ther*. 265:649-656.

Baier, C.J., J. Fantini, and F.J. Barrantes. 2011. Disclosure of cholesterol recognition motifs in transmembrane domains of the human nicotinic acetylcholine receptor. *Sci Rep*. 1:69.

Banati, R.B., R.J. Middleton, R. Chan, C.R. Hatty, W. Wai-Ying Kam, C. Quin, M.B. Graeber, A. Parmar, D. Zahra, P. Callaghan, S. Fok, N.R. Howell, M. Gregoire, A. Szabo, T. Pham, E. Davis, and G.J. Liu. 2014. Positron emission tomography and functional characterization of a complete PBR/TSPO knockout. *Nature communications*. 5:5452.

Banati, R.B., J. Newcombe, R.N. Gunn, A. Cagnin, F. Turkheimer, F. Heppner, G. Price, F. Wegner, G. Giovannoni, D.H. Miller, G.D. Perkin, T. Smith, A.K. Hewson, G. Bydder, G.W. Kreutzberg, T. Jones, M.L. Cuzner, and R. Myers. 2000. The peripheral benzodiazepine binding site in the brain in multiple sclerosis: quantitative in vivo imaging of microglia as a measure of disease activity. *Brain*. 123 (Pt 11):2321-2337.

Barnea, E.R., F. Fares, and M. Gavish. 1989. Modulatory action of benzodiazepines on human term placental steroidogenesis in vitro. *Molecular and cellular endocrinology*. 64:155-159.

Barron, A.M., L.M. Garcia-Segura, D. Caruso, A. Jayaraman, J.W. Lee, R.C. Melcangi, and C.J. Pike. 2013. Ligand for translocator protein reverses pathology in a mouse model of Alzheimer's disease. *J Neurosci*. 33:8891-8897.

Basile, A.S., and P. Skolnick. 1986. Subcellular localization of "peripheral-type" binding sites for benzodiazepines in rat brain. *J Neurochem*. 46:305-308.

Batarseh, A., K.D. Barlow, D.B. Martinez-Arguelles, and V. Papadopoulos. 2012. Functional characterization of the human translocator protein (18kDa) gene promoter in human breast cancer cell lines. *Biochim Biophys Acta*. 1819:38-56.

Batarseh, A., C. Giatzakis, and V. Papadopoulos. 2008. Phorbol-12-myristate 13-acetate acting through protein kinase Cepsilon induces translocator protein (18-kDa) TSPO gene expression. *Biochemistry*. 47:12886-12899.

Batarseh, A., and V. Papadopoulos. 2010. Regulation of translocator protein 18 kDa (TSPO) expression in health and disease states. *Molecular and cellular endocrinology*. 327:1-12.

Benavides, J., C. Malgouris, F. Imbault, F. Begassat, A. Uzan, C. Renault, M.C. Dubroeucq, C. Gueremy, and G. Le Fur. 1983a. "Peripheral type" benzodiazepine binding sites in rat adrenals: binding studies with [3H]PK 11195 and autoradiographic localization. *Arch Int Pharmacodyn Ther*. 266:38-49.

Benavides, J., D. Quarteronet, F. Imbault, C. Malgouris, A. Uzan, C. Renault, M.C. Dubroeucq, C. Gueremy, and G. Le Fur. 1983b. Labelling of "peripheral-type" benzodiazepine binding sites in the rat brain by using [3H]PK 11195, an isoquinoline carboxamide derivative: kinetic studies and autoradiographic localization. *J Neurochem*. 41:1744-1750.

Bernardi, P., A. Rasola, M. Forte, and G. Lippe. 2015. The Mitochondrial Permeability Transition Pore: Channel Formation by F-ATP Synthase, Integration in Signal Transduction, and Role in Pathophysiology. *Physiol Rev*. 95:1111-1155.

Bloksgaard, M., S. Bek, A.B. Marcher, D. Neess, J. Brewer, H.K. Hannibal-Bach, T. Helledie, C. Fenger, M. Due, Z. Berzina, R. Neubert, J. Chemnitz, B. Finsen, A. Clemmensen, J. Wilbertz, H. Saxtorph, J. Knudsen, L. Bagatolli, and S. Mandrup. 2012. The acyl-CoA binding protein is required for normal epidermal barrier function in mice. *J Lipid Res*. 53:2162-2174.

Bose, H.S., V.R. Lingappa, and W.L. Miller. 2002. Rapid regulation of steroidogenesis by mitochondrial protein import. *Nature*. 417:87-91.

Boujrad, N., J.R. Hudson, Jr., and V. Papadopoulos. 1993. Inhibition of hormone-stimulated steroidogenesis in cultured Leydig tumor cells by a cholesterol-linked phosphorothioate oligodeoxynucleotide antisense to diazepam-binding inhibitor. *Proc Natl Acad Sci U S A*. 90:5728-5731.

Braestrup, C., R. Albrechtsen, and R.F. Squires. 1977. High densities of benzodiazepine receptors in human cortical areas. *Nature*. 269:702-704.

Braestrup, C., and R.F. Squires. 1977. Specific benzodiazepine receptors in rat brain characterized by high-affinity (3H)diazepam binding. *Proc Natl Acad Sci U S A*. 74:3805-3809.

Braunersreuther, V., F. Montecucco, M. Asrih, G. Pelli, K. Galan, M. Frias, F. Burger, A.L. Quindere, C. Montessuit, K.H. Krause, F. Mach, and V. Jaquet. 2013. Role of NADPH oxidase isoforms NOX1, NOX2 and NOX4 in myocardial ischemia/reperfusion injury. *J Mol Cell Cardiol*. 64:99-107.

Bucan, M., B. Gatalica, P. Nolan, A. Chung, A. Leroux, M.H. Grossman, J.H. Nadeau, B.S. Emanuel, and M. Budarf. 1993. Comparative mapping of 9 human chromosome 22q loci in the laboratory mouse. *Human molecular genetics*. 2:1245-1252.

Cavallaro, S., A. Korneyev, A. Guidotti, and E. Costa. 1992. Diazepam-binding inhibitor (DBI)-processing products, acting at the mitochondrial DBI receptor, mediate adrenocorticotropic hormone-induced steroidogenesis in rat adrenal gland. *Proc Natl Acad Sci U S A*. 89:10598-10602.

Cavallaro, S., L. Pani, A. Guidotti, and E. Costa. 1993. ACTH-induced mitochondrial DBI receptor (MDR) and diazepam binding inhibitor (DBI) expression in adrenals of hypophysectomized rats is not cause-effect related to its immediate steroidogenic action. *Life Sci*. 53:1137-1147.

Chauveau, F., H. Boutin, N. Van Camp, F. Dolle, and B. Tavitian. 2008. Nuclear imaging of neuroinflammation: a comprehensive review of [11C]PK11195 challengers. *Eur J Nucl Med Mol Imaging*. 35:2304-2319.

Chen, M.K., and T.R. Guilarte. 2008. Translocator protein 18 kDa (TSPO): molecular sensor of brain injury and repair. *Pharmacol Ther*. 118:1-17.

Clark, B.J., J. Wells, S.R. King, and D.M. Stocco. 1994. The purification, cloning, and expression of a novel luteinizing hormone-induced mitochondrial protein in MA-10 mouse Leydig tumor cells. Characterization of the steroidogenic acute regulatory protein (StAR). *J Biol Chem*. 269:28314-28322.

Costa, B., S. Pini, P. Gabelloni, E. Da Pozzo, M. Abelli, L. Lari, M. Preve, A. Lucacchini, G.B. Cassano, and C. Martini. 2009a. The spontaneous Ala147Thr amino acid substitution within the translocator protein influences pregnenolone production in lymphomonocytes of healthy individuals. *Endocrinology*. 150:5438-5445.

Costa, B., S. Pini, C. Martini, M. Abelli, P. Gabelloni, S. Landi, M. Muti, C. Gesi, L. Lari, A. Cardini, S. Galderisi, A. Mucci, A. Lucacchini, and G.B. Cassano. 2009b. Ala147Thr substitution in translocator protein is associated with adult separation anxiety in patients with depression. *Psychiatr Genet*. 19:110-111.

Daugherty, D.J., V. Selvaraj, O.V. Chechneva, X.B. Liu, D.E. Pleasure, and W. Deng. 2013. A TSPO ligand is protective in a mouse model of multiple sclerosis. *EMBO Mol Med*. 5:891-903.

Davies, L.P., and V. Huston. 1981. Peripheral benzodiazepine binding sites in heart and their interaction with dipyridamole. *Eur J Pharmacol*. 73:209-211.

Deane, H.W., and R.O. Greep. 1946. A morphological and histochemical study of the rat's adrenal cortex after hypoph ysectomy, with comments on the liver. *Am J Anat*. 79:117-145.

Delavoie, F., H. Li, M. Hardwick, J.C. Robert, C. Giatzakis, G. Peranzi, Z.X. Yao, J. Maccario, J.J. Lacapere, and V. Papadopoulos. 2003. In vivo and in vitro peripheral-type benzodiazepine receptor polymerization: functional significance in drug ligand and cholesterol binding. *Biochemistry*. 42:4506-4519.

Ding, X., K. Lichti, I. Kim, F.J. Gonzalez, and J.L. Staudinger. 2006. Regulation of constitutive androstane receptor and its target genes by fasting, cAMP, hepatocyte nuclear factor alpha, and the coactivator peroxisome proliferator-activated receptor gamma coactivator-1alpha. *J Biol Chem*. 281:26540-26551.

Fan, J., P. Lindemann, M.G. Feuilloley, and V. Papadopoulos. 2012. Structural and functional evolution of the translocator protein (18 kDa). *Curr Mol Med*. 12:369-386.

Fan, J., and V. Papadopoulos. 2012. Transcriptional regulation of translocator protein (Tspo) via a SINE B2-mediated natural antisense transcript in MA-10 Leydig cells. *Biol Reprod*. 86:147, 141-115.

Fan, J., M.B. Rone, and V. Papadopoulos. 2009. Translocator protein 2 is involved in cholesterol redistribution during erythropoiesis. *J Biol Chem*. 284:30484-30497.

Farges, R., E. Joseph-Liauzun, D. Shire, D. Caput, G. Le Fur, and P. Ferrara. 1994. Site-directed mutagenesis of the peripheral benzodiazepine receptor: identification of amino acids implicated in the binding site of Ro5-4864. *Mol Pharmacol*. 46:1160-1167.

Frye, C.A., J.J. Paris, and M.E. Rhodes. 2009. Increasing 3alpha,5alpha-THP following inhibition of neurosteroid biosynthesis in the ventral tegmental area reinstates anti-anxiety, social, and sexual behavior of naturally receptive rats. *Reproduction*. 137:119-128.

Gaigg, B., T.B. Neergaard, R. Schneiter, J.K. Hansen, N.J. Faergeman, N.A. Jensen, J.R. Andersen, J. Friis, R. Sandhoff, H.D. Schroder, and J. Knudsen. 2001. Depletion of acyl-coenzyme A-binding protein affects sphingolipid synthesis and causes vesicle accumulation and membrane defects in Saccharomyces cerevisiae. *Mol Biol Cell*. 12:1147-1160.

Garnier, M., N. Boujrad, S.O. Ogwuegbu, J.R. Hudson, Jr., and V. Papadopoulos. 1994. The polypeptide diazepam-binding inhibitor and a higher affinity mitochondrial peripheral-type benzodiazepine receptor sustain constitutive steroidogenesis in the R2C Leydig tumor cell line. *J Biol Chem*. 269:22105-22112.

Garnier, M., N. Boujrad, B.O. Oke, A.S. Brown, J. Riond, P. Ferrara, M. Shoyab, C.A. Suarez-Quian, and V. Papadopoulos. 1993. Diazepam binding inhibitor is a paracrine/autocrine regulator of Leydig cell proliferation and steroidogenesis: action via peripheral-type benzodiazepine receptor and independent mechanisms. *Endocrinology*. 132:444-458.

Gatliff, J., and M. Campanella. 2012. The 18 kDa translocator protein (TSPO): a new perspective in mitochondrial biology. *Curr Mol Med*. 12:356-368.

Gatliff, J., D. East, J. Crosby, R. Abeti, R. Harvey, W. Craigen, P. Parker, and M. Campanella. 2014. TSPO interacts with VDAC1 and triggers a ROS-mediated inhibition of mitochondrial quality control. *Autophagy*. 10:2279-2296.

Gavish, M., I. Bachman, R. Shoukrun, Y. Katz, L. Veenman, G. Weisinger, and A. Weizman. 1999. Enigma of the peripheral benzodiazepine receptor. *Pharmacol Rev*. 51:629-650.

Giatzakis, C., A. Batarseh, L. Dettin, and V. Papadopoulos. 2007. The role of Ets transcription factors in the basal transcription of the translocator protein (18 kDa). *Biochemistry*. 46:4763-4774.

Giatzakis, C., and V. Papadopoulos. 2004. Differential utilization of the promoter of peripheral-type benzodiazepine receptor by steroidogenic versus nonsteroidogenic cell lines and the role of Sp1 and Sp3 in the regulation of basal activity. *Endocrinology*. 145:1113-1123.

Ginter, C., I. Kiburu, and O. Boudker. 2013. Chemical catalysis by the translocator protein (18 kDa). *Biochemistry*. 52:3609-3611.

Gonzalez-Polo, R.A., G. Carvalho, T. Braun, D. Decaudin, C. Fabre, N. Larochette, J.L. Perfettini, M. Djavaheri-Mergny, I. Youlyouz-Marfak, P. Codogno, M. Raphael, J. Feuillard, and G. Kroemer. 2005. PK11195 potently sensitizes to apoptosis induction independently from the peripheral benzodiazepin receptor. *Oncogene*. 24:7503-7513.

Guilarte, T.R., M.K. Loth, and S.R. Guariglia. 2016. TSPO Finds NOX2 in Microglia for Redox Homeostasis. *Trends Pharmacol Sci*.

Guo, Y., R.C. Kalathur, Q. Liu, B. Kloss, R. Bruni, C. Ginter, E. Kloppmann, B. Rost, and W.A. Hendrickson. 2015. Protein structure. Structure and activity of tryptophan-rich TSPO proteins. *Science*. 347:551-555.

Gut, P. 2015. Targeting mitochondrial energy metabolism with TSPO ligands. *Biochem Soc Trans*. 43:537-542.

Gut, P., B. Baeza-Raja, O. Andersson, L. Hasenkamp, J. Hsiao, D. Hesselson, K. Akassoglou, E. Verdin, M.D. Hirschey, and D.Y. Stainier. 2013. Whole-organism screening for gluconeogenesis identifies activators of fasting metabolism. *Nat Chem Biol*. 9:97-104.

Hans, G., S. Wislet-Gendebien, F. Lallemend, P. Robe, B. Rogister, S. Belachew, L. Nguyen, B. Malgrange, G. Moonen, and J.M. Rigo. 2005. Peripheral benzodiazepine receptor (PBR) ligand cytotoxicity unrelated to PBR expression. *Biochem Pharmacol*. 69:819-830.

Hardwick, M., D. Fertikh, M. Culty, H. Li, B. Vidic, and V. Papadopoulos. 1999. Peripheral-type benzodiazepine receptor (PBR) in human breast cancer: correlation of breast cancer cell aggressive phenotype with PBR expression, nuclear localization, and PBR-mediated cell proliferation and nuclear transport of cholesterol. *Cancer research*. 59:831-842.

Hatty, C.R., A.P. Le Brun, V. Lake, L.A. Clifton, G.J. Liu, M. James, and R.B. Banati. 2014. Investigating the interactions of the 18kDa translocator protein and its ligand PK11195 in planar lipid bilayers. *Biochim Biophys Acta*. 1838:1019-1030.

Hauet, T., Z.X. Yao, H.S. Bose, C.T. Wall, Z. Han, W. Li, D.B. Hales, W.L. Miller, M. Culty, and V. Papadopoulos. 2005. Peripheral-type benzodiazepine receptor-mediated action of steroidogenic acute regulatory protein on cholesterol entry into leydig cell mitochondria. *Mol Endocrinol*. 19:540-554.

Haworth, R.A., and D.R. Hunter. 1979. The Ca2+-induced membrane transition in mitochondria. II. Nature of the Ca2+ trigger site. *Archives of biochemistry and biophysics*. 195:460-467.

Herrera, J.L., M. Diaz, J.R. Hernandez-Fernaud, E. Salido, R. Alonso, C. Fernandez, A. Morales, and R. Marin. 2011. Voltage-dependent anion channel as a resident protein of lipid rafts: post-transductional regulation by estrogens and involvement in neuronal preservation against Alzheimer's disease. *J Neurochem*. 116:820-827.

Hunter, D.R., and R.A. Haworth. 1979a. The Ca2+-induced membrane transition in mitochondria. I. The protective mechanisms. *Archives of biochemistry and biophysics*. 195:453-459.

Hunter, D.R., and R.A. Haworth. 1979b. The Ca2+-induced membrane transition in mitochondria. III. Transitional Ca2+ release. *Archives of biochemistry and biophysics*. 195:468-477.

Jaremko, L., M. Jaremko, K. Giller, S. Becker, and M. Zweckstetter. 2014. Structure of the mitochondrial translocator protein in complex with a diagnostic ligand. *Science (New York, N.Y.)*. 343:1363-1366.

Joo, H.K., Y.R. Lee, G. Kang, S. Choi, C.S. Kim, S. Ryoo, J.B. Park, and B.H. Jeon. 2015. The 18-kDa Translocator Protein Inhibits Vascular Cell Adhesion Molecule-1 Expression via Inhibition of Mitochondrial Reactive Oxygen Species. *Mol Cells*. 38:1064-1070.

Joo, H.K., Y.R. Lee, S.Y. Lim, E.J. Lee, S. Choi, E.J. Cho, M.S. Park, S. Ryoo, J.B. Park, and B.H. Jeon. 2012. Peripheral benzodiazepine receptor regulates vascular endothelial activations via suppression of the voltage-dependent anion channel-1. *FEBS Lett*. 586:1349-1355.

Kim, T., and A.N. Pae. 2016. Translocator protein (TSPO) ligands for the diagnosis or treatment of neurodegenerative diseases: a patent review (2010-2015; part 1). *Expert Opin Ther Pat*. 26:1325-1351.

Kimura, T. 1969. Effects of hypophysectomy and ACTH administration on the level of adrenal cholesterol side-chain desmolase. *Endocrinology*. 85:492-499.

Kinnally, K.W., D.B. Zorov, Y.N. Antonenko, S.H. Snyder, M.W. McEnery, and H. Tedeschi. 1993. Mitochondrial benzodiazepine receptor linked to inner membrane ion channels by nanomolar actions of ligands. *Proc Natl Acad Sci U S A*. 90:1374-1378.

Kletsas, D., W. Li, Z. Han, and V. Papadopoulos. 2004. Peripheral-type benzodiazepine receptor (PBR) and PBR drug ligands in fibroblast and fibrosarcoma cell proliferation: role of ERK, c-Jun and ligand-activated PBR-independent pathways. *Biochem Pharmacol*. 67:1927-1932.

Knudsen, J., M.V. Jensen, J.K. Hansen, N.J. Faergeman, T.B. Neergaard, and B. Gaigg. 1999. Role of acylCoA binding protein in acylCoA transport, metabolism and cell signaling. *Mol Cell Biochem*. 192:95-103.

Korkhov, V.M., C. Sachse, J.M. Short, and C.G. Tate. 2010. Three-dimensional structure of TspO by electron cryomicroscopy of helical crystals. *Structure*. 18:677-687.

Korneyev, A., B.S. Pan, A. Polo, E. Romeo, A. Guidotti, and E. Costa. 1993. Stimulation of brain pregnenolone synthesis by mitochondrial diazepam binding inhibitor receptor ligands in vivo. *J Neurochem*. 61:1515-1524.

Krueger, K.E., and V. Papadopoulos. 1990. Peripheral-type benzodiazepine receptors mediate translocation of cholesterol from outer to inner mitochondrial membranes in adrenocortical cells. *J Biol Chem*. 265:15015-15022.

Lacapere, J.J., F. Delavoie, H. Li, G. Peranzi, J. Maccario, V. Papadopoulos, and B. Vidic. 2001. Structural and functional study of reconstituted peripheral benzodiazepine receptor. *Biochem Biophys Res Commun*. 284:536-541.

Landrock, D., B.P. Atshaves, A.L. McIntosh, K.K. Landrock, F. Schroeder, and A.B. Kier. 2010. Acyl-CoA binding protein gene ablation induces pre-implantation embryonic lethality in mice. *Lipids*. 45:567-580.

Larcher, J.C., J.L. Vayssiere, F.J. Le Marquer, L.R. Cordeau, P.E. Keane, A. Bachy, F. Gros, and B.P. Croizat. 1989. Effects of peripheral benzodiazepines upon the O2 consumption of neuroblastoma cells. *Eur J Pharmacol*. 161:197-202.

Le Fur, G., M.L. Perrier, N. Vaucher, F. Imbault, A. Flamier, J. Benavides, A. Uzan, C. Renault, M.C. Dubroeucq, and C. Gueremy. 1983a. Peripheral benzodiazepine binding sites: effect of PK 11195, 1-(2-chlorophenyl)-N-methyl-N-(1-methylpropyl)-3-isoquinolinecarboxamide. I. In vitro studies. *Life Sci*. 32:1839-1847.

Le Fur, G., N. Vaucher, M.L. Perrier, A. Flamier, J. Benavides, C. Renault, M.C. Dubroeucq, C. Gueremy, and A. Uzan. 1983b. Differentiation between two ligands for peripheral benzodiazepine binding sites, [3H]RO5-4864 and [3H]PK 11195, by thermodynamic studies. *Life Sci*. 33:449-457.

Leduc, M.S., R.S. Hageman, R.A. Verdugo, S.W. Tsaih, K. Walsh, G.A. Churchill, and B. Paigen. 2011. Integration of QTL and bioinformatic tools to identify candidate genes for triglycerides in mice. *J Lipid Res*. 52:1672-1682.

Lee, L., C.A. DeBono, D.R. Campagna, D.C. Young, D.B. Moody, and M.D. Fleming. 2007. Loss of the acyl-CoA binding protein (Acbp) results in fatty acid metabolism abnormalities in mouse hair and skin. *J Invest Dermatol*. 127:16-23.

Lehtonen, M.T., M. Akita, W. Frank, R. Reski, and J.P. Valkonen. 2012. Involvement of a class III peroxidase and the mitochondrial protein TSPO in oxidative burst upon treatment of moss plants with a fungal elicitor. *Molecular plant-microbe interactions : MPMI*. 25:363-371.

Li, F., J. Liu, Y. Zheng, R.M. Garavito, and S. Ferguson-Miller. 2015. Protein structure. Crystal structures of translocator protein (TSPO) and mutant mimic of a human polymorphism. *Science (New York, N.Y.)*. 347:555-558.

Li, H., and V. Papadopoulos. 1998. Peripheral-type benzodiazepine receptor function in cholesterol transport. Identification of a putative cholesterol recognition/interaction amino acid sequence and consensus pattern. *Endocrinology*. 139:4991-4997.

Li, H., Z. Yao, B. Degenhardt, G. Teper, and V. Papadopoulos. 2001. Cholesterol binding at the cholesterol recognition/ interaction amino acid consensus (CRAC) of the peripheral-type benzodiazepine receptor and inhibition of steroidogenesis by an HIV TAT-CRAC peptide. *Proc Natl Acad Sci U S A*. 98:1267-1272.

Li, L., T. Chen, J.D. Stanton, T. Sueyoshi, M. Negishi, and H. Wang. 2008. The peripheral benzodiazepine receptor ligand 1-(2-chlorophenyl-methylpropyl)-3-isoquinoline-carboxamide is a novel antagonist of human constitutive androstane receptor. *Mol Pharmacol*. 74:443-453.

Lin, D., Y.J. Chang, J.F. Strauss, 3rd, and W.L. Miller. 1993. The human peripheral benzodiazepine receptor gene: cloning and characterization of alternative splicing in normal tissues and in a patient with congenital lipoid adrenal hyperplasia. *Genomics*. 18:643-650.

Lin, D., T. Sugawara, J.F. Strauss, 3rd, B.J. Clark, D.M. Stocco, P. Saenger, A. Rogol, and W.L. Miller. 1995. Role of steroidogenic acute regulatory protein in adrenal and gonadal steroidogenesis. *Science (New York, N.Y.)*. 267:1828-1831.

Lin, R., A. Angelin, F. Da Settimo, C. Martini, S. Taliani, S. Zhu, and D.C. Wallace. 2014. Genetic analysis of dTSPO, an outer mitochondrial membrane protein, reveals its functions in apoptosis, longevity, and Aβ42-induced neurodegeneration. *Aging Cell*. 13:507-518.

Lin, R., D. Rittenhouse, K. Sweeney, P. Potluri, and D.C. Wallace. 2015. TSPO, a Mitochondrial Outer Membrane Protein, Controls Ethanol-Related Behaviors in Drosophila. *PLoS Genet*. 11:e1005366.

Luo, X., D. Sharma, H. Inouye, D. Lee, R.L. Avila, M. Salmona, and D.A. Kirschner. 2007. Cytoplasmic domain of human myelin protein zero likely folded as beta-structure in compact myelin. *Biophys J*. 92:1585-1597.

Macdonald, R., and J.L. Barker. 1978. Benzodiazepines specifically modulate GABA-mediated postsynaptic inhibition in cultured mammalian neurones. *Nature*. 271:563-564.

Maglich, J.M., J. Watson, P.J. McMillen, B. Goodwin, T.M. Willson, and J.T. Moore. 2004. The nuclear receptor CAR is a regulator of thyroid hormone metabolism during caloric restriction. *J Biol Chem*. 279:19832-19838.

Mandrup, S., R. Jepsen, H. Skott, J. Rosendal, P. Hojrup, K. Kristiansen, and J. Knudsen. 1993. Effect of heterologous expression of acyl-CoA-binding protein on acyl-CoA level and composition in yeast. *Biochem J*. 290 (Pt 2):369-374.

Manku, G., Y. Wang, R. Thuillier, C. Rhodes, and M. Culty. 2012. Developmental expression of the translocator protein 18 kDa (TSPO) in testicular germ cells. *Curr Mol Med*. 12:467-475.

McEnery, M.W., A.M. Snowman, R.R. Trifiletti, and S.H. Snyder. 1992. Isolation of the mitochondrial benzodiazepine receptor: association with the voltage-dependent anion channel and the adenine nucleotide carrier. *Proc Natl Acad Sci U S A*. 89:3170-3174.

Mizrahi, R., P.M. Rusjan, J. Kennedy, B. Pollock, B. Mulsant, I. Suridjan, V. De Luca, A.A. Wilson, and S. Houle. 2012. Translocator protein (18 kDa) polymorphism (rs6971) explains in-vivo brain binding affinity of the PET radioligand [(18)F]-FEPPA. *J Cereb Blood Flow Metab*. 32:968-972.

Morohaku, K., S.H. Pelton, D.J. Daugherty, W.R. Butler, W. Deng, and V. Selvaraj. 2014. Translocator protein/peripheral benzodiazepine receptor is not required for steroid hormone biosynthesis. *Endocrinology*. 155:89-97.

Morohaku, K., N.S. Phuong, and V. Selvaraj. 2013. Developmental expression of translocator protein/peripheral benzodiazepine receptor in reproductive tissues. *PLoS One*. 8:e74509.

Mukhin, A.G., V. Papadopoulos, E. Costa, and K.E. Krueger. 1989. Mitochondrial benzodiazepine receptors regulate steroid biosynthesis. *Proc Natl Acad Sci U S A*. 86:9813-9816.

Murail, S., J.C. Robert, Y.M. Coic, J.M. Neumann, M.A. Ostuni, Z.X. Yao, V. Papadopoulos, N. Jamin, and J.J. Lacapere. 2008. Secondary and tertiary structures of the transmembrane domains of the translocator protein TSPO determined by NMR. Stabilization of the TSPO tertiary fold upon ligand binding. *Biochim Biophys Acta*. 1778:1375-1381.

Nakazawa, F., C. Alev, M. Shin, Y. Nakaya, L.M. Jakt, and G. Sheng. 2009. PBRL, a putative peripheral benzodiazepine receptor, in primitive erythropoiesis. *Gene Expr Patterns*. 9:114-121.

Neess, D., S. Bek, M. Bloksgaard, A.B. Marcher, N.J. Faergeman, and S. Mandrup. 2013. Delayed hepatic adaptation to weaning in ACBP-/- mice is caused by disruption of the epidermal barrier. *Cell Rep*. 5:1403-1412.

Neess, D., M. Bloksgaard, S. Bek, A.B. Marcher, I.C. Elle, T. Helledie, M. Due, V. Pagmantidis, B. Finsen, J. Wilbertz, M. Kruhoffer, N. Faergeman, and S. Mandrup. 2011. Disruption of the acyl-CoA-binding protein gene delays hepatic adaptation to metabolic changes at weaning. *J Biol Chem*. 286:3460-3472.

Obame, F.N., R. Zini, R. Souktani, A. Berdeaux, and D. Morin. 2007. Peripheral benzodiazepine receptor-induced myocardial protection is mediated by inhibition of mitochondrial membrane permeabilization. *J Pharmacol Exp Ther*. 323:336-345.

Ohgami, R.S., D.R. Campagna, B. Antiochos, E.B. Wood, J.J. Sharp, J.E. Barker, and M.D. Fleming. 2005a. nm1054: a spontaneous, recessive, hypochromic, microcytic anemia mutation in the mouse. *Blood*. 106:3625-3631.

Ohgami, R.S., D.R. Campagna, E.L. Greer, B. Antiochos, A. McDonald, J. Chen, J.J. Sharp, Y. Fujiwara, J.E. Barker, and M.D. Fleming. 2005b. Identification of a ferrireductase required for efficient transferrin-dependent iron uptake in erythroid cells. *Nat Genet*. 37:1264-1269.

Oke, B.O., C.A. Suarez-Quian, J. Riond, P. Ferrara, and V. Papadopoulos. 1992. Cell surface localization of the peripheral-type benzodiazepine receptor (PBR) in adrenal cortex. *Molecular and cellular endocrinology*. 87:R1-6.

Olson, J.M., B.J. Ciliax, W.R. Mancini, and A.B. Young. 1988. Presence of peripheral-type benzodiazepine binding sites on human erythrocyte membranes. *Eur J Pharmacol*. 152:47-53.

Owen, D.R., and P.M. Matthews. 2011. Imaging brain microglial activation using positron emission tomography and translocator protein-specific radioligands. *Int Rev Neurobiol*. 101:19-39.

Owen, D.R., A.J. Yeo, R.N. Gunn, K. Song, G. Wadsworth, A. Lewis, C. Rhodes, D.J. Pulford, I. Bennacef, C.A. Parker, P.L. StJean, L.R. Cardon, V.E. Mooser, P.M. Matthews, E.A. Rabiner, and J.P. Rubio. 2012. An 18-kDa translocator protein (TSPO) polymorphism explains differences in binding affinity of the PET radioligand PBR28. *J Cereb Blood Flow Metab*. 32:1-5.

Palmer, M. 2004. Cholesterol and the activity of bacterial toxins. *FEMS Microbiol Lett*. 238:281-289.

Papadopoulos, V., H. Amri, N. Boujrad, C. Cascio, M. Culty, M. Garnier, M. Hardwick, H. Li, B. Vidic, A.S. Brown, J.L. Reversa, J.M. Bernassau, and K. Drieu. 1997a. Peripheral benzodiazepine receptor in cholesterol transport and steroidogenesis. *Steroids*. 62:21-28.

Papadopoulos, V., H. Amri, H. Li, N. Boujrad, B. Vidic, and M. Garnier. 1997b. Targeted disruption of the peripheral-type benzodiazepine receptor gene inhibits steroidogenesis in the R2C Leydig tumor cell line. *J Biol Chem*. 272:32129-32135.

Papadopoulos, V., A. Berkovich, and K.E. Krueger. 1991a. The role of diazepam binding inhibitor and its processing products at mitochondrial benzodiazepine receptors: regulation of steroid biosynthesis. *Neuropharmacology*. 30:1417-1423.

Papadopoulos, V., A. Berkovich, K.E. Krueger, E. Costa, and A. Guidotti. 1991b. Diazepam binding inhibitor and its processing products stimulate mitochondrial steroid biosynthesis via an interaction with mitochondrial benzodiazepine receptors. *Endocrinology*. 129:1481-1488.

Papadopoulos, V., P. Guarneri, K.E. Kreuger, A. Guidotti, and E. Costa. 1992. Pregnenolone biosynthesis in C6-2B glioma cell mitochondria: regulation by a mitochondrial diazepam binding inhibitor receptor. *Proc Natl Acad Sci U S A*. 89:5113-5117.

Papadopoulos, V., and L. Lecanu. 2009. Translocator protein (18 kDa) TSPO: an emerging therapeutic target in neurotrauma. *Exp Neurol*. 219:53-57.

Papadopoulos, V., and W.L. Miller. 2012. Role of mitochondria in steroidogenesis. *Best Pract Res Clin Endocrinol Metab*. 26:771-790.

Papadopoulos, V., A.G. Mukhin, E. Costa, and K.E. Krueger. 1990. The peripheral-type benzodiazepine receptor is functionally linked to Leydig cell steroidogenesis. *J Biol Chem*. 265:3772-3779.

Papadopoulos, V., F.B. Nowzari, and K.E. Krueger. 1991c. Hormone-stimulated steroidogenesis is coupled to mitochondrial benzodiazepine receptors. Tropic hormone action on steroid biosynthesis is inhibited by flunitrazepam. *J Biol Chem*. 266:3682-3687.

Paradis, S., V. Leoni, C. Caccia, A. Berdeaux, and D. Morin. 2013. Cardioprotection by the TSPO ligand 4'-chlorodiazepam is associated with inhibition of mitochondrial accumulation of cholesterol at reperfusion. *Cardiovasc Res*. 98:420-427.

Qi, X., J. Xu, F. Wang, and J. Xiao. 2012. Translocator protein (18 kDa): a promising therapeutic target and diagnostic tool for cardiovascular diseases. *Oxid Med Cell Longev*. 2012:162934.

Rampon, C., M. Bouzaffour, M.A. Ostuni, P. Dufourcq, C. Girard, J.M. Freyssinet, J.J. Lacapere, G. Schweizer-Groyer, and S. Vriz. 2009. Translocator protein (18 kDa) is involved in primitive erythropoiesis in zebrafish. *Faseb J*. 23:4181-4192.

Ratcliffe, S.L., and E.K. Matthews. 1995. Modification of the photodynamic action of delta-aminolaevulinic acid (ALA) on rat pancreatoma cells by mitochondrial benzodiazepine receptor ligands. *Br J Cancer*. 71:300-305.

Regan, J.W., H.I. Yamamura, S. Yamada, and W.R. Roeske. 1981. High affinity [3H]flunitrazepam binding: characterization, localization, and alteration in hypertension. *Life Sci*. 28:991-998.

Riond, J., M.G. Mattei, M. Kaghad, X. Dumont, J.C. Guillemot, G. Le Fur, D. Caput, and P. Ferrara. 1991. Molecular cloning and chromosomal localization of a human peripheral-type benzodiazepine receptor. *European journal of biochemistry / FEBS*. 195:305-311.

Romeo, E., S. Cavallaro, A. Korneyev, A.P. Kozikowski, D. Ma, A. Polo, E. Costa, and A. Guidotti. 1993. Stimulation of brain steroidogenesis by 2-aryl-indole-3-acetamide derivatives acting at the mitochondrial diazepam-binding inhibitor receptor complex. *J Pharmacol Exp Ther*. 267:462-471.

Rone, M.B., J. Fan, and V. Papadopoulos. 2009. Cholesterol transport in steroid biosynthesis: role of protein-protein interactions and implications in disease states. *Biochim Biophys Acta*. 1791:646-658.

Rosenberg, N., O. Rosenberg, A. Weizman, L. Veenman, and M. Gavish. 2013. In vitro catabolic effect of protoporphyrin IX in human osteoblast-like cells: possible role of the 18 kDa mitochondrial translocator protein. *Journal of bioenergetics and biomembranes*. 45:333-341.

Rupprecht, R., V. Papadopoulos, G. Rammes, T.C. Baghai, J. Fan, N. Akula, G. Groyer, D. Adams, and M. Schumacher. 2010. Translocator protein (18 kDa) (TSPO) as a therapeutic target for neurological and psychiatric disorders. *Nat Rev Drug Discov*. 9:971-988.

Seneviratne, M.S., D. Faccenda, V. De Biase, and M. Campanella. 2012. PK11195 inhibits mitophagy targeting the F1Fo-ATPsynthase in Bcl-2 knock-down cells. *Curr Mol Med*. 12:476-482.

Sileikyte, J., E. Blachly-Dyson, R. Sewell, A. Carpi, R. Menabo, F. Di Lisa, F. Ricchelli, P. Bernardi, and M. Forte. 2014. Regulation of the Mitochondrial Permeability Transition Pore by the Outer Membrane does not Involve the Peripheral Benzodiazepine Receptor (TSPO). *J Biol Chem*.

Sileikyte, J., V. Petronilli, A. Zulian, F. Dabbeni-Sala, G. Tognon, P. Nikolov, P. Bernardi, and F. Ricchelli. 2011. Regulation of the inner membrane mitochondrial permeability transition by the outer membrane translocator protein (peripheral benzodiazepine receptor). *J Biol Chem*. 286:1046-1053.

Stocco, D.M. 2001. StAR protein and the regulation of steroid hormone biosynthesis. *Annu Rev Physiol*. 63:193-213.

Takahashi, H., A. Nagashima, and C. Koshino. 1958. Effect of gamma-aminobutyryl-choline upon the electrical activity of the cerebral cortex. *Nature*. 182:1443-1444.

Takai, N., N. Kira, T. Ishii, T. Yoshida, M. Nishida, Y. Nishida, K. Nasu, M. Takano, H. Midori, S. Koga, and H. Narahara. 2012. A translocator protein ligand PK11195 shows antigrowth activity in human choriocarcinoma cells. *Tumour biology : the journal of the International Society for Oncodevelopmental Biology and Medicine*. 33:1505-1510.

Taketani, S., H. Kohno, M. Okuda, T. Furukawa, and R. Tokunaga. 1994. Induction of peripheral-type benzodiazepine receptors during differentiation of mouse erythroleukemia cells. A possible involvement of these receptors in heme biosynthesis. *J Biol Chem*. 269:7527-7531.

Tsuda, M., T. Suzuki, and M. Misawa. 1998. Subsensitivity to mitochondrial diazepam binding inhibitor receptor agonist FGIN-1-27-induced antiseizure effect in diazepam-withdrawn mice. *Life Sci*. 62:PL213-217.

Tu, L.N., K. Morohaku, P.R. Manna, S.H. Pelton, W.R. Butler, D.M. Stocco, and V. Selvaraj. 2014. Peripheral Benzodiazepine Receptor/Translocator Protein Global Knock-out Mice Are Viable with No Effects on Steroid Hormone Biosynthesis. *J Biol Chem*. 289:27444-27454.

Tu, L.N., A.H. Zhao, M. Hussein, D.M. Stocco, and V. Selvaraj. 2016. Translocator Protein (TSPO) Affects Mitochondrial Fatty Acid Oxidation in Steroidogenic Cells. *Endocrinology*. 157:1110-1121.

Ueda, A., H.K. Hamadeh, H.K. Webb, Y. Yamamoto, T. Sueyoshi, C.A. Afshari, J.M. Lehmann, and M. Negishi. 2002. Diverse roles of the nuclear orphan receptor CAR in regulating hepatic genes in response to phenobarbital. *Molecular pharmacology*. 61:1-6.

Venturini, I., M.L. Zeneroli, L. Corsi, R. Avallone, F. Farina, H. Alho, C. Baraldi, C. Ferrarese, N. Pecora, M. Frigo, G. Ardizzone, A. Arrigo, R. Pellicci, and M. Baraldi. 1998. Up-regulation of peripheral benzodiazepine receptor system in hepatocellular carcinoma. *Life Sci*. 63:1269-1280.

Verma, A., J.S. Nye, and S.H. Snyder. 1987. Porphyrins are endogenous ligands for the mitochondrial (peripheral-type) benzodiazepine receptor. *Proc Natl Acad Sci U S A*. 84:2256-2260.

Wade, F.M., C. Wakade, V.B. Mahesh, and D.W. Brann. 2005. Differential expression of the peripheral benzodiazepine receptor and gremlin during adipogenesis. *Obes Res*. 13:818-822.

Walter, R.B., J.L. Pirga, M.R. Cronk, S. Mayer, F.R. Appelbaum, and D.E. Banker. 2005. PK11195, a peripheral benzodiazepine receptor (pBR) ligand, broadly blocks drug efflux to chemosensitize leukemia and myeloma cells by a pBR-independent, direct transporter-modulating mechanism. *Blood*. 106:3584-3593.

Wang, H.J., J. Fan, and V. Papadopoulos. 2012. Translocator protein (Tspo) gene promoter-driven green fluorescent protein synthesis in transgenic mice: an in vivo model to study Tspo transcription. *Cell Tissue Res*. 350:261-275.

Wang, X., Z. Liu, S. Eimerl, R. Timberg, A.M. Weiss, J. Orly, and D.M. Stocco. 1998. Effect of truncated forms of the steroidogenic acute regulatory protein on intramitochondrial cholesterol transfer. *Endocrinology*. 139:3903-3912.

Weizman, R., S. Leschiner, W. Schlegel, and M. Gavish. 1997. Peripheral-type benzodiazepine receptor ligands and serum steroid hormones. *Brain Res*. 772:203-208.

Wendler, G., P. Lindemann, J.J. Lacapere, and V. Papadopoulos. 2003. Protoporphyrin IX binding and transport by recombinant mouse PBR. *Biochem Biophys Res Commun*. 311:847-852.

Wu, X., and K.A. Gallo. 2013. The 18-kDa translocator protein (TSPO) disrupts mammary epithelial morphogenesis and promotes breast cancer cell migration. *PLoS One*. 8:e71258.

Xiao, J., D. Liang, H. Zhang, Y. Liu, F. Li, and Y.H. Chen. 2010. 4'-Chlorodiazepam, a translocator protein (18 kDa) antagonist, improves cardiac functional recovery during postischemia reperfusion in rats. *Exp Biol Med (Maywood)*. 235:478-486.

Yang, G., H. Xu, Z. Li, and F. Li. 2014. Interactions of caveolin-1 scaffolding and intramembrane regions containing a CRAC motif with cholesterol in lipid bilayers. *Biochim Biophys Acta*. 1838:2588-2599.

Yeliseev, A.A., and S. Kaplan. 1995. A sensory transducer homologous to the mammalian peripheral-type benzodiazepine receptor regulates photosynthetic membrane complex formation in Rhodobacter sphaeroides 2.4.1. *J Biol Chem*. 270:21167-21175.

Yeliseev, A.A., K.E. Krueger, and S. Kaplan. 1997. A mammalian mitochondrial drug receptor functions as a bacterial "oxygen" sensor. *Proc Natl Acad Sci U S A*. 94:5101-5106.

Zeno, S., L. Veenman, Y. Katz, J. Bode, M. Gavish, and M. Zaaroor. 2012. The 18 kDa mitochondrial translocator protein (TSPO) prevents accumulation of protoporphyrin IX. Involvement of reactive oxygen species (ROS). *Curr Mol Med*. 12:494-501.

Zhao, A.H., L.N. Tu, C. Mukai, M.P. Sirivelu, V.V. Pillai, K. Morohaku, R. Cohen, and V. Selvaraj. 2016. Mitochondrial Translocator Protein (TSPO) Function Is Not Essential for Heme Biosynthesis. *J Biol Chem*. 291:1591-1603.

Zulian, A., J. Sileikyte, V. Petronilli, S. Bova, F. Dabbeni-Sala, G. Cargnelli, D. Rennison, M.A. Brimble, B. Hopkins, P. Bernardi, and F. Ricchelli. 2011. The translocator protein (peripheral benzodiazepine receptor) mediates rat-selective activation of the mitochondrial permeability transition by norbormide. *Biochim Biophys Acta*. 1807:1600-1605.

CHAPTER 2

Peripheral Benzodiazepine Receptor/Translocator Protein Global Knockout Mice Are Viable with No Effects on Steroid Hormone Biosynthesis

Tu, L. N., Morohaku, K., Manna, P. R., Pelton, S. H., Butler, W. R., Stocco, D. M., & Selvaraj, V. (2014). Peripheral benzodiazepine receptor/translocator protein global knock-out mice are viable with no effects on steroid hormone biosynthesis. *J Biol Chem, 289*(40), 27444-27454

ABSTRACT

Translocator protein (TSPO), previously known as the peripheral benzodiazepine receptor (PBR) is a mitochondrial outer membrane protein implicated as essential for cholesterol import to the inner mitochondrial membrane, the rate-limiting step in steroid hormone biosynthesis. Previous research on TSPO was based entirely on *in vitro* experiments and its critical role was reinforced by an early report that claimed TSPO knockout mice were embryonic lethal. In a previous publication, we examined Leydig cell specific TSPO conditional knockout mice that suggested TSPO was not required for testosterone production *in vivo*. This raised controversy and several questions regarding TSPO function. To examine the definitive role of TSPO in steroidogenesis and embryo development, we generated global TSPO null (*Tspo*$^{-/-}$) mice. Contrary to the early report, *Tspo*$^{-/-}$ mice survived with no apparent phenotypic abnormalities and were fertile. Examination of adrenal and gonadal steroidogenesis showed no defects in *Tspo*$^{-/-}$ mice. Adrenal transcriptome comparison of gene expression profiles showed that genes involved in steroid hormone biosynthesis (*Star, Cyp11a1, and Hsd3b1*), were unchanged in *Tspo*$^{-/-}$ mice. Adrenocortical ultrastructure illustrated no morphological alterations in *Tspo*$^{-/-}$ mice. In an attempt to correlate our *in vivo* findings to previously used *in vitro* models, we also determined that siRNA-knockdown or absence of TSPO in different mouse and human steroidogenic cell lines had no effect on steroidogenesis. These findings directly refute the dogma that TSPO is indispensable for steroid hormone biosynthesis and viability. By amending the current model, this study advances our understanding of steroidogenesis with broad implications in biology and medicine.

INTRODUCTION

The peripheral benzodiazepine receptor (PBR) was first identified as a protein with distinct pharmacology and high binding affinity to benzodiazepines in 'peripheral' sites, as opposed to 'central' sites found in brain tissue (Braestrup et al., 1977; Braestrup and Squires, 1977; Davies and Huston, 1981; Regan et al., 1981). The 'central' benzodiazepine receptor is the γ-aminobutyric acid type A ($GABA_A$) receptor that has specific function in inhibitory neurotransmission (Macdonald and Barker, 1978; Takahashi et al., 1958). However, the function for the PBR has remained a topic of debate for decades (Gatliff and Campanella, 2012; Gavish et al., 1999), despite its prominence as a therapeutic target in a variety of diseases/disorders (Daugherty et al., 2013; Qi et al., 2012; Rupprecht et al., 2010; Vlodavsky et al., 2013).

Genetic sequence comparisons show that the PBR gene is highly conserved from archea to metazoans (Yeliseev and Kaplan, 1995). In mammals, highly prominent PBR protein expression has been identified in steroidogenic tissues (Anholt et al., 1985b; Manku et al., 2012; Morohaku et al., 2013). Binding sites for PBR ligands have also been identified in other tissues including: heart, brain, adrenal, kidney, salivary gland, platelets, brown adipose tissue, skin and liver (Gavish et al., 1999). In sub-cellular fractions, binding sites for the PBR were identified to be present in the outer mitochondrial membrane (OMM) (Anholt et al., 1985b; Anholt et al., 1986).

The transport of cholesterol from intracellular stores and the OMM to the inner mitochondrial membrane (IMM) forms the first and rate-limiting step in steroid hormone biosynthesis (Simpson and Boyd, 1967; Simpson et al., 1978). Cholesterol is then converted to the first steroid, pregnenolone, by CYP11A1 (cytochrome P450 side chain cleavage), an enzyme located on the matrix side of the IMM (Churchill and Kimura, 1979; Yago and Ichii, 1969). The initial link between PBR and steroid hormone biosynthesis emerged by studying the effect of a PBR-binding chemical PK11195 that triggered steroidogenesis in the Y1 mouse adrenal tumor cell line (Mukhin et al., 1989). In agreement, targeted

disruption of PBR in the R2C rat Leydig tumor cell line inhibited steroidogenesis (Papadopoulos et al., 1997b).

The structure of murine PBR showed a five alpha helix fold, each forming a transmembrane segment (Murail et al., 2008), and the possibility of a channel-like structure with an interior surface for potential substrate translocation (Korkhov et al., 2010). Cholesterol binding to PBR was defined by the identification of a cholesterol recognition amino acid consensus (CRAC) sequence at the C terminal region (Li and Papadopoulos, 1998). These structural features combined with functional considerations led to the modeling of PBR as a membrane-associated cholesterol transport protein (Lacapere et al., 2001; Rupprecht et al., 2010). Based on these findings, to more accurately represent its subcellular role, PBR was renamed as translocator protein (TSPO) (Papadopoulos et al., 2006).

Independent of studies on PBR/TSPO, another mitochondrial protein that is expressed in rapid response to steroidogenic stimuli, the steroidogenic acute regulatory protein (StAR), was identified in the MA-10 Leydig tumor cell line (Clark et al., 1994). Induced expression of StAR resulted in increased steroid hormone production even in the absence of hormonal stimulation (Clark et al., 1994). Anchoring StAR in a mitochondria-affixed StAR-Tom20 fusion protein in MA-10 cells resulted in the constitutive production of steroid hormone (Bose et al., 2002). In humans, StAR mutations cause lipoid congenital adrenal hyperplasia that ranges from an almost complete inability to synthesize steroids (Lin et al., 1995), to less severe forms that retain partial StAR protein activity (Baker et al., 2006). Also in support, StAR gene-deleted mice showed an almost complete inability to synthesize steroid hormones underscoring its critical role in steroidogenesis (Caron et al., 1997).

Two key experiments appeared to cement a functional link between StAR and PBR/TSPO. First, inhibition of protein synthesis that blocks StAR production and steroidogenesis (Privalle et al., 1983), did not affect the ability of PK11195 to trigger steroidogenesis (Krueger and Papadopoulos, 1990). Second, knockdown of PBR/TSPO in mitochondria-affixed StAR-Tom20 fusion protein expressing MA-10 cells

resulted in a reduction in their steroidogenic capacity (Hauet et al., 2005). Thus, the PBR function was linked to transport of cholesterol from the OMM to the IMM (Papadopoulos et al., 1990).

In a recent study, we questioned this model showing that PBR/TSPO expression is not required for *in vivo* testicular steroidogenesis (Morohaku et al., 2014). This result has indeed raised a lot of questions and controversy regarding current understanding of the precise PBR/TSPO-mediated functions in steroid hormone production (Papadopoulos, 2014). Moving forward, there remained an absolute need to examine specific deficits in TSPO global knockout mice to gain additional functional understanding of this protein (Stocco, 2014).

In a review article published in 1997, it was claimed that efforts to generate a PBR/TSPO gene-deleted model failed as a result of early embryonic mortality in PBR/TSPO deficient mice (Papadopoulos et al., 1997a). This led to the conclusion that in addition to steroidogenesis, TSPO is involved in basic functions that are critically necessary for embryonic development. However, this review article failed to explain experimental methods covering the recombination strategy used and the exact stage of embryonic mortality; these specific methods/results were never published. Given the current gap in understanding PBR/TSPO function *in vivo*, we decided to revisit this global knockout question.

With a primary objective of studying the role of PBR/TSPO in steroidogenesis and other vital functions (if any) that may be critical for embryonic development, we used a germ cell specific knockout approach to generate PBR/TSPO global gene-deleted mice. Our results are unexpected and contrary to the prevailing view in that we find PBR/TSPO knockout mice are viable and fertile with no effects on steroid hormone biosynthesis.

MATERIALS AND METHODS

Generation of *Tspo*$^{-/-}$ mice

Mice with floxed alleles for PBR/TSPO with loxP sites flanking exons 2 and 3 (*Tspo*$^{fl/fl}$) were generated and validated as previously described (Morohaku et al., 2014). In this study, *Tspo*$^{fl/fl}$ female mice were crossed with Ddx4-*cre*+ [FVB-Tg$^{(Ddx4\text{-}cre)1Dcas/J}$, (Gallardo et al., 2007)] males to generate a germ cell-specific deletion of *Tspo* (*TspocΔ/*+) in both male and female mice. *TspocΔ/*+ Ddx4*cre*+ positive offspring were then backcrossed to generate *TspocΔ/Δ* mice of both sexes. These sperm and oocyte-specific knockouts were bred to generate global PBR/TSPO null (*Tspo*$^{-/-}$) offspring in the C57BL/6 background. We also observed that oocyte-specific *TspocΔ/*+ Ddx4-*cre*+ mice induced global recombination directly as previously described for the Ddx4-*cre*+ strain of mice (Gallardo et al., 2007). Cre was subsequently bred out from *Tspo*$^{-/-}$ mice (Figure 1). Breeding colonies for *Tspo*$^{-/-}$ and *Tspo*$^{fl/fl}$ mice were maintained separately and offspring were genotyped for all experiments (Figure 1) using primers that have been previously validated (Morohaku et al., 2014). ROSA26-tdTomato (R26-tdTom) reporter females [B6.Cg-Gt(ROSA)26Sor$^{tm14(CAG\text{-}tdTomato)Hze}$, (Madisen et al., 2010)] were used to confirm recombination, and bred to generate *Tspo*$^{fl/fl}$-R26-tdTom homozygous mice to directly mark *Tspo* deletion. Animals were maintained in accordance with the National Institute of Health Guide for the Care and Use of Laboratory Animals. The Institutional Animal Care and Use Committee of Cornell University approved all experiments in this manuscript.

Phenotypic analysis

Growth rate of *Tspo*$^{fl/fl}$ and *Tspo*$^{-/-}$ mice were examined from postnatal day 0 to week 5. Litter sizes from homozygous crosses in *Tspo*$^{fl/fl}$ and *Tspo*$^{-/-}$ mouse colonies were examined in at least 8 unique pairings. Recombination was examined in different tissues by both PCR of genomic DNA using specific primers as previously validated (Morohaku et al., 2014), and td-Tomato reporter expression indicating cre-mediated recombination as previously described (Morohaku et al., 2014).

Histology

Tissues were processed for hematoxylin and eosin staining as described (Morohaku et al., 2014). Immunohistochemistry for PBR/TSPO was performed using a rabbit monoclonal anti-TSPO antibody (Abcam) that specifically recognizes amino acids 156-169 at the C-terminal of Exon 4 as described (Morohaku et al., 2014; Morohaku et al., 2013). For examining neutral lipid deposits, 9 μm frozen sections were prepared and Lipid staining was performed using Oil Red O (Matheson Coleman & Bell) in 60% Isopropanol for 30 minutes. Fluorescent tdTomato was also visualized in 9 μm frozen sections in multiple tissues. Images were acquired using either a DFC365FX or an ICC50HD camera (Leica) or a Meta 510 confocal scope (Zeiss). Density of Oil Red O staining density was quantified using ImageJ (Schneider et al., 2012).

Immunoblots

Proteins were separated by SDS-PAGE and immunoblotted using rabbit monoclonal primary antibodies against TSPO (Abcam) and isocitrate dehydrogenase 2 (IDH2) (Abcam), and a rabbit polyclonal StAR antibody (Bose et al., 1999). Each primary antibody was multiplexed with the loading control β-actin (Li-Cor). Simultaneous detection was performed using IRDye 700 and 800 under a laser fluorescence scanner (Li-Cor) and quantified as described previously (Morohaku et al., 2014). For immunoblots performed in knockdown experiments, a TSPO polyclonal (Cell Signaling) and β-actin (Life Technologies) primary antibodies were used. Specific band intensities in knockdown experiments were calculated by image analysis using Quantity One Software (Bio-Rad).

Hormone assays

Plasma was collected from 8-10 week old *Tspo*$^{fl/fl}$ and *Tspo*$^{-/-}$ mice. Levels of different steroid hormones were measured using radioimmunoassay: corticosterone, aldosterone and testosterone (Siemens), estradiol and progesterone (Serono Maia), as previously described (Beam and Butler, 1997; Morohaku et al., 2014). For adrenal/corticosterone stimulation test, 500 ng/g body weight (BW) of

adrenocorticotropin (ACTH) fragment 1-24 (Sigma) was administered subcutaneously and plasma was collected after 1 hr. For testis/testosterone stimulation test, 10 IU of human chorionic gonadotropin (hCG; EMD biosciences) was administered intraperitoneal to male mice and plasma was collected after 1 hr.

Transmission electron microscopy

Adrenal glands were fixed in Karnovsky's fixative (2.5% glutaraldehyde, 2% paraformaldehyde in 0.08 M phosphate buffer) overnight. After fixation, tissues were processed for transmission electron microscopy as previously described (Daugherty et al., 2013). Stained sections were examined in a Tecnai™ T12 Spirit electron microscope (FEI), at 120 kV. High magnification images were acquired using a high-resolution CCD camera Megaview III (Olympus Soft Imaging System) to examine cellular and mitochondrial morphology within regions in the adrenal cortex.

RT-PCR and quantitative PCR

Total RNA was extracted from adrenal glands of 8-10 week old *Tspo*$^{fl/fl}$ and *Tspo*$^{-/-}$ mice using RNeasy Lipid Tissue Mini Kit (Qiagen). For human A172 and H295R cells, total RNA was extracted using Trizol (Life Technologies). Reverse transcription was carried out using Multiscribe™ reverse transcriptase (Life Technologies). Validated Taqman gene expression assays were used for quantitative PCR estimation of murine *Tspo* (Mm00437828_m1), human *Tspo* (Hs00559362_m1), *Tspo2* (Mm01281420_m1), *Star* (Mm00441556), *Cyp11a1* (Mm00490735_m1), and *Hsd3b1* (Mm00476184_g1). For all other genes, expressions were quantified by SYBR® Green detection method using validated primer sequences obtained from PrimerBank database (Spandidos et al., 2010). *Vdac1*: 5' AAGTGAACAACTCCAGCC TGA 3' and 5' CACCAGCATTGACGTTCTTG 3', *Vdac2*: 5' CTCCACCCTATGCTGACCTC 3' and 5' CCCGCTAACTTTACCAGTGTCT 3', *Vdac3*: 5' CAAAGGGTATGGGTTTGGCAT 3' and 5' TTGGTCTCTAGGTTGCCTGAT 3', *Ant1*: 5' CTGGTGTCCTACCCCTTTGA 3' and 5' TGGCTCCTTCGTCTTTTGCA 3', *Ant2*: 5' CAAGACAGCGGTAGCACCC 3' and 5' CGC AGTCTATGATGCCCTTGTA 3', *Hxk2*: 5' GG GCATGAAGGGCGTGTCCC 3' and 5' TCTTC ACCCTCGCAGCCGGA 3', *Acbp*: 5' TTTCGG

CATCCGTATCACCT 3' and 5' TTTGTCAAAT TCAGCCTGAGACA 3', *Pap7*: 5' GAGGAGC TTTACGGCCTGG 3' and 5' CTTATGCAG TGCCACGAACTT 3'. All expressions were normalized to an internal control gene, *Gapdh*. Relative quantification of fold-change was performed using the $2^{-\Delta\Delta Ct}$ method (Livak and Schmittgen, 2001).

Adrenal transcriptome shotgun sequencing

Adrenal gland total RNA from *Tspo*$^{fl/fl}$ and *Tspo*$^{-/-}$ mice were extracted and polyA RNA were isolated using oligo(dT)25 Dynabeads (Life Technologies). Fragmentation and strand-specific RNA-seq library preparation was performed as described (Zhong et al., 2011). Each sample with unique bar codes was pooled to one lane for obtaining short single-reads in a HiSeq 2000 sequencer (Illumina). RNA-seq reads were first aligned to the ribosomal RNA gene database (Quast et al., 2013) using Bowtie (Langmead et al., 2009) and the mapped reads were discarded. The resulting filtered reads were aligned to the mouse genome (Ensembl) using TopHat (Trapnell et al., 2009). Subsequent to alignments, raw counts for each mouse gene were derived and normalized to reads per kilobase of exon model per million mapped reads (RPKM). Differentially expressed genes were identified using the DESeq package (Anders and Huber, 2010). Raw p-values of multiple tests were corrected using false discovery rate (FDR) (Benjamini and Hochberg, 1995).

TSPO knockdown in different steroidogenic cell lines

Specific small interfering RNAs (siRNAs) were used to knockdown endogenous TSPO expression in different steroidogenic cell lines as previously described for other genes (Manna et al., 2013). *Tspo* siRNAs and the Silencer® negative control (scrambled) were obtained as annealed oligos (Life Technologies). Sense strand sequences for *Tspo* siRNAs utilized were: (1) 5'-GGAAA GAGCUGGGAGGUUUtt-3', (2) 5'-GCUCCUAC AUAGUCUGGAAtt-3', and (3) 5'-UGGGCCUG CUAGUCUGUCAtt-3'. Cell lines: MA-10, Y-1, H295R, R2C and MLTC cells (from ATCC) were transfected with 100 nM of *Tspo* siRNA #1, #2, #3 or control using Lipofectamine 2000 (Life Technologies). Forty-eight hours after transfection, cells were examined for TSPO protein expression and

used to estimate steroidogenic potential with 0.5 mM dibutryl cyclic AMP [$(Bu)_2$cAMP] as previously described (Manna et al., 2013).

RESULTS

Tspo$^{-/-}$ mice are viable and fertile

The *Tspo*$^{fl/fl}$ locus allows *cre*-mediated deletion of exon 2 and 3 of the *Tspo* gene (Figure 2.1A). Exon 1 does not contain any start codons. Removal of exon 2 and 3 eliminates the start codon and exon 4 does not have any in-frame start codons. Therefore, deletion of exon 2 and 3 will completely eliminate TSPO protein expression (Morohaku et al., 2014). Germ cell-specific Ddx4-cre mice were used to induce germ cell *Tspo* deletion in F1 and global recombination in F2 generations. Litters from all crosses were genotyped and the Ddx4-cre transgene was subsequently bred out from this colony (Figure 2.1B). Using a *Tspo*$^{fl/fl}$-R26-tdTom reporter line, we confirmed that *cre*-mediated recombination occurred in all tissues globally (Figure 2.2 A and C). Recombination at the *Tspo*$^{-/-}$genomic locus was also confirmed by PCR in different tissues (Figure 2.1C). The complete absence of TSPO protein expression in different tissues in *Tspo*$^{-/-}$ mice was confirmed by both Western blots (Figure 2.2B) and immunohistochemistry (not shown), using a monoclonal antibody that recognizes protein coded by Exon 4. This proved that no partial TSPO peptide was produced in mice deleted for TSPO Exons 2 and 3 as previously shown (Morohaku et al., 2014). All *Tspo*$^{-/-}$ mice were viable and showed no apparent phenotypic abnormalities. Litter sizes from *Tspo*$^{-/-}$ pair mating were not different from *Tspo*$^{fl/fl}$ pair litters (Table 2.1). Growth rate in *Tspo*$^{-/-}$ mice measured up to 5 weeks of age were quite similar to *Tspo*$^{fl/fl}$ cohorts. However, when analyzed based on sex, *Tspo*$^{-/-}$ female mice showed a very modest (~1g) but significantly higher body weight than *Tspo*$^{fl/fl}$ mice at 1-5 weeks of age; males body weights at this same age interval were not different between the two genotypes (not shown).

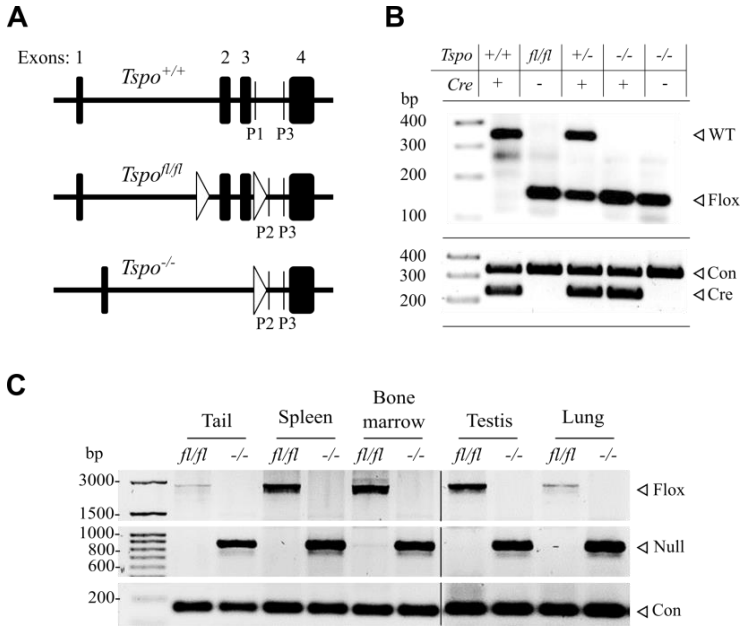

Figure 2.1. Generation of TSPO knockout mice. (A) Schematic showing genomic TSPO locus in wildtype (TSPO$^{+/+}$), intact floxed (*Tspo*$^{fl/fl}$) and knockout (*Tspo*$^{-/-}$) mice. *Tspo*$^{fl/fl}$ mice contained exons 2 and 3 flanked with LoxP sites (open arrow heads). *Tspo*$^{fl/fl}$ female mice were bred with Ddx4-cre male mice to generate germ cell-specific deletion of TSPO as heterozygotes. These sperm and oocyte-specific knockout mice were bred to generate *Tspo*$^{-/-}$ offspring. Ddx4-cre transgene was subsequently bred out from this colony. (B) Panel showing genotyping for floxed alleles and cre transgene in Ddx4-cre mice, *Tspo*$^{fl/fl}$ mice, TSPO$^{+/-}$ Ddx4-cre mice, *Tspo*$^{-/-}$ Ddx4-cre mice, and *Tspo*$^{-/-}$ mice. (C) Genomic DNA PCR for recombination at the TSPO locus detects deletion of Exon 2 and 3 in *Tspo*$^{-/-}$ mice [Product sizes: Flox-2697 bp, Null-872 bp, Con-161 bp].

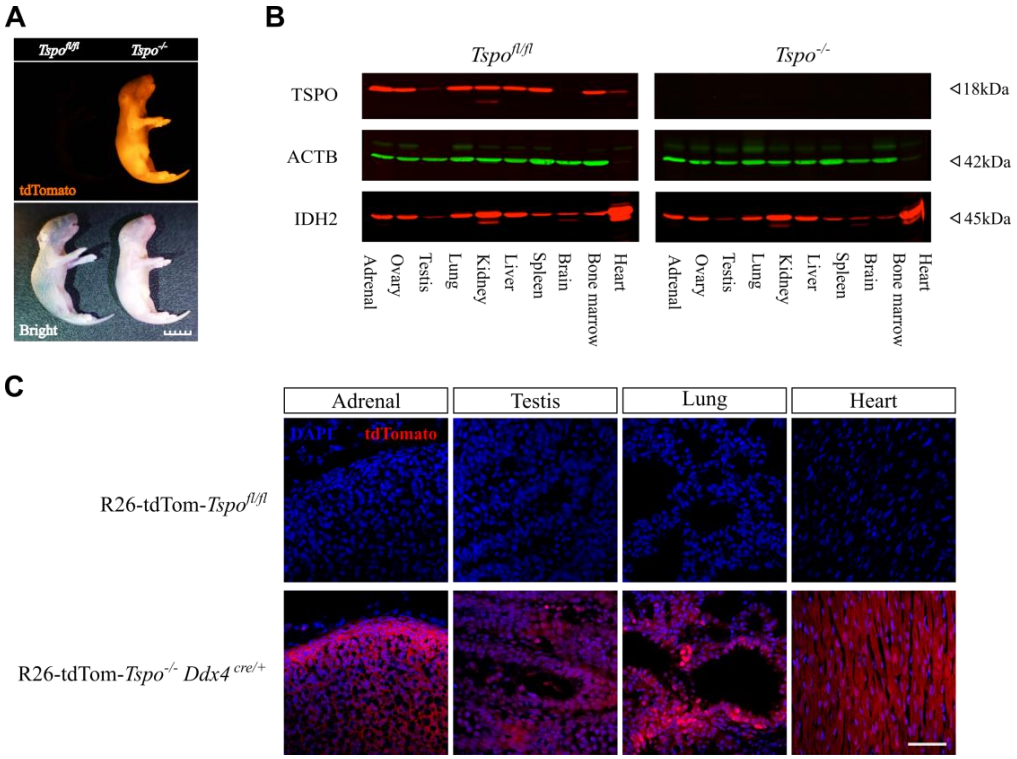

Figure 2.2. Validation of *Tspo*$^{-/-}$ genotype. (A) *Tspo*$^{fl/fl}$-ROSA26-tdTomato reporter mice were used to examine cre-mediated recombination induced in offspring from germ-cell specific deletions. Global recombination was clear in R26-tdTom-*Tspo*$^{-/-}$ P3 pups. (B) TSPO monoclonal antibody specific for peptide corresponding to TSPO exon 4 detected a protein of expected size (18 kDa) in *Tspo*$^{fl/fl}$ tissues but not in *Tspo*$^{-/-}$ tissues. Actin and mitochondrial IDH2 were used as controls. Scale bar: 1 cm. (C) Representative images of different tissues from an R26-tdTom-*Tspo*$^{fl/fl}$ mouse with no tdTomato fluorescence in contrast to tissues from an R26-tdTom-*Tspo*$^{-/-}$ mouse showing tdTomato fluorescence (red) indicating recombination. Nuclei were counterstained with DAPI (blue). Scale bar: 50 µm.

Table 2.1. Litter sizes from *Tspo*$^{fl/fl}$ and *Tspo*$^{-/-}$ male and female mice

Mating pairs	n	Litter size* ± SE
Tspo$^{fl/fl}$ female x *Tspo*$^{fl/fl}$ male	17	8.11 ± 0.44
Tspo$^{-/-}$ female x *Tspo*$^{-/-}$ male	8	8.00 ± 0.53

* No significant differences in litter size were detected between the two crosses. Sex ratios in these litters were also not different.

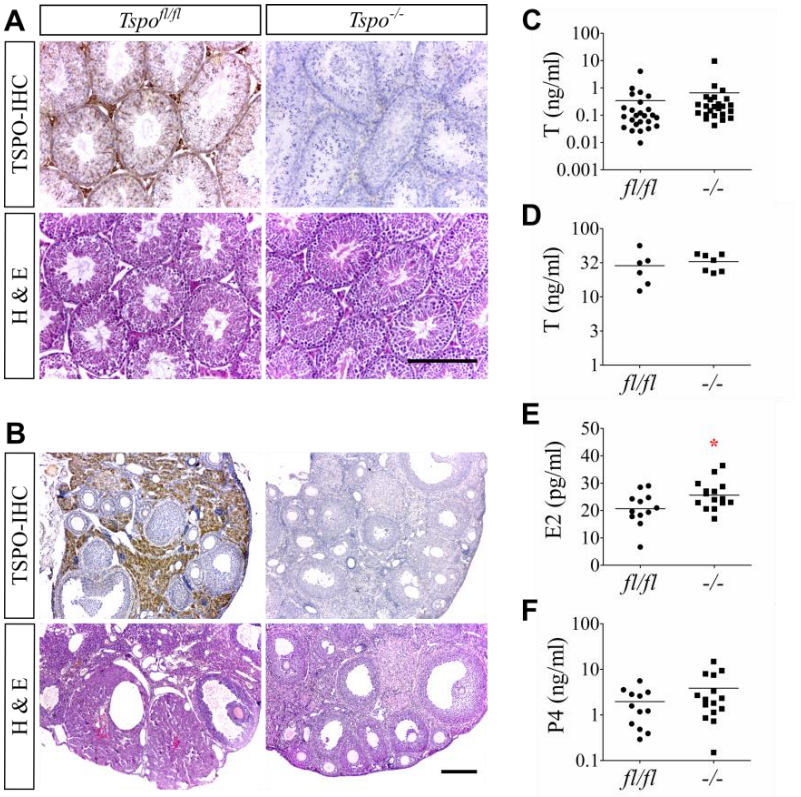

Figure 2.3. TSPO deletion does not affect gonadal steroidogenesis. (A) Testes sections showing TSPO localization in Leydig and Sertoli cells in *Tspo*$^{fl/fl}$ but not in *Tspo*$^{-/-}$ testis. Functional morphology of seminiferous tubules was not affected in *Tspo*$^{-/-}$ testis. (B) Ovary sections showing TSPO localization in interstitial cells and surface epithelium, weak in theca and granulosa cells in *Tspo*$^{fl/fl}$ ovary; no staining was observed in *Tspo*$^{-/-}$ ovary. Functional morphology was not affected in *Tspo*$^{-/-}$ ovary. (C) Baseline plasma testosterone levels were not different between *Tspo*$^{fl/fl}$ and *Tspo*$^{-/-}$ male mice (n=24-25/group). (D) Increase in plasma testosterone levels after hCG stimulation was similar between *Tspo*$^{fl/fl}$ and *Tspo*$^{-/-}$ male mice (n=6-7/group). (E) Baseline plasma estradiol levels were significantly higher in *Tspo*$^{-/-}$ compared to *Tspo*$^{fl/fl}$ mice ($p<0.05$), but the difference was modest (n=12-15/group). (F) Baseline plasma progesterone levels were not different between *Tspo*$^{fl/fl}$ and *Tspo*$^{-/-}$ mice (n=12-15/group). Scale bar: 200 µm.

Gonadal steroid hormone production is not affected in *Tspo*$^{-/-}$ mice

The lack of TSPO did not affect the functional morphology of the testis (Figure 2.3A) or the ovary (Figure 2.3B) in *Tspo*$^{-/-}$ mice compared to *Tspo*$^{fl/fl}$ controls. In male mice, examination of plasma testosterone concentration showed that baseline levels were not different between *Tspo*$^{-/-}$ and *Tspo*$^{fl/fl}$ mice (Figure 2.3C). Increase in plasma testosterone in response to hCG *in vivo* was not different between *Tspo*$^{-/-}$ and *Tspo*$^{fl/fl}$ mice (Figure 2.3D). Cauda epididymal sperm counts were not different between *Tspo*$^{-/-}$ and

Tspo$^{fl/fl}$ mice (not shown). In female mice, examination of plasma estradiol and progesterone concentration showed that TSPO deletion did not decrease baseline values (Figure 2.3E-F). In actuality, *Tspo*$^{-/-}$ mice showed modest but significantly higher estradiol levels compared to *Tspo*$^{fl/fl}$ cohorts. We did not observe any abnormalities in gonad size, reproductive behavior and fecundity in *Tspo*$^{-/-}$ mice (not shown).

Adrenal steroid hormone production is not affected in *Tspo*$^{-/-}$ mice

The lack of TSPO expression did not affect the functional morphology of the adrenal cortex (Figure 2.4A) in *Tspo*$^{-/-}$ mice. Quantitation of neutral lipid staining in the adrenal cortex did not indicate any major steroid transport defects in *Tspo*$^{-/-}$ mice (Figure 2.4 B-C). Baseline levels of aldosterone (Figure 2.5A), and corticosterone (Figure 2.5B), two major hormones produced by the adrenal cortex were not different between *Tspo*$^{-/-}$ and *Tspo*$^{fl/fl}$ mice. Increase in plasma corticosterone in response to ACTH *in vivo* was not different between *Tspo*$^{-/-}$ and *Tspo*$^{fl/fl}$ mice (Figure 2.5C). There was also no evidence for compensatory increase in StAR expression in adrenals of *Tspo*$^{-/-}$ mice compared to *Tspo*$^{fl/fl}$ mice after ACTH treatment (Figure 2.5 D-F).

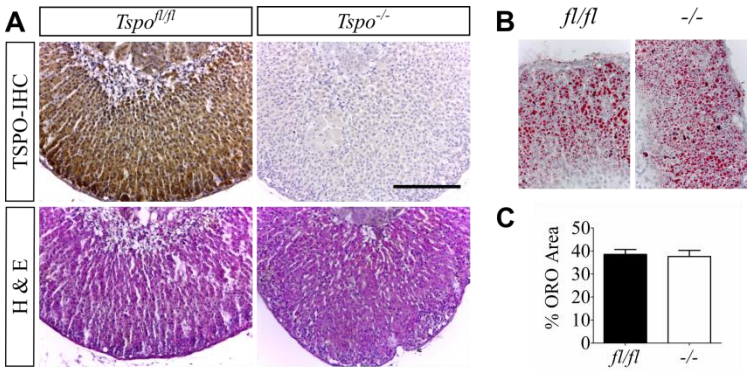

Figure 2.4. TSPO deletion has no effect on morphology and lipid deposits in the adrenal cortex. (A) Adrenal sections from *Tspo*$^{fl/fl}$ and *Tspo*$^{-/-}$ mice showing TSPO localization in adrenocortical cells with a higher density in the zona glomerulosa; no staining was observed in *Tspo*$^{-/-}$ adrenal. No difference in adrenocortical morphology was apparent between two genotypes. (B) Oil Red O staining of adrenal glands showed no difference in neutral lipid deposits between *Tspo*$^{fl/fl}$ and *Tspo*$^{-/-}$ adrenal glands. (C) Quantification of Oil Red O (ORO) labeling density was similar in both *Tspo*$^{fl/fl}$ and *Tspo*$^{-/-}$ adrenal cortex (n=5/group; mean ± SEM). Scale bar: 200 µm.

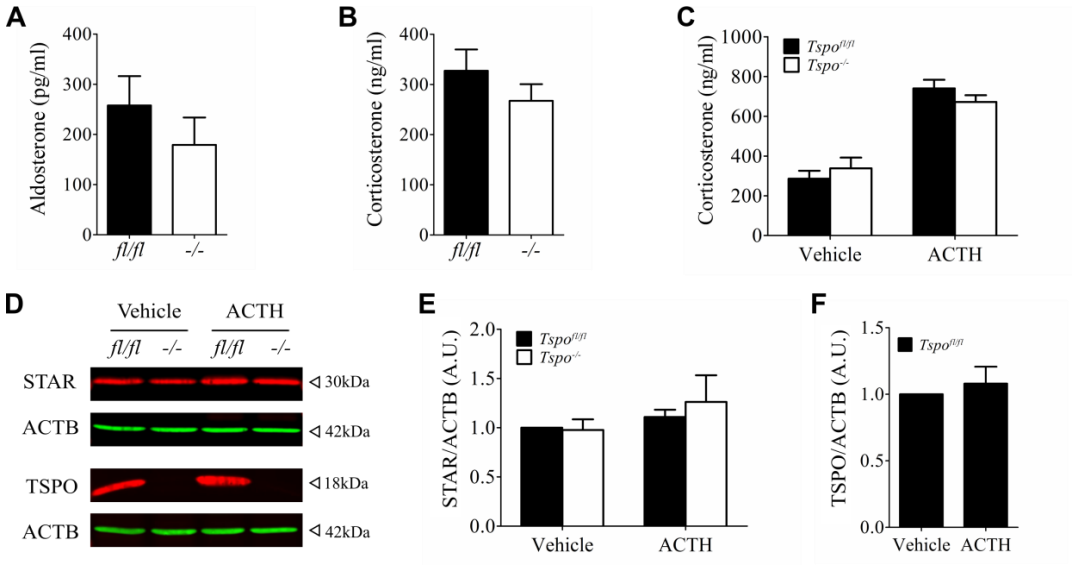

Figure 2.5. TSPO deletion has no effect on adrenal steroid hormone production. (A) Plasma aldosterone baseline levels were not significantly different between *Tspo*$^{fl/fl}$ and *Tspo*$^{-/-}$ mice (n=7/group). (B) Plasma corticosterone baseline levels were not significantly different between *Tspo*$^{fl/fl}$ and *Tspo*$^{-/-}$ mice (n=24-30/group). (C) Increase in plasma corticosterone in response to ACTH stimulation was similar between *Tspo*$^{fl/fl}$ and *Tspo*$^{-/-}$ mice (n=10-14/group). (D) Representative Western blot showing no compensatory increase in StAR and TSPO protein expression after ACTH stimulation in both *Tspo*$^{fl/fl}$ and *Tspo*$^{-/-}$ mice. Quantification of (E) StAR, and (F) TSPO protein levels also showed no significant increase at 1 hour after ACTH stimulation (n=3). (Data are represented as mean ± SEM).

Loss of TSPO does not affect steroidogenic gene expression in adrenal glands

Comparison of gene expression profiles by transcriptome shotgun sequencing of *Tspo*$^{-/-}$ and *Tspo*$^{fl/fl}$ adrenals revealed only a short list of differentially expressed genes (Table 2.2), none of which were directly associated with steroidogenesis. Mining reads representing *Tspo* mRNA confirmed deletion of exon 2 and exon 3. A majority of the differentially expressed genes were involved in immune activity. Validated expression of genes involved in the steroid hormone biosynthetic pathway: *Star*, *Cyp11a1* and *Hsd3b1* (Figure 2.6 A-C), and TSPO-interacting proteins: *Vdac*, *Ant*, *Hxk2*, *Pap-7* and *Acbp* were not affected in *Tspo*$^{-/-}$ adrenals (Figure 2.6 E-L). Complete dataset available through NCBI-SRA SRP043599. To evaluate possible functional redundancy, we also examined expression levels for *Tspo2*, a TSPO paralog (Fan et al., 2009). We did not detect *Tspo2* expression in both *Tspo*$^{fl/fl}$ and *Tspo*$^{-/-}$ adrenal glands (Figure 2.6D).

Table 2.2. Genes differentially expressed between *Tspo*$^{fl/fl}$ and *Tspo*$^{-/-}$ adrenal glands

Genes*	Gene Name/Description	*Tspo*$^{fl/fl}$ [mean]	*Tspo*$^{-/-}$ [mean]	Ratio	P value
BC018473	Unclassified non-coding RNA gene	0.01	1.86	186.33	1.77E-13
Trim12a	Tripartite motif-containing 12A	1.97	0.01	0.01	1.19E-12
Gm12196	Predicted gene 12196	0.26	40.59	156.12	5.94E-12
Pydc4	Pyrin domain containing 4	1.63	0.02	0.01	7.36E-10
Gm4955	Predicted gene 4955	3.25	0.07	0.02	9.45E-09
Gm16510	Predicted pseudogene 16510	1.19	23.5	19.81	5.15E-06
Gm5540	Predicted pseudogene 5540	0.71	19.88	28.14	0.0018
Prrc2a	Proline-rich coiled-coil 2A	1.16	20.69	17.78	0.0084
RP23-81C12.1	Known lincRNA	0.93	22.69	24.49	0.0084
Atxn2l	Ataxin 2-like	1.1	16.44	14.99	0.0147
Abhd1	Abhydrolase domain containing 1	1.34	10.53	7.84	0.0157
Ankrd52	Ankyrin repeat domain 52	0.35	5.62	15.91	0.0166
Nxpe2	Neurexophilin and PC-esterase domain family, member 2	0.8	0.12	0.15	0.0173
Tmem178	Transmembrane protein 178	16.36	3.04	0.19	0.0188
Epn1	Epsin 1	0.8	9.97	12.47	0.0320
Zbtb7b	Zinc finger and BTB domain containing 7B	0.38	5.51	14.64	0.0346
Osgin1	Oxidative stress induced growth inhibitor 1	2.46	19.15	7.79	0.0346
Cyp21a2-ps	Cytochrome P450, family 21, subfamily a, polypeptide 2 pseudogene	159.04	1352.39	8.5	0.0346
Abca2	ATP-binding cassette, sub-family A (ABC1), member 2	0.41	3.38	8.24	0.0414

*Presented in the order of significance based on P value.

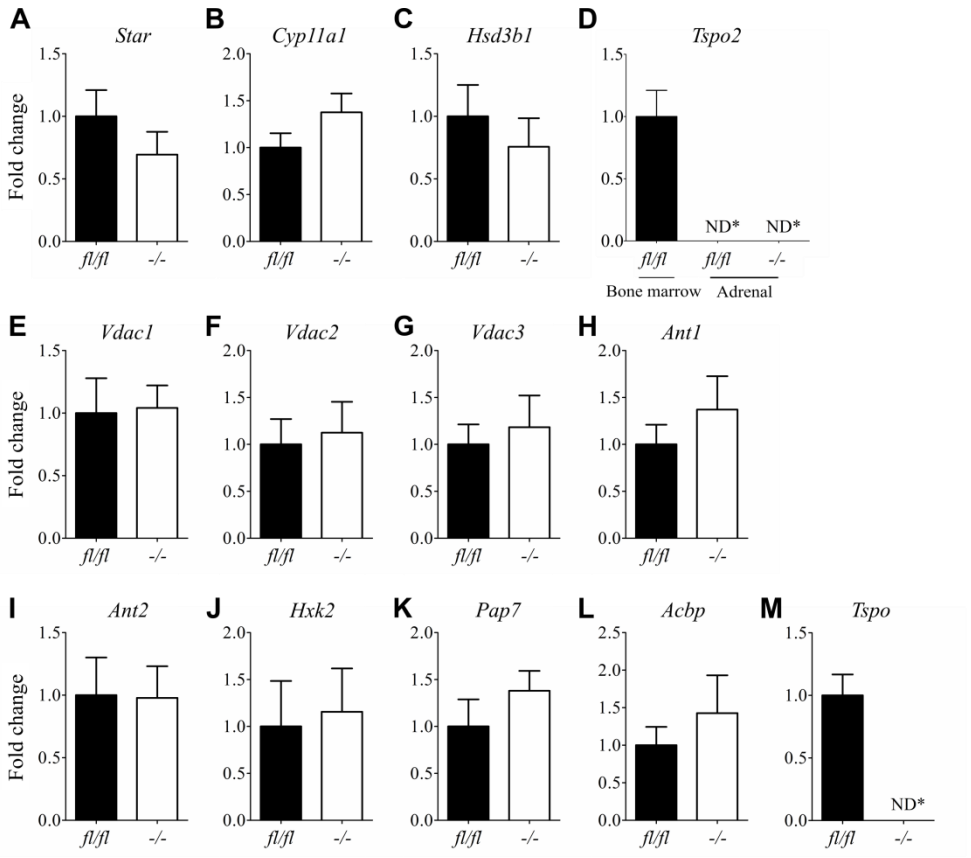

Figure 2.6. TSPO deletion does not alter expression levels of steroidogenic genes and TSPO-interacting proteins in the adrenal glands. Expression levels of steroidogenic genes StAR (A), CYP11A1 (B) and HSD3B1 (C) were similar between *Tspo*$^{fl/fl}$ and *Tspo*$^{-/-}$ mice. TSPO2 expression (D) was not detected in both *Tspo*$^{fl/fl}$ and *Tspo*$^{-/-}$ adrenal glands.. Genes encoding TSPO-interacting proteins VDAC1 (E), VDAC2 (F), VDAC3 (G), ANT1 (H), ANT2 (I), HXK2 (J), PAP7 (K), and ACBP (L) showed similar expression levels between *Tspo*$^{fl/fl}$ and *Tspo*$^{-/-}$ mice. TSPO expression (M) was not detected in *Tspo*$^{-/-}$ adrenal glands. (n=6/group; data are represented as mean ± SEM).

Ultrastructure of adrenal cortex remains the same in *Tspo*$^{-/-}$ mice

Examination of steroidogenic cells of the adrenal cortex using transmission electron microscopy did not show any aberrations in cellular ultrastructure in *Tspo*$^{-/-}$ mice (Figure 2.7). Despite its presence in the OMM, TSPO deficiency did not affect mitochondrial morphology. Lipid droplet distribution was also identical between regions within adrenal cortex (zona glomerulosa, zona fasciculata and zona reticularis) in both *Tspo*$^{fl/fl}$ and *Tspo*$^{-/-}$ mice. TSPO deficiency also did not affect mitochondrial volume in cells, as

assessed in *Tspo*$^{fl/fl}$ and *Tspo*$^{-/-}$ primary fibroblasts that showed no quantitative differences between the two genotypes (not shown).

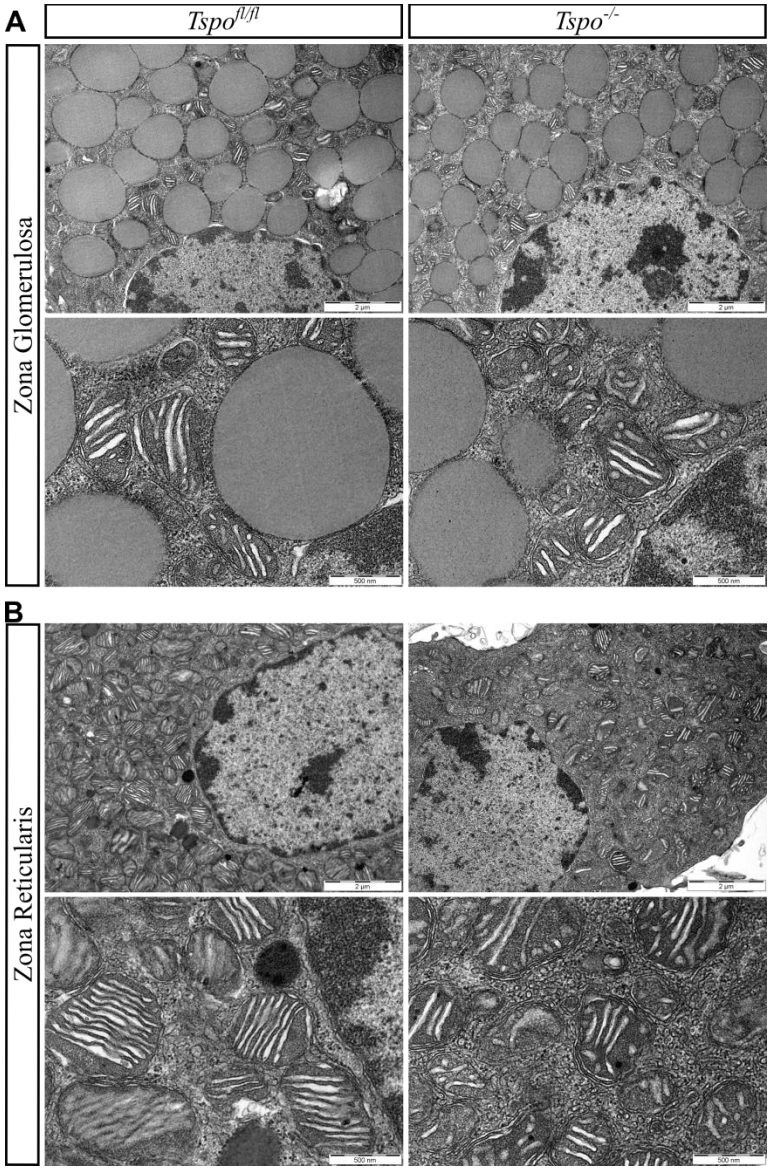

Figure 2.7. Ultrastructure of cells in the adrenal cortex is not affected by TSPO deletion. Transmission electron micrographs showing cell morphology in the zona glomerulosa (A) and zona reticularis (B) of the adrenal cortex. Subcellular organelle morphology including mitochondria and lipid droplets are identical between both *Tspo*$^{fl/fl}$ and *Tspo*$^{-/-}$ mice.

TSPO knockdown in steroidogenic cell lines does not affect steroidogenesis

Progesterone production after $(Bu)_2$cAMP treatment by the different murine (MA-10, Y1 and MLTC) and human (H295R) steroidogenic cell lines was not adversely affected by knockdown of TSPO expression (Figure 2.8 A-D). TSPO protein expression in murine cell lines decreased by approximately 85%, 75% and 82% respectively; surprisingly, baseline TSPO protein expression was not detectable in human H295R cells, [confirmed by extremely low levels of TSPO mRNA (Figure 2.8 F-G)]. This observation showed that H295R cells are capable of making steroid hormones without TSPO. In all conditions, TSPO knockdown did not have an effect on StAR expression. In the case of MA-10 cells, progesterone production showed a significant increase after $(Bu)_2$cAMP treatment in TSPO knockdown cells compared to scrambled controls. This is in direct contrast with another study using the same MA-10 cells that showed significantly decreased progesterone production after just 60% knockdown of TSPO protein expression (Hauet et al., 2005). However, such increases were not observed in Y1 and MLTC cells after TSPO knockdown under identical conditions. In R2C cells that abnormally display constitutively high levels of steroidogenesis, TSPO knockdown showed a modest but significant decrease in progesterone production in conditions with and without $(Bu)_2$cAMP treatment compared to scrambled controls (Figure 2.8E). Mono-allelic TSPO gene deletion in R2C cells was reported to abolish TSPO expression and inhibit steroidogenesis (Papadopoulos et al., 1997b). We find this hard to reconcile, as we do not find any evidence for allele-specific TSPO expression in our *in vivo* studies (Figure 2.9). Moreover, R2C cells are pathologically constitutive in steroid hormone production, the mechanism of regulation of which is not physiologically relevant. Data from TSPO knockdown experiments in 3 different murine cell lines together with the discovery that TSPO expression is below detection levels in H295R cells confirm that TSPO is not essential for steroidogenesis *in vitro*.

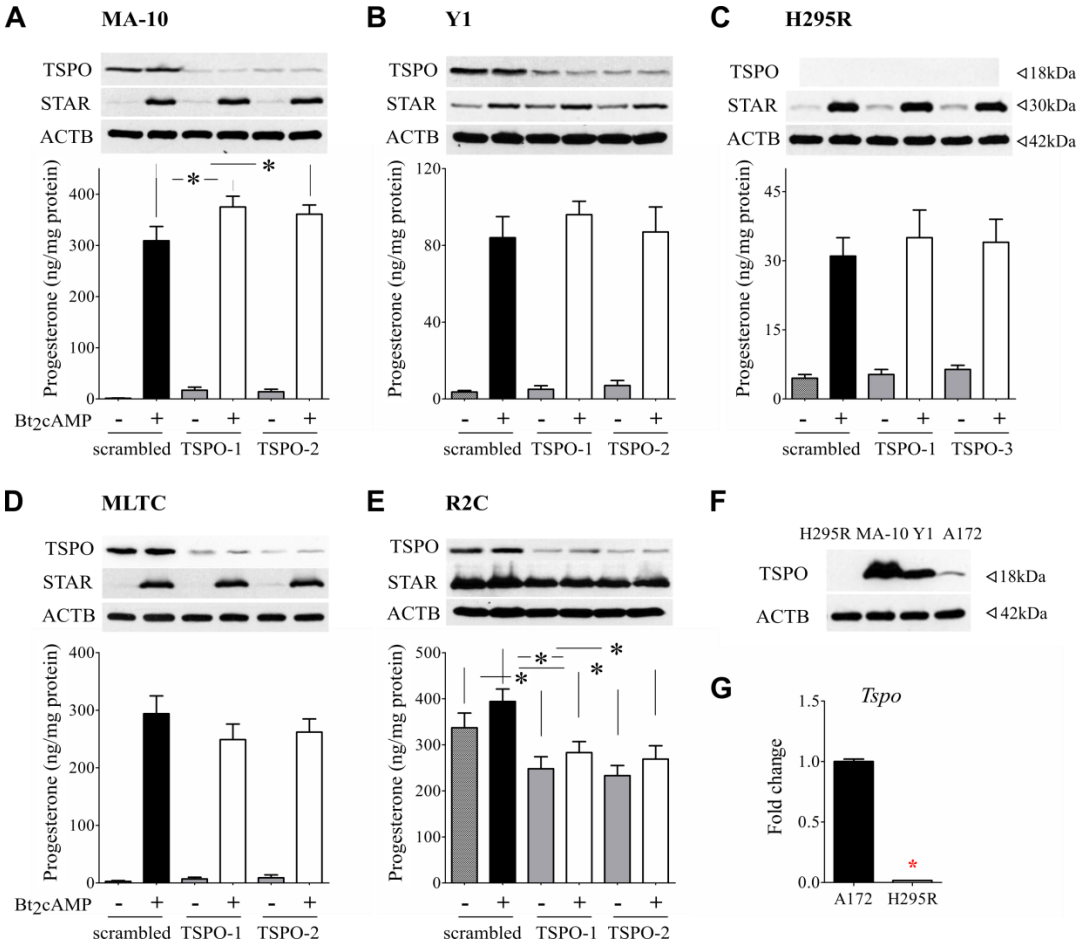

Figure 2.8. TSPO knockdown in steroidogenic cells does not affect steroid hormone biosynthesis. TSPO knockdown (#1 and #2) resulted in substantial decrease in TSPO protein compared to controls (scrambled) in MA-10 (A), Y1 (B), MLTC (D), and R2C cells (E). No baseline TSPO was detected in H295R cells (C). $(Bu)_2$cAMP treatment resulted in a similar increase in StAR protein expression in MA-10, Y1, MLTC and H295R cells and higher progesterone production. TSPO knockdown MA-10 cells showed significantly higher progesterone production ($p<0.05$) compared to scrambled controls. Progesterone production in TSPO knockdown Y1 and MLTC cells was similar to the scrambled controls. H295R cells did not show TSPO expression but still produced progesterone upon $(Bu)_2$cAMP treatment. Careful re-examination confirmed that H295R cells do not express both TSPO protein and mRNA (F and G). Abnormal R2C cells constitutively expressed high StAR protein levels and constantly produced high levels of progesterone. TSPO knockdown in R2C resulted in a modest but statistically significant decrease in progesterone production ($p<0.05$), both with and without $(Bu)_2$cAMP treatment.

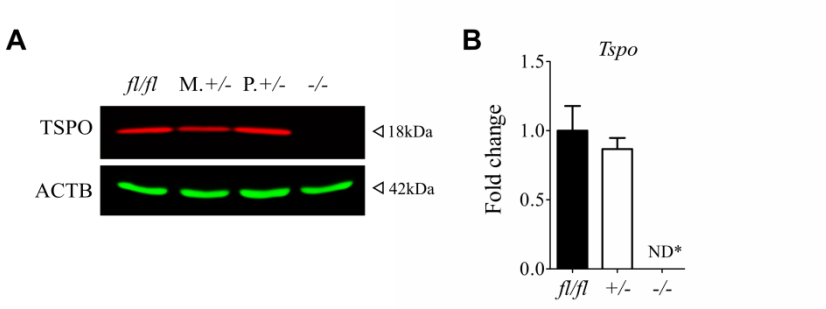

Figure 2.9. TSPO expression is not allele-specific. (A) TSPO monoclonal antibody detected similar expression levels in *Tspo*$^{fl/fl}$, maternal-transmitted heterozygous TSPO$^{+/-}$ and paternal-transmitted heterozygous TSPO$^{+/-}$; no TSPO was detected in *Tspo*$^{-/-}$ adrenal glands. (B) There was no significant difference in TSPO mRNA expression levels between *Tspo*$^{fl/fl}$ and maternal heterozygous TSPO$^{+/-}$adrenal glands; no TSPO mRNA was detected in *Tspo*$^{-/-}$ adrenals (n=4/group; ND*-not detected).

DISCUSSION

According to existing literature, TSPO function is absolutely essential for steroid hormone biosynthesis (Papadopoulos et al., 1997b), and global TSPO gene deletion results in early embryonic lethality in mice (Papadopoulos et al., 1997a). In direct contrast to those observations, our experimental findings disprove these functional arguments and definitively demonstrate that TSPO is not essential for steroidogenesis, and that *Tspo*$^{-/-}$ mice are viable and fertile. These concrete results form a key step towards rectifying the prevailing model of steroidogenesis and underscore that the precise role of TSPO in mammalian physiology is yet to be uncovered.

In a previous study, we demonstrated that conditional TSPO gene deletion in testicular Leydig cells did not affect testosterone production (Morohaku et al., 2014). At that time, the finding was met with skepticism that Amhr2 cre-mediated recombination may not have complete penetrance in Leydig cells, and criticism that it may not be the case for all steroid-synthesizing cells (Papadopoulos, 2014). But from observations in this present study in which TSPO has been deleted globally, it is clear that TSPO is not involved in physiologically relevant steroid hormone biosynthesis. This calls into question the previously suggested functional cooperation between StAR and TSPO for mitochondrial cholesterol import (Rone et al., 2009).

It could be argued that *Tspo*$^{-/-}$ mice respond to the loss of TSPO with some unknown compensatory mechanism. If this is the case, it is surprising that redundant mechanisms were not evident in earlier studies that claimed an indispensable role for TSPO in the steroidogenic machinery (Papadopoulos et al., 1997b). TSPO2, a paralog of TSPO (35% homology) and a likely candidate for functional compensation is restricted to the adult bone marrow and not expressed in steroidogenic tissues (Fan et al., 2009), negating such a possibility. Moreover, there is no experimental evidence that multiple mechanisms are involved in mitochondrial cholesterol import. Based on observations in StAR knockout mice, it appears unmistakable that there is one rate-limiting mechanism of mitochondrial cholesterol import that is governed by StAR (Caron et al., 1997). Therefore, a model for TSPO in mitochondrial cholesterol transport is highly unlikely.

Given these results, it is unclear how the global TSPO knockout reported in an earlier study by Papadopoulos *et al.,* could be embryonic lethal (Papadopoulos et al., 1997a). As exact experimental details for that study were not published, we can only speculate that an error occurred in genome manipulation during this previous attempt. Similarly, a study from this same research group reported that more than 70% TSPO knockdown in cell lines resulted in cell death (Veenman et al., 2007). This is certainly not the case in both our *in vivo* and *in vitro* experimental observations and indicates that experimental conditions used in these earlier studies may have not been optimal. This conclusion is supported by another recent study that independently generated conditional liver and heart specific *Tspo*$^{-/-}$ mice and did not report any incidence of cell death after abolishing TSPO expression; TSPO was found to be not involved in mitochondrial permeability transition and cell death (Sileikyte et al., 2014).

At baseline physiology, gene expression differences between *Tspo*$^{fl/fl}$ and *Tspo*$^{-/-}$ adrenals were surprisingly few. A majority of these genes were involved in immune modulation: *Tmem178* is a negative regulator of inflammatory cytokine production (Decker, 2012); *Prrc2a* is a gene within the major histocompatibility complex class III region and is involved in the inflammatory process (Nieters et al., 2012); *Osgin1* is an oxidative stress response protein that regulates inflammation (Li et al., 2007), *Zbtb7b*

is a regulator of T cell mediated tumor-induced immunity (Mariani et al., 2013), *Pydc4* is part of a PYHIN domain family of proteins involved in innate immunity (Keating et al., 2011), *Trim12a* is a putative anti-viral gene (Schaller et al., 2007). Two genes were involved in vesicular transport and lipid sequestration: *Epn1* is an endocytic adaptor involved in clathrin-mediated endocytosis (Chen et al., 2009), *Abca2* is an endolysosomal protein with a role in intracellular lipid trafficking (Mack et al., 2007). Three genes expressed were of unknown function: *Ankrd52*, *Abhd1* and *Atxn2l*. The remainders were 2 non-coding RNA genes, 2 predicted genes and 3 pseudogenes. Careful consideration of these differentially expressed genes and the phenotype observed in $Tspo^{-/-}$ mice indicate that TSPO is not essential for sustaining physiological function.

TSPO binding chemicals have been shown to increase steroid hormone production in isolated mitochondria from steroidogenic cells (Krueger and Papadopoulos, 1990), MA-10 cells (Papadopoulos et al., 1990), and even live rats (Chung et al., 2013). Given our current findings, we can offer two possible explanations for these pharmacological effects. With ligand binding, TSPO may undergo a conformational change [as previously suggested (Lacapere and Papadopoulos, 2003; Murail et al., 2008)], resulting in the release of bound cholesterol that subsequently becomes available to mitochondrial transport systems and steroidogenesis. Alternatively, the effect of pharmacological agents could be due to drug-membrane interactions resulting in TSPO-independent biological effects (Seneviratne et al., 2012). It has also been discovered that TSPO ligands like PK11195 can insert themselves into lipid bilayers affecting membrane properties (Hatty et al., 2014), something that can modulate cholesterol availability to the steroidogenic machinery and also the nature of TSPO-ligand interactions. Nevertheless, as TSPO is considered a therapeutic target for numerous inflammatory conditions (Daugherty et al., 2013; Qi et al., 2012; Rupprecht et al., 2010; Vlodavsky et al., 2013), these properties of TSPO ligands may be important to assess specificity and side effects.

The sexual disparity in body weight differences in that only female $Tspo^{-/-}$ mice showed subtle but higher growth weights than their $Tspo^{fl/fl}$ cohorts suggests a hormone-dependent metabolic mechanism

(Anholt et al., 1985a). But the overall lack of phenotype in *Tspo*$^{-/-}$ mice appears to suggest that TSPO function could be more relevant only in pathological disease states. We have now observed *Tspo*$^{-/-}$ mice for up to 16 months of age with no apparent abnormalities/problems. Comparison of gene expression profiles after TSPO deletion also suggests potential changes to immune system function associated with TSPO deletion. We intend to investigate this further in future studies to gain insight into TSPO function.

In summary, this study provides irrefutable evidence that PBR/TSPO is not essential for steroid hormone biosynthesis, and that *Tspo*$^{-/-}$ mice are viable and fertile. These findings form a critical step towards understanding TSPO function and will help rebuild a defined model for steroid hormone biosynthesis. In addition, this understanding also forces reevaluation of interpretations made for TSPO function across multiple fields including neuroscience, immunology and oncology.

REFERENCES

Anders, S., and W. Huber. 2010. Differential expression analysis for sequence count data. *Genome Biol*. 11:R106.

Anholt, R.R., E.B. De Souza, M.J. Kuhar, and S.H. Snyder. 1985a. Depletion of peripheral-type benzodiazepine receptors after hypophysectomy in rat adrenal gland and testis. *Eur J Pharmacol*. 110:41-46.

Anholt, R.R., E.B. De Souza, M.L. Oster-Granite, and S.H. Snyder. 1985b. Peripheral-type benzodiazepine receptors: autoradiographic localization in whole-body sections of neonatal rats. *J Pharmacol Exp Ther*. 233:517-526.

Anholt, R.R., P.L. Pedersen, E.B. De Souza, and S.H. Snyder. 1986. The peripheral-type benzodiazepine receptor. Localization to the mitochondrial outer membrane. *J Biol Chem*. 261:576-583.

Baker, B.Y., L. Lin, C.J. Kim, J. Raza, C.P. Smith, W.L. Miller, and J.C. Achermann. 2006. Nonclassic congenital lipoid adrenal hyperplasia: a new disorder of the steroidogenic acute regulatory protein with very late presentation and normal male genitalia. *J Clin Endocrinol Metab*. 91:4781-4785.

Beam, S.W., and W.R. Butler. 1997. Energy balance and ovarian follicle development prior to the first ovulation postpartum in dairy cows receiving three levels of dietary fat. *Biol Reprod*. 56:133-142.

Benjamini, Y., and Y. Hochberg. 1995. Controlling the False Discovery Rate: A Practical and Powerful Approach to Multiple Testing. *Journal of the Royal Statistical Society. Series B (Methodological)*. 57:289-300.

Bose, H.S., V.R. Lingappa, and W.L. Miller. 2002. Rapid regulation of steroidogenesis by mitochondrial protein import. *Nature*. 417:87-91.

Bose, H.S., R.M. Whittal, M.A. Baldwin, and W.L. Miller. 1999. The active form of the steroidogenic acute regulatory protein, StAR, appears to be a molten globule. *Proc Natl Acad Sci U S A*. 96:7250-7255.

Braestrup, C., R. Albrechtsen, and R.F. Squires. 1977. High densities of benzodiazepine receptors in human cortical areas. *Nature*. 269:702-704.

Braestrup, C., and R.F. Squires. 1977. Specific benzodiazepine receptors in rat brain characterized by high-affinity (3H)diazepam binding. *Proc Natl Acad Sci U S A*. 74:3805-3809.

Caron, K.M., S.C. Soo, W.C. Wetsel, D.M. Stocco, B.J. Clark, and K.L. Parker. 1997. Targeted disruption of the mouse gene encoding steroidogenic acute regulatory protein provides insights into congenital lipoid adrenal hyperplasia. *Proc Natl Acad Sci U S A*. 94:11540-11545.

Chen, H., G. Ko, A. Zatti, G. Di Giacomo, L. Liu, E. Raiteri, E. Perucco, C. Collesi, W. Min, C. Zeiss, P. De Camilli, and O. Cremona. 2009. Embryonic arrest at midgestation and disruption of Notch signaling produced by the absence of both epsin 1 and epsin 2 in mice. *Proc Natl Acad Sci U S A*. 106:13838-13843.

Chung, J.Y., H. Chen, A. Midzak, A.L. Burnett, V. Papadopoulos, and B.R. Zirkin. 2013. Drug ligand-induced activation of translocator protein (TSPO) stimulates steroid production by aged brown Norway rat Leydig cells. *Endocrinology*. 154:2156-2165.

Churchill, P.F., and T. Kimura. 1979. Topological studies of cytochromes P-450scc and P-45011 beta in bovine adrenocortical inner mitochondrial membranes. Effects of controlled tryptic digestion. *J Biol Chem*. 254:10443-10448.

Clark, B.J., J. Wells, S.R. King, and D.M. Stocco. 1994. The purification, cloning, and expression of a novel luteinizing hormone-induced mitochondrial protein in MA-10 mouse Leydig tumor cells. Characterization of the steroidogenic acute regulatory protein (StAR). *J Biol Chem*. 269:28314-28322.

Daugherty, D.J., V. Selvaraj, O.V. Chechneva, X.B. Liu, D.E. Pleasure, and W. Deng. 2013. A TSPO ligand is protective in a mouse model of multiple sclerosis. *EMBO Mol Med*. 5:891-903.

Davies, L.P., and V. Huston. 1981. Peripheral benzodiazepine binding sites in heart and their interaction with dipyridamole. *Eur J Pharmacol*. 73:209-211.

Decker, C. 2012. TMEM178 Is a Novel Negative Regulator of Inflammatory Cytokine Production and Osteoclastogenesis during Rheumatoid Arthritis. *In* The American Society for Bone and Mineral Research 2012 Annual Meeting, Minneapolis, Minnesota, USA.

Fan, J., M.B. Rone, and V. Papadopoulos. 2009. Translocator protein 2 is involved in cholesterol redistribution during erythropoiesis. *J Biol Chem*. 284:30484-30497.

Gallardo, T., L. Shirley, G.B. John, and D.H. Castrillon. 2007. Generation of a germ cell-specific mouse transgenic Cre line, Vasa-Cre. *Genesis*. 45:413-417.

Gatliff, J., and M. Campanella. 2012. The 18 kDa translocator protein (TSPO): a new perspective in mitochondrial biology. *Curr Mol Med*. 12:356-368.

Gavish, M., I. Bachman, R. Shoukrun, Y. Katz, L. Veenman, G. Weisinger, and A. Weizman. 1999. Enigma of the peripheral benzodiazepine receptor. *Pharmacol Rev*. 51:629-650.

Hatty, C.R., A.P. Le Brun, V. Lake, L.A. Clifton, G.J. Liu, M. James, and R.B. Banati. 2014. Investigating the interactions of the 18kDa translocator protein and its ligand PK11195 in planar lipid bilayers. *Biochim Biophys Acta*. 1838:1019-1030.

Hauet, T., Z.X. Yao, H.S. Bose, C.T. Wall, Z. Han, W. Li, D.B. Hales, W.L. Miller, M. Culty, and V. Papadopoulos. 2005. Peripheral-type benzodiazepine receptor-mediated action of steroidogenic acute regulatory protein on cholesterol entry into leydig cell mitochondria. *Mol Endocrinol*. 19:540-554.

Keating, S.E., M. Baran, and A.G. Bowie. 2011. Cytosolic DNA sensors regulating type I interferon induction. *Trends Immunol*. 32:574-581.

Korkhov, V.M., C. Sachse, J.M. Short, and C.G. Tate. 2010. Three-dimensional structure of TspO by electron cryomicroscopy of helical crystals. *Structure*. 18:677-687.

Krueger, K.E., and V. Papadopoulos. 1990. Peripheral-type benzodiazepine receptors mediate translocation of cholesterol from outer to inner mitochondrial membranes in adrenocortical cells. *J Biol Chem*. 265:15015-15022.

Lacapere, J.J., F. Delavoie, H. Li, G. Peranzi, J. Maccario, V. Papadopoulos, and B. Vidic. 2001. Structural and functional study of reconstituted peripheral benzodiazepine receptor. *Biochem Biophys Res Commun*. 284:536-541.

Lacapere, J.J., and V. Papadopoulos. 2003. Peripheral-type benzodiazepine receptor: structure and function of a cholesterol-binding protein in steroid and bile acid biosynthesis. *Steroids*. 68:569-585.

Langmead, B., C. Trapnell, M. Pop, and S.L. Salzberg. 2009. Ultrafast and memory-efficient alignment of short DNA sequences to the human genome. *Genome Biol*. 10:R25.

Li, H., and V. Papadopoulos. 1998. Peripheral-type benzodiazepine receptor function in cholesterol transport. Identification of a putative cholesterol recognition/interaction amino acid sequence and consensus pattern. *Endocrinology*. 139:4991-4997.

Li, R., W. Chen, R. Yanes, S. Lee, and J.A. Berliner. 2007. OKL38 is an oxidative stress response gene stimulated by oxidized phospholipids. *J Lipid Res*. 48:709-715.

Lin, D., T. Sugawara, J.F. Strauss, 3rd, B.J. Clark, D.M. Stocco, P. Saenger, A. Rogol, and W.L. Miller. 1995. Role of steroidogenic acute regulatory protein in adrenal and gonadal steroidogenesis. *Science*. 267:1828-1831.

Livak, K.J., and T.D. Schmittgen. 2001. Analysis of relative gene expression data using real-time quantitative PCR and the 2(-Delta Delta C(T)) Method. *Methods*. 25:402-408.

Macdonald, R., and J.L. Barker. 1978. Benzodiazepines specifically modulate GABA-mediated postsynaptic inhibition in cultured mammalian neurones. *Nature*. 271:563-564.

Mack, J.T., V. Beljanski, A.M. Soulika, D.M. Townsend, C.B. Brown, W. Davis, and K.D. Tew. 2007. "Skittish" Abca2 knockout mice display tremor, hyperactivity, and abnormal myelin ultrastructure in the central nervous system. *Mol Cell Biol*. 27:44-53.

Madisen, L., T.A. Zwingman, S.M. Sunkin, S.W. Oh, H.A. Zariwala, H. Gu, L.L. Ng, R.D. Palmiter, M.J. Hawrylycz, A.R. Jones, E.S. Lein, and H. Zeng. 2010. A robust and high-throughput Cre reporting and characterization system for the whole mouse brain. *Nat Neurosci*. 13:133-140.

Manku, G., Y. Wang, R. Thuillier, C. Rhodes, and M. Culty. 2012. Developmental expression of the translocator protein 18 kDa (TSPO) in testicular germ cells. *Curr Mol Med*. 12:467-475.

Manna, P.R., J. Cohen-Tannoudji, R. Counis, C.W. Garner, I. Huhtaniemi, F.B. Kraemer, and D.M. Stocco. 2013. Mechanisms of action of hormone-sensitive lipase in mouse Leydig cells: its role in the regulation of the steroidogenic acute regulatory protein. *J Biol Chem*. 288:8505-8518.

Mariani, F., P. Sena, M. Pedroni, P. Benatti, P. Manni, C. Di Gregorio, A. Manenti, C. Palumbo, M.P. de Leon, and L. Roncucci. 2013. Th inducing POZ-Kruppel Factor (ThPOK) is a key regulator of the immune response since the early steps of colorectal carcinogenesis. *PLoS One*. 8:e54488.

Morohaku, K., S.H. Pelton, D.J. Daugherty, W.R. Butler, W. Deng, and V. Selvaraj. 2014. Translocator protein/peripheral benzodiazepine receptor is not required for steroid hormone biosynthesis. *Endocrinology*. 155:89-97.

Morohaku, K., N.S. Phuong, and V. Selvaraj. 2013. Developmental expression of translocator protein/peripheral benzodiazepine receptor in reproductive tissues. *PLoS One*. 8:e74509.

Mukhin, A.G., V. Papadopoulos, E. Costa, and K.E. Krueger. 1989. Mitochondrial benzodiazepine receptors regulate steroid biosynthesis. *Proc Natl Acad Sci U S A*. 86:9813-9816.

Murail, S., J.C. Robert, Y.M. Coic, J.M. Neumann, M.A. Ostuni, Z.X. Yao, V. Papadopoulos, N. Jamin, and J.J. Lacapere. 2008. Secondary and tertiary structures of the transmembrane domains of the translocator protein TSPO determined by NMR. Stabilization of the TSPO tertiary fold upon ligand binding. *Biochim Biophys Acta*. 1778:1375-1381.

Nieters, A., L. Conde, S.L. Slager, A. Brooks-Wilson, L. Morton, D.R. Skibola, A.J. Novak, J. Riby, S.M. Ansell, E. Halperin, T.D. Shanafelt, L. Agana, A.H. Wang, A.J. De Roos, R.K. Severson, W. Cozen, J. Spinelli, K. Butterbach, N. Becker, S. de Sanjose, Y. Benavente, P. Cocco, A. Staines, M. Maynadie, L. Foretova, P. Boffetta, P. Brennan, Q. Lan, Y. Zhang, T. Zheng, M. Purdue, B. Armstrong, A. Kricker, C.M. Vajdic, A. Grulich, M.T. Smith, P.M. Bracci, S.J. Chanock, P. Hartge, J.R. Cerhan, S.S. Wang, N. Rothman, and C.F. Skibola. 2012. PRRC2A and BCL2L11 gene variants influence risk of non-Hodgkin lymphoma: results from the InterLymph consortium. *Blood*. 120:4645-4648.

Papadopoulos, V. 2014. On the Role of the Translocator Protein (18-kDa) TSPO in Steroid Hormone Biosynthesis. *Endocrinology*. 155:15-20.

Papadopoulos, V., H. Amri, N. Boujrad, C. Cascio, M. Culty, M. Garnier, M. Hardwick, H. Li, B. Vidic, A.S. Brown, J.L. Reversa, J.M. Bernassau, and K. Drieu. 1997a. Peripheral benzodiazepine receptor in cholesterol transport and steroidogenesis. *Steroids*. 62:21-28.

Papadopoulos, V., H. Amri, H. Li, N. Boujrad, B. Vidic, and M. Garnier. 1997b. Targeted disruption of the peripheral-type benzodiazepine receptor gene inhibits steroidogenesis in the R2C Leydig tumor cell line. *J Biol Chem*. 272:32129-32135.

Papadopoulos, V., M. Baraldi, T.R. Guilarte, T.B. Knudsen, J.J. Lacapere, P. Lindemann, M.D. Norenberg, D. Nutt, A. Weizman, M.R. Zhang, and M. Gavish. 2006. Translocator protein (18kDa): new nomenclature for the peripheral-type benzodiazepine receptor based on its structure and molecular function. *Trends Pharmacol Sci*. 27:402-409.

Papadopoulos, V., A.G. Mukhin, E. Costa, and K.E. Krueger. 1990. The peripheral-type benzodiazepine receptor is functionally linked to Leydig cell steroidogenesis. *J Biol Chem*. 265:3772-3779.

Privalle, C.T., J.F. Crivello, and C.R. Jefcoate. 1983. Regulation of intramitochondrial cholesterol transfer to side-chain cleavage cytochrome P-450 in rat adrenal gland. *Proc Natl Acad Sci U S A*. 80:702-706.

Qi, X., J. Xu, F. Wang, and J. Xiao. 2012. Translocator protein (18 kDa): a promising therapeutic target and diagnostic tool for cardiovascular diseases. *Oxid Med Cell Longev*. 2012:162934.

Quast, C., E. Pruesse, P. Yilmaz, J. Gerken, T. Schweer, P. Yarza, J. Peplies, and F.O. Glockner. 2013. The SILVA ribosomal RNA gene database project: improved data processing and web-based tools. *Nucleic Acids Res*. 41:D590-596.

Regan, J.W., H.I. Yamamura, S. Yamada, and W.R. Roeske. 1981. High affinity [3H]flunitrazepam binding: characterization, localization, and alteration in hypertension. *Life Sci*. 28:991-998.

Rone, M.B., J. Fan, and V. Papadopoulos. 2009. Cholesterol transport in steroid biosynthesis: role of protein-protein interactions and implications in disease states. *Biochim Biophys Acta*. 1791:646-658.

Rupprecht, R., V. Papadopoulos, G. Rammes, T.C. Baghai, J. Fan, N. Akula, G. Groyer, D. Adams, and M. Schumacher. 2010. Translocator protein (18 kDa) (TSPO) as a therapeutic target for neurological and psychiatric disorders. *Nat Rev Drug Discov*. 9:971-988.

Schaller, T., S. Hue, and G.J. Towers. 2007. An active TRIM5 protein in rabbits indicates a common antiviral ancestor for mammalian TRIM5 proteins. *J Virol*. 81:11713-11721.

Schneider, C.A., W.S. Rasband, and K.W. Eliceiri. 2012. NIH Image to ImageJ: 25 years of image analysis. *Nat Methods*. 9:671-675.

Seneviratne, M.S., D. Faccenda, V. De Biase, and M. Campanella. 2012. PK11195 inhibits mitophagy targeting the F1Fo-ATPsynthase in Bcl-2 knock-down cells. *Curr Mol Med*. 12:476-482.

Sileikyte, J., E. Blachly-Dyson, R. Sewell, A. Carpi, R. Menabo, F. Di Lisa, F. Ricchelli, P. Bernardi, and M. Forte. 2014. Regulation of the Mitochondrial Permeability Transition Pore by the Outer Membrane does not Involve the Peripheral Benzodiazepine Receptor (TSPO). *J Biol Chem*.

Simpson, E.R., and G.S. Boyd. 1967. The cholesterol side-chain cleavage system of bovine adrenal cortex. *Eur J Biochem*. 2:275-285.

Simpson, E.R., J.L. McCarthy, and J.A. Peterson. 1978. Evidence that the cycloheximide-sensitive site of adrenocorticotropic hormone action is in the mitochondrion. Changes in pregnenolone formation, cholesterol content, and the electron paramagnetic resonance spectra of cytochrome P-450. *J Biol Chem*. 253:3135-3139.

Spandidos, A., X. Wang, H. Wang, and B. Seed. 2010. PrimerBank: a resource of human and mouse PCR primer pairs for gene expression detection and quantification. *Nucleic Acids Res*. 38:D792-799.

Stocco, D.M. 2014. The Role of PBR/TSPO in Steroid Biosynthesis Challenged. *Endocrinology*. 155:6-9.

Takahashi, H., A. Nagashima, and C. Koshino. 1958. Effect of gamma-aminobutyryl-choline upon the electrical activity of the cerebral cortex. *Nature*. 182:1443-1444.

Trapnell, C., L. Pachter, and S.L. Salzberg. 2009. TopHat: discovering splice junctions with RNA-Seq. *Bioinformatics*. 25:1105-1111.

Veenman, L., V. Papadopoulos, and M. Gavish. 2007. Channel-like functions of the 18-kDa translocator protein (TSPO): regulation of apoptosis and steroidogenesis as part of the host-defense response. *Curr Pharm Des*. 13:2385-2405.

Vlodavsky, E., E. Palzur, and J.F. Soustiel. 2013. 18 kDa Translocator Protein as a Potential Therapeutic Target for Traumatic Brain Injury. *CNS Neurol Disord Drug Targets*.

Yago, N., and S. Ichii. 1969. Submitochondrial distribution of components of the steroid 11 beta-hydroxylase and cholesterol sidechain-cleaving enzyme systems in hog adrenal cortex. *J Biochem*. 65:215-224.

Yeliseev, A.A., and S. Kaplan. 1995. A sensory transducer homologous to the mammalian peripheral-type benzodiazepine receptor regulates photosynthetic membrane complex formation in Rhodobacter sphaeroides 2.4.1. *J Biol Chem*. 270:21167-21175.

Zhong, S., J.G. Joung, Y. Zheng, Y.R. Chen, B. Liu, Y. Shao, J.Z. Xiang, Z. Fei, and J.J. Giovannoni. 2011. High-throughput illumina strand-specific RNA sequencing library preparation. *Cold Spring Harb Protoc*. 2011:940-949.

CHAPTER 3

PK11195 Effect on Steroidogenesis Is Not Mediated Through the Translocator Protein (TSPO)

Tu, L. N., Zhao, A. H., Stocco, D. M., & Selvaraj, V. (2015). PK11195 effect on steroidogenesis is not mediated through the translocator protein (TSPO). *Endocrinology, 156*(3), 1033-1039.

ABSTRACT

Translocator protein (TSPO) is a mitochondrial outer membrane protein of unknown function with high physiological expression in steroidogenic cells. Using TSPO gene-deleted mice, we recently demonstrated that TSPO function is not essential for steroidogenesis. The first link between TSPO and steroidogenesis was established in studies showing modest increases in progesterone production by adrenocortical and Leydig tumor cell lines after treatment with PK11195. In order to reconcile discrepancies between physiological and pharmacological interpretations of TSPO function, we generated TSPO-knockout MA-10 mouse Leydig tumor cells (MA-10:*Tspo*Δ/Δ) and examined their steroidogenic potential after exposure to either dibutyryl-cAMP or PK11195. Progesterone production in MA-10:*Tspo*Δ/Δ after dibutyryl-cAMP was not different from control MA-10:*Tspo*+/+ cells confirming that TSPO function is not essential for steroidogenesis. Interestingly, when treated with increasing concentrations of PK11195, both control MA-10:*Tspo*+/+ cells and MA-10:*Tspo*Δ/Δ cells responded in a similar dose-dependent manner showing increases in progesterone production. These results show that the pharmacological effect of PK11195 on steroidogenesis is not mediated through TSPO.

INTRODUCTION

Translocator protein (TSPO), previously known as peripheral benzodiazepine receptor (PBR), is a highly conserved protein across kingdoms (Yeliseev and Kaplan, 1995). It was first identified for its high binding affinity to benzodiazepines in distinct peripheral sites, as opposed to the central benzodiazepine receptor (γ-aminobutyric acid type A receptor) sites in the brain (Braestrup et al., 1977; Braestrup and Squires, 1977; Davies and Huston, 1981; Regan et al., 1981). The isoquinoline carboxamine, PK11195 [N-butan-2-yl-1-(2-chlorophenyl)-N-methylisoquinoline-3-carboxamide], was then identified as a selective high-affinity TSPO/PBR binding chemical (Le Fur et al., 1983), and has been widely used in most binding/functional studies. Binding sites of TSPO ligands have been found in multiple tissues including: heart, brain, adrenal, kidney, salivary gland, platelets, brown adipose tissue, skin and liver (Gavish et al., 1999), but were noted to be highest in steroidogenic cells (Anholt et al., 1985; Morohaku et al., 2013; Wang et al., 2012).

Sub-cellular fractionation and drug displacement studies showed that TSPO was enriched in the outer mitochondrial membrane (OMM) (Anholt et al., 1985; Anholt et al., 1986). A putative cholesterol recognition amino acid consensus (CRAC) sequence was identified at the C terminal region (Li and Papadopoulos, 1998), distinct from its PK11195 binding site (Jaremko et al., 2014). The structure of murine TSPO is described as a five transmembrane alpha helix (Murail et al., 2008), that was initially modeled to form a hydrophobic interior core containing the CRAC domain for cholesterol translocation (Korkhov et al., 2010). However, a more recent nuclear magnetic resonance structure of TSPO showed that the CRAC domain is located on the outside of the TSPO pointing towards the membrane environment (Jaremko et al., 2014). Therefore, the ability of cholesterol to dimerize has been proposed to induce oligomerization of TSPO leading to the potential transporter function (Jaremko et al., 2014).

For the past 25 years, TSPO has been depicted in the steroidogenic pathway as a critical transporter of cholesterol from the OMM to the mitochondrial matrix (Midzak et al., 2011). Conversion of cholesterol to pregnenolone by the enzyme CYP11A1 is restricted to the matrix side of the inner

mitochondrial membrane, therefore mitochondrial cholesterol import forms the first and the rate-limiting step for the acute production of all steroid hormones. The very first link between TSPO and steroid hormone biosynthesis emerged from a pharmacological study of different high affinity TSPO-binding chemicals on steroidogenesis. In Y1 mouse adrenal tumor cells, three out of nine chemicals, including PK11195, could induce steroid production at maximum 2-fold of the baseline (Mukhin et al., 1989). A follow-up report using the MA-10 mouse Leydig tumor cell line showed the same phenomenon with PK11195 being capable of inducing a 4-fold increase in baseline steroid production (Papadopoulos et al., 1990). These responses were independent of induction of the steroidogenic acute regulatory protein (STAR), a key player in mitochondrial cholesterol transport required for steroidogenesis (Caron et al., 1997; Clark et al., 1994). A subsequent publication reported that mono-allelic targeted disruption of the *Tspo* gene by homologous recombination in the R2C rat Leydig tumor cell line abolished TSPO protein expression and consequently inhibited progesterone level to only ~5% of control values (Papadopoulos et al., 1997b); it was concluded that TSPO has an indispensable role in steroidogenesis.

Using Leydig cell-specific TSPO conditional knockout mice, we recently demonstrated that TSPO does not have a role in testosterone production (Morohaku et al., 2014). In direct contrast to a previous study (Papadopoulos et al., 1997a), we subsequently found that global TSPO knockout mice were viable and fertile with no effects on steroidogenesis (Tu et al., 2014). We also showed in different steroidogenic cell lines: Y1, MA-10, MLTC and R2C, that TSPO knockdown did not affect their ability to produce steroid hormones (Tu et al., 2014). In fact, the steroidogenic human adrenocortical cell line H295R, is deficient of TSPO, yet is capable of making steroid hormones (Tu et al., 2014). These results provided compelling genetic evidence that TSPO physiology is not associated with steroidogenesis. However, this did not agree with TSPO pharmacology, as TSPO binding chemicals are reported to induce steroid hormone production (Chung et al., 2013; Mukhin et al., 1989; Papadopoulos et al., 1990).

In order to reconcile this discrepancy, we generated TSPO-knockout MA-10 Leydig tumor (MA-10:*Tspo*Δ/Δ) cells and tested the ability of PK11195 to induce steroid hormone production. Our results

demonstrate that TSPO deletion in MA-10 cells had no effect on its ability to produce steroid hormones and that the pharmacological effect of PK11195 on steroidogenesis is not mediated through TSPO.

MATERIALS AND METHODS

Generation of TSPO-deleted MA-10 cells

MA-10 cells were cultured in Dulbecco's modified Eagle medium (DMEM) with glutamine and pyruvate containing 10% fetal bovine serum as previously described (Morohaku et al., 2013). The clustered regularly interspaced short palindromic repeats (CRISPR) system was used to generate MA-10:*Tspo*Δ/Δ cells by targeting exon 2 of the *Tspo* gene (NCBI: Gene ID: 12257; Reference Sequence: NM_009775.4). The specific guide RNA sequence 5' – GCCTACTTTGTACGTGGCGA – 3' was cloned in the pX330-U6-Chimeric_BB-cBh-hSpCas9 plasmid (Cong et al., 2013), transfected into MA-10 cells using TransIT-X2 (Mirus Bio) and cultured for 48 hrs. Transfected cells were then seeded in 96 well plates at the density of ~1 cell/well for clonal selection. Clones originating from single cells were screened for absence of TSPO protein expression by performing Western blots using a monoclonal antibody (Abcam) that recognizes amino acid 156-169 coded by the TSPO exon 4. Three MA-10:*Tspo*Δ/Δ cell clones were identified and mutations in the *Tspo* gene were confirmed by sequencing after cloning both the respective *Tspo* cDNAs and *Tspo* exon 2 genomic DNA into TOPO-TA vectors (Life Technologies), and ZR Plasmid Miniprep (Zymo Research) purification. The list of primers used for cloning and sequencing is provided in Supplemental Table 1.

Immunocytochemistry

Cells were incubated with 300 nM Mitotracker® Deep Red FM (Life Technologies) in culture medium for 1 hour at 37˚C, washed with PBS and fixed with 2% paraformaldehyde. Cells were blocked with 5% horse serum in PBS to prevent non-specific binding, stained with a primary rabbit monoclonal TSPO antibody (Abcam) and secondary Alexa Fluor 488 antibody as previously described (Morohaku et

al., 2013). Images were captured using a LSM 510 confocal microscope (Zeiss) and visualized using Image J.

Hormone assays

For dibutyryl-cAMP (Bt_2cAMP) stimulation experiments, 5 x 10^4 cells were plated per well in a 96 well plate and allowed to attach overnight. Cells were then washed with PBS and incubated with 0.5 mM Bt_2cAMP (Sigma) in DMEM medium without serum for 6 hrs. For PK11195 stimulation experiments, 15 x 10^4 cells were plated per well in a 12 well plate and allowed to attach overnight. Cells were washed with PBS, changed to DMEM medium without serum, and different doses of PK11195 (Sigma) in equal volume of vehicle (ethanol, 0.1% v/v final) was added (Treatments: Vehicle only, 100 nM, 1 µM, and 10 µM final concentrations of PK11195), and incubated for 2 hrs. For both stimulations, supernatants were collected and progesterone was measured as previously described (Manna et al., 2013), and values were normalized to total protein in each well.

Immunoblots

Proteins were separated by SDS-PAGE and immunoblotted using rabbit monoclonal primary antibodies against TSPO (Abcam) and a rabbit polyclonal STAR antibody (Clark et al., 1994). Each primary antibody was multiplexed with the control for protein loading, mouse monoclonal β-actin (Li-Cor). Simultaneous detection was performed using IRDye 700 and 800 labeled secondary antibodies using a laser fluorescence scanner (Li-Cor) and quantified using ImageJ as described previously (Morohaku et al., 2014; Morohaku et al., 2013).

Statistics

Numeric differences between groups were compared using a Student's t-test; comparisons for more than two groups were performed using ANOVA and *post hoc* Tukey's test; $p<0.05$ was considered significant. All analyses were performed using Prism 5 (GraphPad).

RESULTS

CRISPR/Cas9-mediated deletion of TSPO in MA-10 cells

Tspo has 4 exons with the translation start codon in exon 2. Using the CRISPR/Cas9 system, a guide RNA was used with sequence complementary to 20 nucleotides downstream of the start codon in *Tspo* exon 2 for targeting Cas9 nuclease activity (Figure 3.1A). The resulting DNA double-stranded breaks, which are subject to the error prone non-homologous end joining, caused random indel mutations that induced frame shifts and/or generated a premature stop codon in the mRNA, leading to a truncated and non-functional TSPO protein.

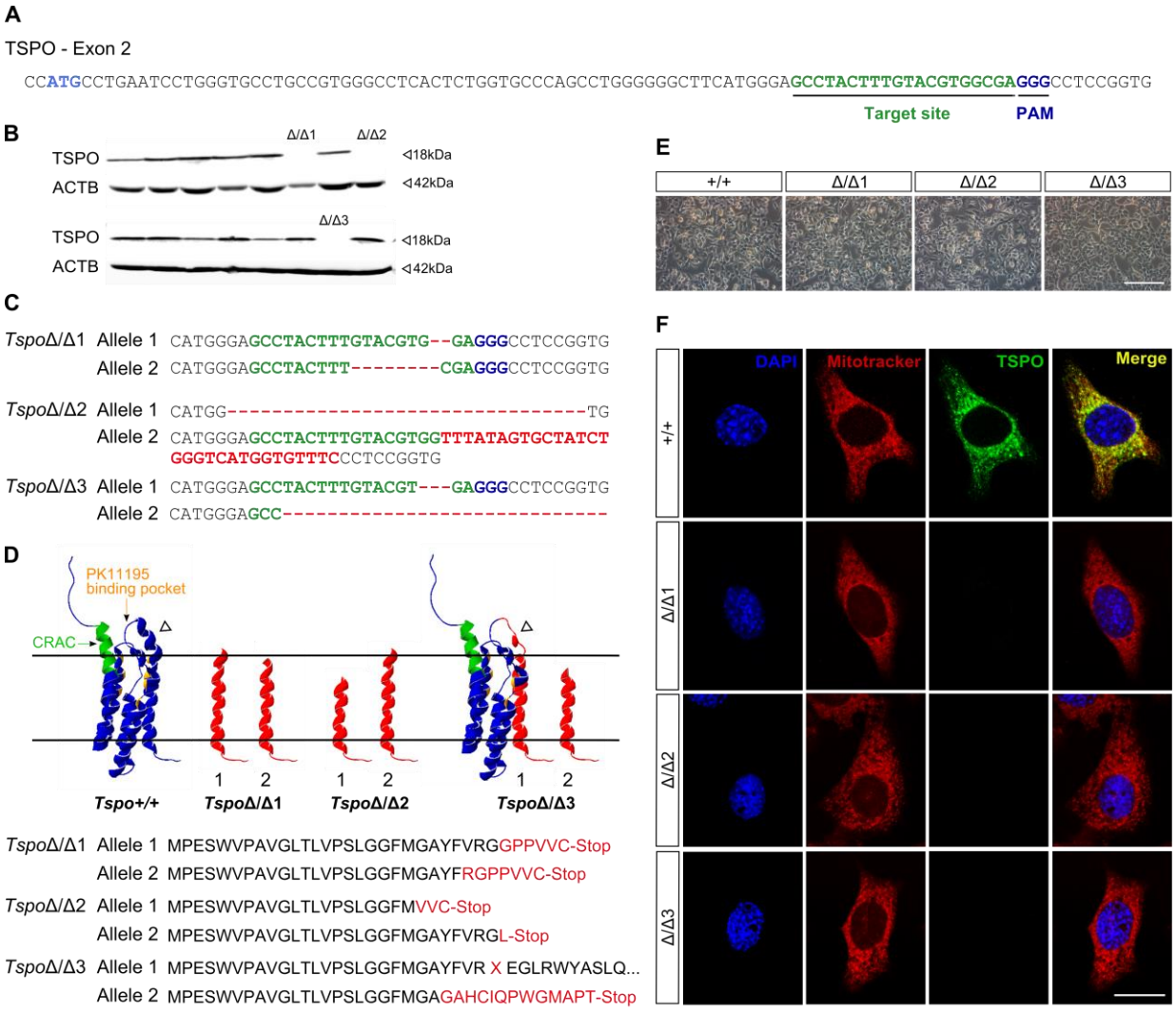

Figure 3.1. CRISPR/Cas9-mediated deletion of TSPO in steroidogenic MA-10 Leydig cells. (A) Sequence of *Tspo* exon 2 showing the start codon and targeted sequence followed by the protospacer adjacent motif (PAM). (B) After transfection with *Tspo*-CRISPR/Cas9 construct, MA-10 clones were screened for TSPO protein expression using a monoclonal TSPO antibody that recognizes amino acids 156-169 encoded by *Tspo* exon 4. Western blots that identified the three TSPO-deleted clones are shown. Control bands are β-Actin (ACTB). (C) Sequencing results of *Tspo* cDNA in 3 MA-10:*Tspo*Δ/Δ clones confirmed indel mutations in the target sites of expressed alleles. Regions corresponding to guide RNA sequences are shown in green, deletions and insertions are shown in red. Deleted regions ranged from 2 bp in MA-10:*Tspo*Δ/Δ1 mutation 1 to 88 bp in MA-10:*Tspo*Δ/Δ3 mutation 2. (D) Mutations in *Tspo* induced a frame shift and/or generated a stop codon, which resulted in a truncation with fragments restricted to TSPO N-terminal 28 and 25 amino acids for alleles in MA-10:*Tspo*Δ/Δ1, 21 and 28 amino acids for alleles in MA-10:*Tspo*Δ/Δ2, and 23 amino acids for the one allele in MA-10:*Tspo*Δ/Δ3. The second allele in MA-10:*Tspo*Δ/Δ3 was a Gly28 mutation that induced a significant change to the short α helix loop (arrowhead) that connects transmembrane region 1 and 2 that ultimately led to complete loss of TSPO protein expression. (E) Representative light microscopy images of MA-10:*Tspo*+/+ and MA-10:*Tspo*Δ/Δ cells showed that MA-10:*Tspo*Δ/Δ cells were healthy with no apparent morphological changes (Scale bar: 200 μm). (F) Immunocytochemistry confirmed complete absence of TSPO in the different MA-10:*Tspo*Δ/Δ clones (Scale bar: 20 μm).

In this study, after transfection with the *Tspo*-CRISPR/Cas9 construct, we screened 36 MA-10 cell clones derived from single transfected cells for TSPO protein expression using a TSPO monoclonal antibody that recognizes amino acids 156-169 at the C-terminal tail of TSPO (coded by exon 4). We identified three TSPO-deleted clones: MA-10:*Tspo*Δ/Δ1, MA-10:*Tspo*Δ/Δ2, MA-10:*Tspo*Δ/Δ3 (Figure 3.1B). Sequencing confirmed that deletion mutations occurred in the targeted region in exon 2 in the expressed alleles of the three clones resulting in loss of TSPO protein expression (Figure 3.1 C-D). In MA-10:*Tspo*Δ/Δ1, truncations resulting from frame shifts resulted in fragments restricted to TSPO N-terminal 28 and 25 amino acids respectively for expressed alleles; similarly, MA-10:*Tspo*Δ/Δ2 resulted in fragments restricted to the N-terminal 21 and 28 amino acids respectively for expressed alleles. In MA-10:*Tspo*Δ/Δ3, one allele was truncated with a fragment restricted to TSPO N-terminal 23 amino acids, and the other allele showed a deletion of Gly28. No mutant clones expressed the cholesterol-binding CRAC domain and the PK11195 binding pocket of the TSPO protein. The Gly28 deletion in one allele of MA-10:*Tspo*Δ/Δ3 was a 3 base pair deletion that could potentially allow the remainder of the TSPO protein to remain in frame; however, we did not detect any TSPO protein expression from this clone (Figure 3.1B). Based on modeling this deletion in the TSPO structure (Jaremko et al., 2014), we identified a significant change to the short α helix loop that connects transmembrane region 1 and 2 (Figure 3.1D), which could potentially trigger the misfolded protein response. However, treatment with the proteasome inhibitor MG132 did not recover TSPO protein detection (data not shown), suggesting that cellular quality control mechanisms for TSPO are yet to be understood. Sequencing the genomic DNA *Tspo* loci from the three MA-10:*Tspo*Δ/Δ clones detected 5-6 copies of TSPO in each clone that were all mutated (data not shown). Although the potential possibility of multiple alleles exists, it is also possible that persistent or repeated cutting by Cas9 at the *Tspo* exon 2 loci that may have occurred during clonal selection, could have resulted in some minor subclonal populations. These different mutations included those that were detected in *Tspo* cDNA from these clones. All MA-10:*Tspo*Δ/Δ cells appeared healthy with no morphological differences compared to the control MA-10:*Tspo*+/+ cells (Figure 3.1E).

Immunocytochemical staining confirmed that TSPO protein was not detectable in MA-10:*Tspo*Δ/Δ cells (Figure 3.1F).

Loss of TSPO does not affect progesterone production in MA-10 cells

We examined the effect of complete TSPO protein deficiency on steroid hormone production in MA-10:*Tspo*Δ/Δ cells compared to control MA-10:*Tspo*+/+ cells. At baseline, progesterone levels were not different between the three MA-10:*Tspo*Δ/Δ clones and control MA-10:*Tspo*+/+ cells (Figure 3.2A). After stimulation with Bt_2cAMP, progesterone levels increased in both MA-10:*Tspo*Δ/Δ and control MA-10:*Tspo*+/+ cells to identical levels showing no defects in steroid hormone production (Figure 3.2A). In fact, progesterone levels in one clone MA-10:*Tspo*Δ/Δ3, were even significantly higher than control MA-10:*Tspo*+/+ cells. Expression of the steroidogenic acute regulatory (STAR) protein, a critical player in the steroid hormone synthesis pathway, was similar at both baseline and after Bt_2cAMP stimulation in MA-10:*Tspo*Δ/Δ clones and control MA-10:*Tspo*+/+ cells (Figure 3.2B). These results indicated that TSPO is not involved in the steroid hormone biosynthetic pathway in MA-10 cells.

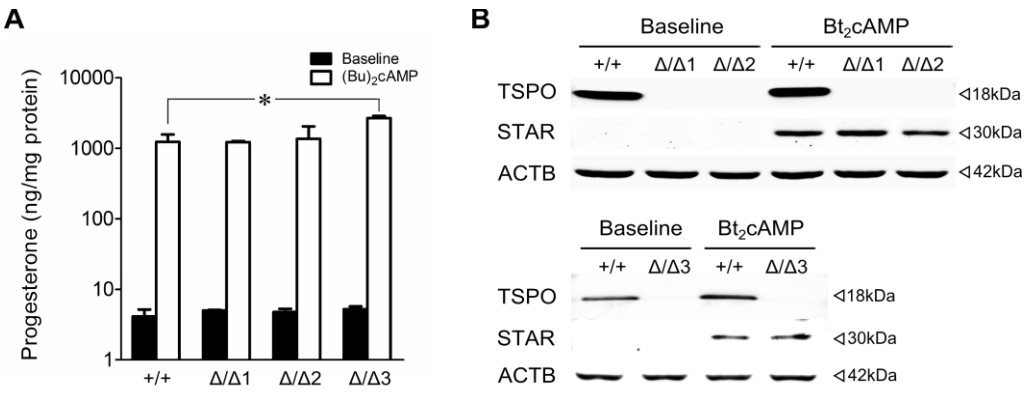

Figure 3.2. **TSPO deficiency does not affect progesterone production in MA-10 cells.** (A) TSPO deletion in the three MA-10:*Tspo*Δ/Δ clones did not affect baseline or Bt_2cAMP stimulated progesterone production. Bt_2cAMP stimulation, increased progesterone levels to a similar extent in both intact MA-10:*Tspo*+/+, and TSPO deleted clones: MA-10:*Tspo*Δ/Δ1, MA-10:*Tspo*Δ/Δ2, and MA-10:*Tspo*Δ/Δ3. Progesterone levels after Bt_2cAMP treatment in clone MA-10:*Tspo*Δ/Δ3 were significantly higher than MA-10:*Tspo*+/+ cells. Mean values were generated from 2-3 experiments conducted in triplicate. (B) Western blots showing absence of TSPO and the induction of STAR after Bt_2cAMP stimulation of MA-10:*Tspo*Δ/Δ clones and MA-10:*Tspo*+/+ cells. Induction of STAR expression after Bt_2cAMP stimulation were identical in the different MA-10:*Tspo*Δ/Δ clones compared to MA-10:*Tspo*+/+ cells. Control bands are β-Actin (ACTB).

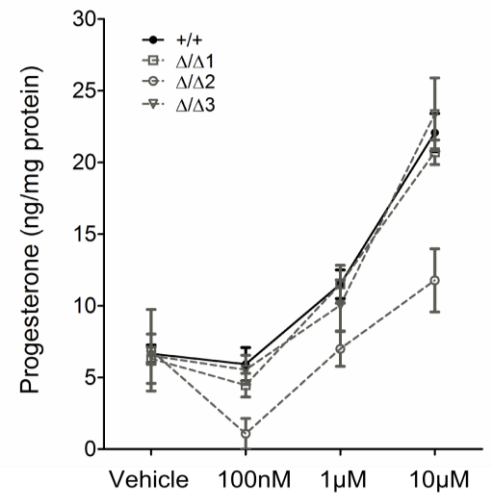

Figure 3.3. PK11195 induced steroidogenesis in the absence of TSPO. PK11195 dose-dependent increase in progesterone production was observed in both MA-10:*Tspo*Δ/Δ clones (1, 2 and 3) and control MA-10:*Tspo*+/+ cells. Mean values were generated from 3-4 independent experiments conducted in triplicate.

Pharmacological effect of PK11195 on steroidogenesis is not mediated by TSPO

Using MA-10:*Tspo*Δ/Δ cells as a tool, we attempted to validate the specific relationship between PK11195 and TSPO in the induction of steroidogenesis, a pharmacological effect demonstrated in previous studies (Mukhin et al., 1989; Papadopoulos et al., 1990). We examined whether PK11195 would induce a steroidogenic response in MA-10:*Tspo*Δ/Δ clones. Our results showed that PK11195 could stimulate progesterone production in a dose-dependent manner in both MA-10:*Tspo*Δ/Δ clones and control MA-10:*Tspo*+/+ cells (Figure 3.3). In control MA-10:*Tspo*+/+ cells, the maximal progesterone levels observed at 10 μM PK11195 was about 3 to 4 fold higher than baseline; this was identical in MA-10:*Tspo*Δ/Δ clones 1 and 3. MA-10:*Tspo*Δ/Δ clone 2 also showed a similar response, but the progesterone production was induced only about 2 fold of the baseline. These results indicated that the pharmacological effect of the TSPO ligand PK11195 on steroid hormone synthesis in MA-10 cells is not mediated via TSPO.

DISCUSSION

Recent evidence that there is no physiological need for TSPO in mitochondrial cholesterol transport for steroid hormone biosynthesis has raised critical questions about the pharmacology of TSPO binding chemicals (Banati et al., 2014; Stocco, 2014; Tu et al., 2014). The core basis for TSPO involvement in steroidogenesis was indicated by early studies reporting that TSPO binding chemicals can induce steroid hormone production (Mukhin et al., 1989; Papadopoulos et al., 1990). Based on our results, it is apparent that the effect of PK11195 on MA-10 cells resulting in the induction of steroid hormone production is not mediated through TSPO.

Hormone production by steroidogenic cells upon treatment with TSPO binding chemicals has been offered as proof of TSPO involvement in steroidogenesis (Mukhin et al., 1989; Papadopoulos et al., 1990). The effect of PK11195 was previously shown to induce progesterone production in a steep dose response curve that plateaued at concentrations higher than 1 μM. However, it is interesting to note that the response itself was very modest and transient; in a time course, there was no progressive increase in progesterone accumulation in cell culture supernatants after the first hour of PK11195 treatment, and levels remained unchanged over the next 4 hours (Papadopoulos et al., 1990). This is in contrast to stimulation with trophic hormones, which show a progressive accumulation of progesterone in the supernatant over the entire 5-hour period (Papadopoulos et al., 1990). We initially interpreted this distinction as an indicator that the effect of TSPO binding chemicals is a physical response to TSPO binding rather than a physiological effect. In a recent commentary, Papadopoulos also offered such an explanation to address why physiological TSPO function might be different from pharmacology (Papadopoulos, 2014). In addition, structural evidence that PK11195-binding stabilizes TSPO also contributed to the logic that such an event might be possible (Jaremko et al., 2014).

In our treatments, maximal induction of progesterone production was 2 to 4 fold higher than baseline at 10 μM PK11195 in both MA-10:*Tspo*Δ/Δ and MA-10:*Tspo*+/+ cells, which is comparable to the extent of induction previously demonstrated for MA-10 cells (Papadopoulos et al., 1990). One of the

three clones MA-10:*Tspo*Δ/Δ2 was less responsive and reached only about 2 fold above baseline, a difference that could be explained by inherent variability that exists in clonal populations within MA-10 cells (Gocze and Freeman, 1994). Interestingly, we did not find induction of progesterone production in either MA-10:*Tspo*Δ/Δ or MA-10:*Tspo*+/+ cells at nanomolar PK11195 concentrations; values for progesterone also did not seem to plateau at 1 μM for these cells as previously reported (Papadopoulos et al., 1990), suggesting an experimental difference in effective ranges for this steroidogenic response by PK11195. We observed that PK11195 ability to induce progesterone production was inversely affected by cell density, and a prominent response could be observed only when cells were less than 50% confluent (not shown). This also suggested that the PK11195 exposure did not generate a typical drug-ligand type response in these cells. Nevertheless, the fact that we observed a PK11195 response in both MA-10:*Tspo*Δ/Δ and MA-10:*Tspo*+/+ cells confirms that TSPO is not involved in this phenomenon.

One possibility for this disconnect is that the pharmacological effect of PK11195 on steroidogenesis could be due to a chemical-membrane interaction. It has been recently demonstrated that TSPO ligands like PK11195 can insert themselves into lipid bilayers affecting membrane properties (Hatty et al., 2014), a phenomenon that could modulate cholesterol availability to the steroidogenic machinery. Another study reported that high concentrations of PK11195 could rapidly displace fluorescent NBD-cholesterol [(22-(*N*-(7-Nitrobenz-2-Oxa-1,3-Diazol-4-yl)Amino)-23,24-Bisnor-5-Cholen-3β-Ol)] from different membrane compartments into lipid droplets, affecting intracellular cholesterol in astrocytes and fibroblasts (Falchi et al., 2007). Although it was not clear if this displacement was mediated by TSPO in these cell types, one plausible explanation for our results in steroidogenic cells is that a similar displacement could potentially release a limited amount of cholesterol from mitochondrial membranes and hence trigger a modest and transient increase in steroid hormone production.

In addition, while there are reports in the literature of TSPO-independent action of several putative binding chemicals, specific cellular targets other than TSPO have not been extensively

characterized. PK11195 has been demonstrated to target the F1F0-ATPsynthase and inhibit mitophagy without the involvement of TSPO (Seneviratne et al., 2012). In another study, an apoptosis-sensitizing effect for PK11195 was observed even after TSPO was completely knocked down (Gonzalez-Polo et al., 2005). The anti-tumor effect of TSPO binding chemicals Ro5-4864 and FGIN-1-27 was identical irrespective of the presence or absence of TSPO in different tumors (Hans et al., 2005). In hematologic cancers, PK11195 showed broad inhibition of adenosine triphosphate (ATP)-binding cassette transporters by binding to plasma membrane sites without involvement of TSPO (Walter et al., 2005). In cells of mesenchymal origin, PK11195 and Ro5-4864 could inhibit cell proliferation through decreases in activation of ERK and c-Jun independent of TSPO (Kletsas et al., 2004). Therefore, we can speculate that the effect of PK11195 on steroidogenesis may be mediated through binding to another unidentified cellular target in steroid hormone producing cells.

Results in this study also contradicted the previous study on R2C cells that disruption of one *Tspo* allele dramatically reduced steroid production to only ~5% of control values (Papadopoulos et al., 1997b). This disruption also caused significant adverse morphological changes and 2-3 times slower cell proliferation in these R2C cells. We did not observe any differences in morphology, viability or proliferation in the three MA-10:*Tspo*Δ/Δ clones generated in this study. Therefore, previous results from the solitary mono-allelic *Tspo*-disrupted R2C clone may require reinvestigation.

In summary, our results show that TSPO deletion in MA-10 cells has no effect on steroid hormone biosynthesis and that the pharmacological activity of PK11195 on the induction of steroidogenesis is not mediated through TSPO.

REFERENCES

Anholt, R.R., E.B. De Souza, M.L. Oster-Granite, and S.H. Snyder. 1985. Peripheral-type benzodiazepine receptors: autoradiographic localization in whole-body sections of neonatal rats. *J Pharmacol Exp Ther*. 233:517-526.

Anholt, R.R., P.L. Pedersen, E.B. De Souza, and S.H. Snyder. 1986. The peripheral-type benzodiazepine receptor. Localization to the mitochondrial outer membrane. *J Biol Chem*. 261:576-583.

Banati, R.B., R.J. Middleton, R. Chan, C.R. Hatty, W. Wai-Ying Kam, C. Quin, M.B. Graeber, A. Parmar, D. Zahra, P. Callaghan, S. Fok, N.R. Howell, M. Gregoire, A. Szabo, T. Pham, E. Davis, and G.J. Liu. 2014. Positron emission tomography and functional characterization of a complete PBR/TSPO knockout. *Nature communications*. 5:5452.

Braestrup, C., R. Albrechtsen, and R.F. Squires. 1977. High densities of benzodiazepine receptors in human cortical areas. *Nature*. 269:702-704.

Braestrup, C., and R.F. Squires. 1977. Specific benzodiazepine receptors in rat brain characterized by high-affinity (3H)diazepam binding. *Proc Natl Acad Sci U S A*. 74:3805-3809.

Caron, K.M., S.C. Soo, W.C. Wetsel, D.M. Stocco, B.J. Clark, and K.L. Parker. 1997. Targeted disruption of the mouse gene encoding steroidogenic acute regulatory protein provides insights into congenital lipoid adrenal hyperplasia. *Proc Natl Acad Sci U S A*. 94:11540-11545.

Chung, J.Y., H. Chen, A. Midzak, A.L. Burnett, V. Papadopoulos, and B.R. Zirkin. 2013. Drug ligand-induced activation of translocator protein (TSPO) stimulates steroid production by aged brown Norway rat Leydig cells. *Endocrinology*. 154:2156-2165.

Clark, B.J., J. Wells, S.R. King, and D.M. Stocco. 1994. The purification, cloning, and expression of a novel luteinizing hormone-induced mitochondrial protein in MA-10 mouse Leydig tumor cells. Characterization of the steroidogenic acute regulatory protein (StAR). *J Biol Chem*. 269:28314-28322.

Cong, L., F.A. Ran, D. Cox, S. Lin, R. Barretto, N. Habib, P.D. Hsu, X. Wu, W. Jiang, L.A. Marraffini, and F. Zhang. 2013. Multiplex genome engineering using CRISPR/Cas systems. *Science*. 339:819-823.

Davies, L.P., and V. Huston. 1981. Peripheral benzodiazepine binding sites in heart and their interaction with dipyridamole. *Eur J Pharmacol*. 73:209-211.

Falchi, A.M., B. Battetta, F. Sanna, M. Piludu, V. Sogos, M. Serra, M. Melis, M. Putzolu, and G. Diaz. 2007. Intracellular cholesterol changes induced by translocator protein (18 kDa) TSPO/PBR ligands. *Neuropharmacology*. 53:318-329.

Gavish, M., I. Bachman, R. Shoukrun, Y. Katz, L. Veenman, G. Weisinger, and A. Weizman. 1999. Enigma of the peripheral benzodiazepine receptor. *Pharmacol Rev*. 51:629-650.

Gocze, P.M., and D.A. Freeman. 1994. Factors underlying the variability of lipid droplet fluorescence in MA-10 Leydig tumor cells. *Cytometry*. 17:151-158.

Gonzalez-Polo, R.A., G. Carvalho, T. Braun, D. Decaudin, C. Fabre, N. Larochette, J.L. Perfettini, M. Djavaheri-Mergny, I. Youlyouz-Marfak, P. Codogno, M. Raphael, J. Feuillard, and G. Kroemer. 2005. PK11195 potently sensitizes to apoptosis induction independently from the peripheral benzodiazepin receptor. *Oncogene*. 24:7503-7513.

Hans, G., S. Wislet-Gendebien, F. Lallemend, P. Robe, B. Rogister, S. Belachew, L. Nguyen, B. Malgrange, G. Moonen, and J.M. Rigo. 2005. Peripheral benzodiazepine receptor (PBR) ligand cytotoxicity unrelated to PBR expression. *Biochem Pharmacol*. 69:819-830.

Hatty, C.R., A.P. Le Brun, V. Lake, L.A. Clifton, G.J. Liu, M. James, and R.B. Banati. 2014. Investigating the interactions of the 18kDa translocator protein and its ligand PK11195 in planar lipid bilayers. *Biochim Biophys Acta*. 1838:1019-1030.

Jaremko, L., M. Jaremko, K. Giller, S. Becker, and M. Zweckstetter. 2014. Structure of the mitochondrial translocator protein in complex with a diagnostic ligand. *Science*. 343:1363-1366.

Kletsas, D., W. Li, Z. Han, and V. Papadopoulos. 2004. Peripheral-type benzodiazepine receptor (PBR) and PBR drug ligands in fibroblast and fibrosarcoma cell proliferation: role of ERK, c-Jun and ligand-activated PBR-independent pathways. *Biochem Pharmacol*. 67:1927-1932.

Korkhov, V.M., C. Sachse, J.M. Short, and C.G. Tate. 2010. Three-dimensional structure of TspO by electron cryomicroscopy of helical crystals. *Structure*. 18:677-687.

Le Fur, G., M.L. Perrier, N. Vaucher, F. Imbault, A. Flamier, J. Benavides, A. Uzan, C. Renault, M.C. Dubroeucq, and C. Gueremy. 1983. Peripheral benzodiazepine binding sites: effect of PK 11195, 1-(2-chlorophenyl)-N-methyl-N-(1-methylpropyl)-3-isoquinolinecarboxamide. I. In vitro studies. *Life Sci*. 32:1839-1847.

Li, H., and V. Papadopoulos. 1998. Peripheral-type benzodiazepine receptor function in cholesterol transport. Identification of a putative cholesterol recognition/interaction amino acid sequence and consensus pattern. *Endocrinology*. 139:4991-4997.

Manna, P.R., J. Cohen-Tannoudji, R. Counis, C.W. Garner, I. Huhtaniemi, F.B. Kraemer, and D.M. Stocco. 2013. Mechanisms of action of hormone-sensitive lipase in mouse Leydig cells: its role in the regulation of the steroidogenic acute regulatory protein. *J Biol Chem*. 288:8505-8518.

Midzak, A., M. Rone, Y. Aghazadeh, M. Culty, and V. Papadopoulos. 2011. Mitochondrial protein import and the genesis of steroidogenic mitochondria. *Mol Cell Endocrinol*. 336:70-79.

Morohaku, K., S.H. Pelton, D.J. Daugherty, W.R. Butler, W. Deng, and V. Selvaraj. 2014. Translocator protein/peripheral benzodiazepine receptor is not required for steroid hormone biosynthesis. *Endocrinology*. 155:89-97.

Morohaku, K., N.S. Phuong, and V. Selvaraj. 2013. Developmental expression of translocator protein/peripheral benzodiazepine receptor in reproductive tissues. *PLoS One*. 8:e74509.

Mukhin, A.G., V. Papadopoulos, E. Costa, and K.E. Krueger. 1989. Mitochondrial benzodiazepine receptors regulate steroid biosynthesis. *Proc Natl Acad Sci U S A*. 86:9813-9816.

Murail, S., J.C. Robert, Y.M. Coic, J.M. Neumann, M.A. Ostuni, Z.X. Yao, V. Papadopoulos, N. Jamin, and J.J. Lacapere. 2008. Secondary and tertiary structures of the transmembrane domains of the translocator protein TSPO determined by NMR. Stabilization of the TSPO tertiary fold upon ligand binding. *Biochim Biophys Acta*. 1778:1375-1381.

Papadopoulos, V. 2014. On the Role of the Translocator Protein (18-kDa) TSPO in Steroid Hormone Biosynthesis. *Endocrinology*. 155:15-20.

Papadopoulos, V., H. Amri, N. Boujrad, C. Cascio, M. Culty, M. Garnier, M. Hardwick, H. Li, B. Vidic, A.S. Brown, J.L. Reversa, J.M. Bernassau, and K. Drieu. 1997a. Peripheral benzodiazepine receptor in cholesterol transport and steroidogenesis. *Steroids*. 62:21-28.

Papadopoulos, V., H. Amri, H. Li, N. Boujrad, B. Vidic, and M. Garnier. 1997b. Targeted disruption of the peripheral-type benzodiazepine receptor gene inhibits steroidogenesis in the R2C Leydig tumor cell line. *J Biol Chem*. 272:32129-32135.

Papadopoulos, V., A.G. Mukhin, E. Costa, and K.E. Krueger. 1990. The peripheral-type benzodiazepine receptor is functionally linked to Leydig cell steroidogenesis. *J Biol Chem*. 265:3772-3779.

Regan, J.W., H.I. Yamamura, S. Yamada, and W.R. Roeske. 1981. High affinity [3H]flunitrazepam binding: characterization, localization, and alteration in hypertension. *Life Sci*. 28:991-998.

Seneviratne, M.S., D. Faccenda, V. De Biase, and M. Campanella. 2012. PK11195 inhibits mitophagy targeting the F1Fo-ATPsynthase in Bcl-2 knock-down cells. *Curr Mol Med*. 12:476-482.

Stocco, D.M. 2014. The Role of PBR/TSPO in Steroid Biosynthesis Challenged. *Endocrinology*. 155:6-9.

Tu, L.N., K. Morohaku, P.R. Manna, S.H. Pelton, W.R. Butler, D.M. Stocco, and V. Selvaraj. 2014. Peripheral Benzodiazepine Receptor/Translocator Protein Global Knock-out Mice Are Viable with No Effects on Steroid Hormone Biosynthesis. *J Biol Chem*. 289:27444-27454.

Walter, R.B., J.L. Pirga, M.R. Cronk, S. Mayer, F.R. Appelbaum, and D.E. Banker. 2005. PK11195, a peripheral benzodiazepine receptor (pBR) ligand, broadly blocks drug efflux to chemosensitize leukemia and myeloma cells by a pBR-independent, direct transporter-modulating mechanism. *Blood*. 106:3584-3593.

Wang, H.J., J. Fan, and V. Papadopoulos. 2012. Translocator protein (Tspo) gene promoter-driven green fluorescent protein synthesis in transgenic mice: an in vivo model to study Tspo transcription. *Cell Tissue Res*. 350:261-275.

Yeliseev, A.A., and S. Kaplan. 1995. A sensory transducer homologous to the mammalian peripheral-type benzodiazepine receptor regulates photosynthetic membrane complex formation in Rhodobacter sphaeroides 2.4.1. *J Biol Chem*. 270:21167-21175.

CHAPTER 4

Translocator Protein (TSPO) Affects Mitochondrial Fatty Acid Oxidation in Steroidogenic Cells

Tu, L. N., Zhao, A. H., Hussein, M., Stocco, D. M., & Selvaraj, V. (2016). Translocator Protein (TSPO) Affects Mitochondrial Fatty Acid Oxidation in Steroidogenic Cells. *Endocrinology, 157*(3), 1110-1121.

ABSTRACT

Translocator protein (TSPO), also known as the peripheral benzodiazepine receptor (PBR), is a highly conserved outer mitochondrial membrane protein present in specific sub-populations of cells within different tissues. In recent studies, the presumptive model depicting mammalian TSPO as a critical cholesterol transporter for steroidogenesis has been refuted by studies examining effects of *Tspo* gene deletion *in vivo* and *in vitro*, biochemical testing of TSPO cholesterol transport function, and specificity of TSPO-mediated pharmacological responses. Nevertheless, high TSPO expression in steroid-producing cells seemed to indicate an alternate function for this protein in steroidogenic mitochondria. To seek an explanation, we used CRISPR/Cas9-mediated TSPO knockout steroidogenic MA-10 Leydig cell (MA-10:*Tspo*Δ/Δ) clones to examine changes to core mitochondrial functions resulting from TSPO deficiency. We observed that, 1) MA-10:*Tspo*Δ/Δ cells had a shift in substrate utilization for energy production from glucose to fatty acids with significantly higher mitochondrial fatty acid oxidation (FAO), and increased reactive oxygen species (ROS) production; 2) oxygen consumption rate (OCR), mitochondrial membrane potential ($\Delta\psi m$), and proton leak were not different between MA-10:*Tspo*Δ/Δ and MA-10:*Tspo*+/+ control cells. Consistent with this finding, TSPO deficient adrenal glands from global TSPO knockout ($Tspo^{-/-}$) mice also showed upregulation of genes involved in FAO compared to the TSPO floxed ($Tspo^{fl/fl}$) controls. These results demonstrate the first experimental evidence that TSPO can affect mitochondrial energy homeostasis through modulation of FAO, a function that appears to be consistent with high levels of TSPO expression observed in cell types active in lipid storage/metabolism.

INTRODUCTION

Translocator protein (TSPO), also known as the peripheral benzodiazepine receptor (PBR), was first identified in 1977 as a secondary target for diazepam-binding (Braestrup and Squires, 1977). Although TSPO protein sequence is highly conserved from bacteria to mammals (Yeliseev and Kaplan, 1995), functions reported for TSPO have been variable depending on organism and sometimes even context (Gatliff and Campanella, 2012; Gavish et al., 1999). Hence, its exact molecular function continues to remain elusive. For more than two decades, mammalian TSPO was depicted as a mitochondrial cholesterol transporter indispensable for steroid hormone biosynthesis (Papadopoulos et al., 1997; Papadopoulos and Miller, 2012). Abundant expression of TSPO in steroidogenic cells, and its localization to the outer mitochondrial membrane (Anholt et al., 1986), appeared to support this functional role. However, recent genetic and pharmacological evidence has refuted this model by showing that TSPO has no role in steroidogenesis both *in vivo* and *in vitro* (Banati et al., 2014; Morohaku et al., 2014; Tu et al., 2014; Tu et al., 2015). This paradigm shift in understanding of TSPO function has precipitated a need to reevaluate functional interpretations made for TSPO in previous studies [reviewed in (Selvaraj et al., 2015)].

Despite these recent findings that TSPO has no role in steroidogenesis, a new model for TSPO function explaining the reason for its high expression in steroidogenic cells is yet to be established (Selvaraj and Stocco, 2015). This gap in knowledge has led to speculations that a role in steroidogenic cell function, unrelated to mitochondrial cholesterol transport might still be relevant for TSPO (Fan et al., 2015). Indeed high expression of TSPO in steroidogenic cells of the adrenals, testes and ovaries is evident from several studies (Bribes et al., 2004; De Souza et al., 1985), and has been reproducible (Morohaku et al., 2013; Tu et al., 2014). This correlation has been the basis of numerous studies attempting to link TSPO function to steroidogenesis, overshadowing the fact that TSPO expression is not particularly confined to steroidogenic cells within tissues (Morohaku et al., 2013). Expression of TSPO in many other cell types that do not produce steroids in tissues such as lungs, kidneys, livers, spleens and bone marrows

(Banati et al., 2014; Tu et al., 2014), suggest perhaps a broader function for TSPO in mitochondrial homeostasis, which remains to be explored in genetic models.

In pharmacological studies, TSPO has been associated with almost all core mitochondrial functions. TSPO binding drugs have been shown to affect mitochondrial energy metabolism (Hirsch et al., 1989; Larcher et al., 1989), apoptosis (Furre et al., 2005; Maaser et al., 2005), intracellular calcium signaling (Campanella et al., 2008; Hong et al., 2006), and reactive oxygen species (ROS) production (Fennell et al., 2001; Zeno et al., 2012). However, interpreting effects observed using TSPO ligands have been confounded by inconsistencies due to inherent binding distinctions/affinities (Scarf et al., 2012), and potential alternate targets in the cell (Li et al., 2008; Seneviratne et al., 2012). As a result, these observations have not been relevant for advancing knowledge of the precise physiological function of TSPO. Another confounding factor of membrane-drug interactions of TSPO binding chemicals has also recently surfaced (Hatty et al., 2014; Scarf et al., 2012). Limitations of pharmacological studies were highlighted when the previously believed role for TSPO in mitochondrial permeability transition (Kinnally et al., 1993), could occur even after TSPO deletion (Sileikyte et al., 2014). Similarly, the prototypical TSPO binding drug PK11195 [N-butan-2-yl-1-(2-chlorophenyl)-N-methylisoquinoline-3-carboxamide] that was used in demonstration of the first pharmacological basis for TSPO function in steroidogenesis (Mukhin et al., 1989), could stimulate steroid hormone production in TSPO deleted steroidogenic cells (Tu et al., 2015). Therefore, it has become important to clarify the different pharmacological effects reported on mitochondrial functions using *Tspo* gene deleted models to advance understanding of its physiological role in steroidogenic cells.

Previously, we generated CRISPR/Cas9-mediated TSPO knockout MA-10 (MA-10:*Tspo*Δ/Δ) Leydig cells and demonstrated that TSPO deletion did not have any effect on viability or steroidogenesis (Tu et al., 2015). In the present study, we examine the effect of TSPO deletion in this cell type on different mitochondrial functions. Our systematic investigation of mitochondrial properties led us to uncover that TSPO-deficient MA-10 cells increased fatty acid uptake, fatty acid oxidation (FAO), and

increased reactive oxygen species (ROS) production. Extending this observation *in vivo*, we found that TSPO deficiency in adrenal glands of global TSPO knockout (*Tspo*$^{-/-}$) mice also resulted in upregulation of genes involved in FAO compared to the TSPO floxed (*Tspo*$^{fl/fl}$) controls. These results indicate that TSPO affects fatty acid metabolism, a function that positively correlates with high levels of TSPO expression observed in cell types active in lipid storage/metabolism.

MATERIALS AND METHODS

Cells and mice

The MA-10 Leydig cell line (Ascoli, 1981), was used as a model for male steroidogenic cells. Two independent clones of TSPO knockout MA-10 cells (MA-10:*Tspo*Δ/Δ) previously generated by CRISPR/Cas9-mediated targeting of Exon 2 of the *Tspo* gene were compared to intact MA-10 cells (MA-10:*Tspo*+/+) in all experiments. Generation and characterization of *Tspo* mutations in these cells have been previously published (Tu et al., 2015). Cells were grown at 37˚C under 5% CO_2 in Dulbecco's modified eagle medium/DMEM high glucose (25 mM glucose, 1 mM pyruvate) containing 10% FBS and 1% penicillin-streptomycin. Generation and validation of *Tspo*$^{fl/fl}$ and *Tspo*$^{-/-}$ mice has been previously described (Tu et al., 2014); both male and female mice were sampled at 8-12 weeks of age. Animals were maintained in accordance with the National Institute of Health Guide for the Care and Use of Laboratory Animals. The Institutional Animal Care and Use Committee of Cornell University approved the experiment described.

Progesterone assay

For dibutyryl-cAMP (Bt_2cAMP) stimulation experiments, 5 x 10^4 cells were plated per well in a 96 well plate and allowed to attach overnight. Cells were then washed with PBS and incubated with 0.5 mM Bt_2cAMP in serum free media for 6 hrs. For both baseline and stimulation, supernatants were

collected and progesterone was measured as previously described (Tu et al., 2015), and normalized to total protein in each well.

Measurement of mitochondrial respiration

Mitochondrial respiration was calculated from oxygen consumption rates (OCR) under specific conditions using an XF24 Extracellular Flux Analyzer (Seahorse Bioscience). For quantifying mitochondrial respiration, MA-10:*Tspo*+/+ cells were paired with one of the MA-10:*Tspo*Δ/Δ clones in different wells at a density of 50,000 cells in the same XF24 cell culture microplates in growth medium overnight. One hour before assay, cells were washed and incubated in XF assay medium (DMEM with no bicarbonate) supplemented with 25 mM glucose and 1 mM pyruvate at 37˚C in a CO_2-free atmosphere. Changes to OCR were measured in real time every 3-5 minutes. Oligomycin, Carbonyl cyanide 4-(trifluoromethoxy)phenylhydrazone (FCCP), Antimycin A and Rotenone were sequentially injected into each well to assess basal respiration, coupling of respiratory chain, proton leak and mitochondrial spare respiratory capacity. OCR values were used to calculate mitochondrial coupling efficiency, spare respiratory capacity and proton leak. Extracellular acidification rates (ECAR) as changes in mpH over time were simultaneously measured.

Measurement of fatty acid oxidation

Fatty acid oxidation (FAO) was calculated from OCR under specific conditions using an XF24 Extracellular Flux Analyzer. For quantifying FAO, MA-10:*Tspo*+/+ and MA-10:*Tspo*Δ/Δ cells were plated at a density of 50,000 cells in the XF24 cell culture microplates overnight. Cells were then starved in substrate-limited medium (DMEM containing 0.5 mM glucose, 1% FBS, 1 mM Glutamax and 0.5 mM carnitine) for 3 hours before it was replaced with FAO assay media (Krebs-Henseleit buffer supplemented with 2.5 mM glucose, 0.5 mM carnitine and 5 mM HEPES). Etomoxir (40 μM) was added 20 minutes before the assay. Bovine serum albumin (BSA) or Palmitate-BSA was added to specific wells right before starting the assay with sequential injections of Oligomycin, FCCP, Antimycin A and Rotenone, and changes to OCR were measured in real time every 3-5 minutes as described above.

Measurement of ATP

MA-10:*Tspo*+/+ and MA-10:*Tspo*Δ/Δ cells in growth phase at 60% confluence were maintained in either high glucose DMEM, or changed to no glucose DMEM, with or without 50 µM Etomoxir for 3 hours. Cells were then collected and lysed in ice-cold trichloroacetic acid (0.5% final conc.) for 5 minutes, and centrifuged at 10,000 x g to precipitate proteins. Supernatant containing ATP was collected and neutralized with 1 M Tris-acetate buffer, 1mM EDTA (pH 7.75), and kept on ice until measurement. ATP measurement was performed using a luciferin-luciferase method with an Enliten® ATP detection kit (Promega), and luminescence was measured using an Infinite® 200Pro reader (Tecan). Measured ATP values were normalized to total protein content for comparison between groups.

Measurement of mitochondrial membrane potential (Δ*ψm*)

Cells in growth phase at 60% confluence were trypsinized and resuspended in phenol red-free high glucose DMEM, 10% FBS. Cells were then incubated with 100 nM Mitotracker® Green FM and 20 nM tetramethylrhodamine methyl ester (TMRM) at 37˚C for 30 minutes in the dark. The labeled MA-10 cells were examined separately using wavelengths 488/520 (excitation/emission) nm for Mitotracker® Green and 488/575 nm for TMRM with a Gallios flow cytometer (Beckman Coulter). Intensity of TMRM was normalized to that of Mitotracker® Green for comparison of Δ*ψm* among samples.

Measurement of reactive oxygen species

Production of reactive oxygen species and superoxide were directly monitored in live cells by flow cytometry using the total ROS/Superoxide detection kit (Enzo Life Science). Cells were grown overnight to 60% density, trypsinized and washed with phosphate buffered saline (PBS). Cells were then incubated with fluorescent dyes: oxidative stress detection reagent (green) for total ROS and reactive nitrogen species (RNS), and superoxide detection reagent (orange) for 30 minutes at 37^0C in the dark. The labeled MA-10 cells from both genotypes were examined using wavelengths 488/520 nm and 550/620 nm in a Gallios flow cytometer (Beckman Coulter). Positive controls (200 µM pyocyanin treatment) and

negative controls (5 mM N-acetyl-L-cysteine treatment) were used to confirm analytical methods. Mean fluorescence intensity was calculated from data collected from the two channels and values were compared between the two genotypes using Kaluza Flow Analysis software (Beckman Coulter).

Lentiviral expression of TSPO in MA-10 cells

Tspo cDNA was cloned in a lentiviral vector [pLenti CMV GFP Puro, (Campeau et al., 2009)] for expression in mammalian cells. Lentiviral particles were packaged using 293T cells by cotransfecting with helper plasmids encoding gag, pol and rev, and viral supernatants were collected at 48h and 72h. Unmodified pLenti vector was used to make GFP control viruses. MA-10:*Tspo*+/+ cells and the two MA-10:*Tspo*Δ/Δ clones were transduced using *Tspo* and control lentiviruses in medium supplemented with 6 μg/ml Polybrene (Sigma) for 24 hours. Infection efficiency was analyzed visualizing GFP fluorescence or TSPO expression after 5 days and used for experiments.

Gene expression

Total RNA was extracted from MA-10 cells and adrenal glands using Trizol (Life Technologies). Reverse transcription was carried out using Multiscribe™ reverse transcriptase (Life Technologies). Gene expressions were quantified using a SYBR® Green detection method (Affymetrix) with validated primer sequences obtained from PrimerBank database (Spandidos et al., 2010). Primer specificity and amplification efficiency were confirmed and sequences are provided in Supplemental Table 1. All expression data were normalized to internal control genes, TATA-binding protein (*Tbp*) or Glyceraldehyde 3-phosphate dehydrogenase (*Gapdh*). Relative quantification of fold-change was calculated using the $2^{-\Delta/\Delta Ct}$ method (Livak and Schmittgen, 2001).

Protein expression

Total protein concentration in each sample was measured using the bicinchoninic acid (BCA) assay (Pierce). Proteins (cells: 30 μg and mouse tissues: 75 μg) were separated by SDS-PAGE and immunoblotted using rabbit monoclonal primary antibodies against TSPO (Abcam) and isocitrate

dehydrogenase 2 (IDH2) (Abcam), mouse monoclonal antibody against voltage-dependent anion channel 1 (VDAC1) (Abcam), or rabbit polyclonal antibody against uncoupling protein 2 (UCP2) (Alpha Diagnostics). Each primary antibody was multiplexed with the loading control β-actin (ACTB) (Li-Cor). Simultaneous detection was performed using IRDye 700 and 800-labeled secondary antibodies under a laser fluorescence scanner (Li-Cor) and quantified using ImageJ as described previously (Morohaku et al., 2014; Morohaku et al., 2013).

Statistics

Numeric differences of interval level data between groups were compared using a Student's t-test; comparisons for more than two groups were performed using ANOVA and *post hoc* Tukey's test ($p<0.05$ was considered significant). All analyses were performed using Prism 5 (GraphPad). Data are represented as mean ± standard error of the mean and replicates are as indicated in figure legends.

RESULTS

TSPO deletion does not affect mitochondrial respiration in MA-10 cells

Complete absence of TSPO in the two MA-10:*Tspo*Δ/Δ clones, compared to high levels of TSPO expression in intact MA-10:*Tspo*+/+ cells (Figure 4.1A), make them excellent comparative models to investigate TSPO function. As demonstrated previously (Tu et al., 2015), deletion of TSPO in these cells had no effect on steroid hormone biosynthesis (Figure 4.1B). We confirmed using Western blots that loss of such an abundant mitochondrial protein did not affect expression of other mitochondrial markers in the two MA-10:*Tspo*Δ/Δ clones: VDAC1, present in the outer mitochondrial membrane and IDH2, present in the mitochondrial matrix were not different between the two MA-10:*Tspo*Δ/Δ clones and MA-10:*Tspo*+/+ cells (Figure 4.1A).

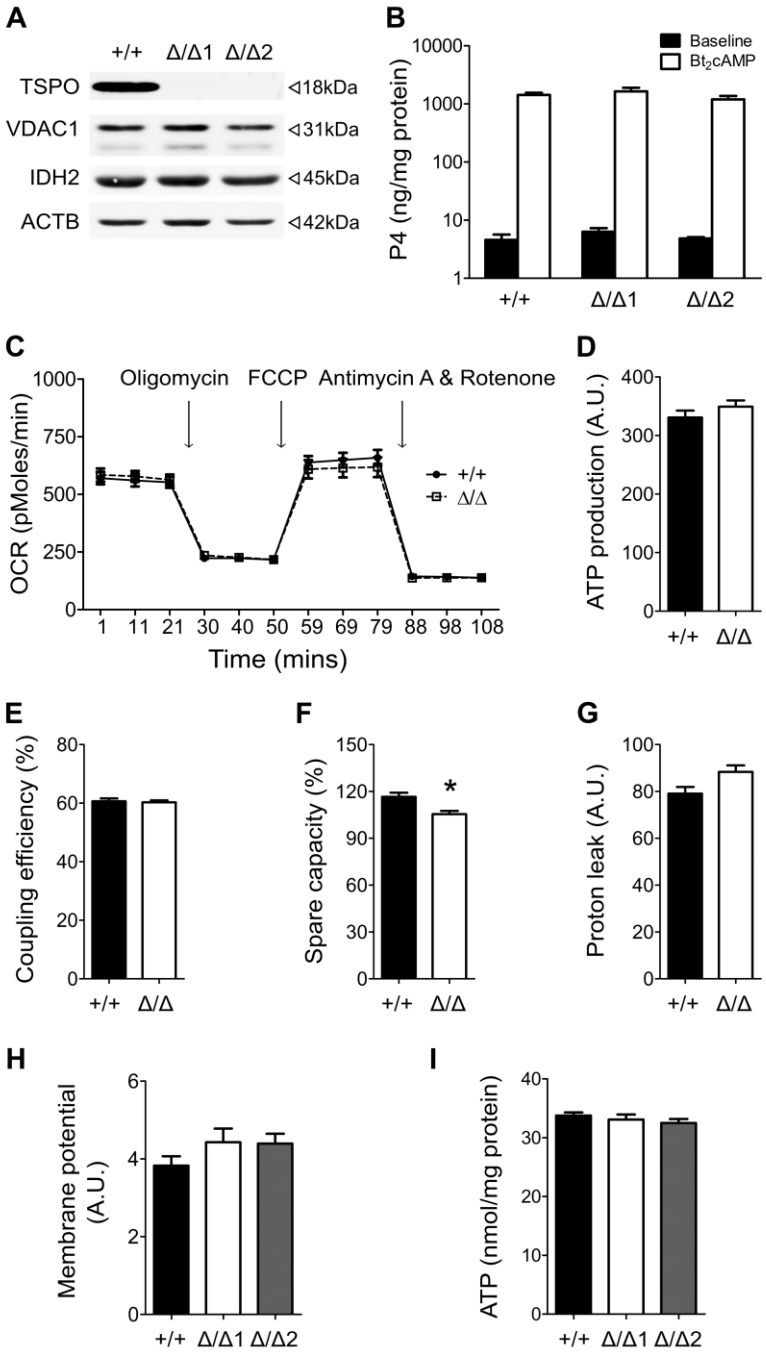

Figure 4.1. TSPO deletion does not alter mitochondrial bioenergetics in MA-10 cells. **(A)** Representative western blots of MA-10:*Tspo*+/+ and the two MA-10:*Tspo*Δ/Δ clones showing that TSPO deletion did not affect expressions of mitochondrial proteins VDAC1 and IDH2. **(B)** TSPO deletion did not affect baseline or Bt_2cAMP stimulated progesterone production in the two MA-10:*Tspo*Δ/Δ clones compared to the intact MA-10:*Tspo*+/+ cells (For A-B, n=3/group). **(C)** Representative results from a paired assay showing that baseline oxygen consumption rate (OCR) and maximal OCR after addition of the protonophore FCCP were not different between MA-10:*Tspo*+/+ and MA-10:*Tspo*Δ/Δ2 cells. OCR declined upon blocking ATP synthase activity using oligomycin, or inhibiting electron transport chain

using antimycin A and rotenone, but these were also not different between the two genotypes. **(D)** Calculated ATP production was not different between MA-10:*Tspo*+/+ and MA-10:*Tspo*Δ/Δ cells. **(E)** Calculated mitochondrial coupling efficiency was not different between MA-10:*Tspo*+/+ and MA-10:*Tspo*Δ/Δ cells. **(F)** Calculated spare respiratory capacity was significantly lower in MA-10:*Tspo*Δ/Δ compared to MA-10:*Tspo*+/+ cells. **(G)** Calculated proton leak was not different between the two genotypes. (For C-G, n=10/group) **(H)** Normalized TMRM/Mitotracker® Green fluorescence intensity comparison between MA-10:*Tspo*+/+ and MA-10:*Tspo*Δ/Δ cells showed no difference in baseline Δψm (n=5-6/group). **(I)** Total ATP levels were not different between MA-10:*Tspo*+/+ and MA-10:*Tspo*Δ/Δ cells in high glucose medium (n=5/group).

Direct measurements of baseline and maximal OCR showed no significant difference between MA-10:*Tspo*+/+ cells and both MA-10:*Tspo*Δ/Δ clones; representative results from one paired assay comparing MA-10:*Tspo*+/+ cells and MA-10:*Tspo*Δ/Δ1 clone is presented (Figure 4.1C). Calculated ATP production, oxidative phosphorylation coupling efficiency and proton leak were also unchanged in MA-10:*Tspo*Δ/Δ cells compared to MA-10:*Tspo*+/+ cells (Figure 4.1 D,E,G). The spare respiratory capacity was significantly reduced in MA-10:*Tspo*Δ/Δ1 clone compared to MA-10:*Tspo*+/+ cells (Figure 4.1F), but the difference was very modest and not observed in MA-10:*Tspo*Δ/Δ2 clone. All other results were consistent in the second MA-10:*Tspo*Δ/Δ2 clone (data not shown).

TSPO deletion does not affect ΔΨm and ATP production in MA-10 cells

Assessment of ΔΨm using the membrane potential-dependent probe TMRM, normalized to Mitotracker® Green showed that MA-10:*Tspo*+/+ cells and the two MA-10:*Tspo*Δ/Δ clones had similar baseline ΔΨm (Figure 4.1H). Provided that oxygen consumption and Δψm were unchanged, ATP production was not expected to be different between MA-10:*Tspo*Δ/Δ cells as compared to the intact MA-10:*Tspo*+/+ cells. In corroboration, total ATP levels measured by luciferin-luciferase assay were not affected by TSPO deletion in the two MA-10:*Tspo*Δ/Δ clones when compared to MA-10:*Tspo*+/+ cells when all cells were maintained in DMEM high glucose growth medium (Figure 4.1I).

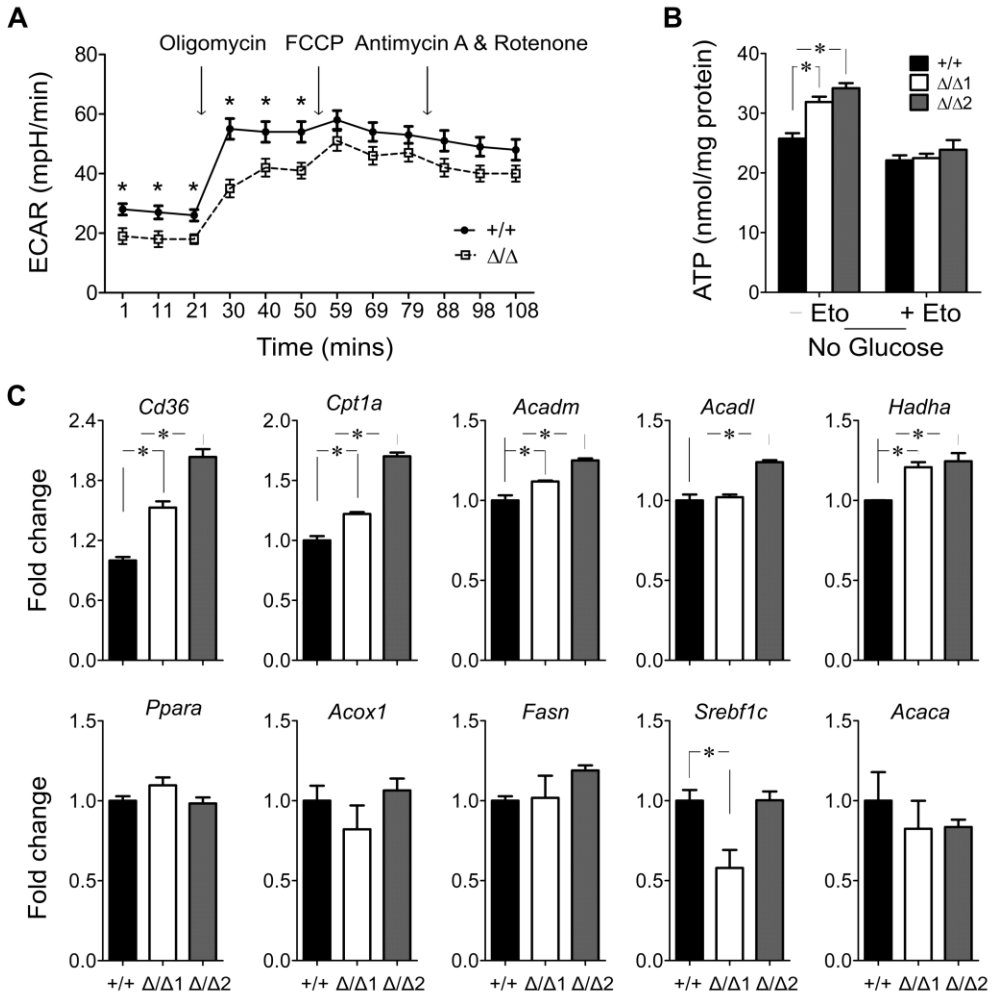

Figure 4.2. Shift in substrate utilization for energy production in TSPO deficient MA-10 cells. (A) Baseline extracellular acidification rates (ECAR) and maximal ECAR after addition of oligomycin were significantly lower in MA-10:*Tspo*Δ/Δ compared to MA-10:*Tspo*+/+ cells (n=10/group). **(B)** When cells were cultured in medium without glucose, ATP production was significantly higher in MA-10:*Tspo*Δ/Δ cells compared to MA-10:*Tspo*+/+ cells. Treatment with etomoxir (Eto), a CPT1A inhibitor, resulted in decrease in ATP production in all cells to similar levels (n=4-6/group). **(C)** Expression of *Cd36*, a key gene for fatty acid uptake is significantly higher in MA-10:*Tspo*Δ/Δ compared to MA-10:*Tspo*+/+ cells. Expression levels of key genes in mitochondrial β-oxidation pathway: *Cpt1a*, *Acadm*, *Acadl*, and *Hadha* were significantly upregulated in MA-10:*Tspo*Δ/Δ compared to MA-10:*Tspo*+/+ cells. There was no difference in the transcription factor *Ppara* and peroxisomal β-oxidation gene *Acox1* between the two genotypes. Expression levels of key genes in lipogenesis pathway: *Srebf1c*, *Fasn*, *Acaca* were not different between MA-10:*Tspo*+/+ and MA-10:*Tspo*Δ/Δ cells, except that *Srebf1c* was significantly lower in one clone MA-10:*Tspo*Δ/Δ1 but not in MA-10:*Tspo*Δ/Δ2, compared to MA-10:*Tspo*+/+ cells (n=3/group; *p<0.05).

TSPO deletion increases mitochondrial fatty acid oxidation in MA-10 cells

The extracellular acidification rates (ECAR), measured simultaneously with OCR were significantly lower in MA-10:*Tspo*Δ/Δ cells compared to MA-10:*Tspo*+/+ cells (Figure 4.2A), which indicated a decrease in glycolysis associated with TSPO deletion. However, the fact that total ATP levels were not different in MA-10:*Tspo*Δ/Δ clones compared to MA-10:*Tspo*+/+ cells (Figure 4.1I), suggested a shift favoring substrate utilization from glucose to fatty acids. To directly examine the contribution of FAO to ATP production, MA-10:*Tspo*Δ/Δ clones and MA-10:*Tspo*+/+ cells were incubated in no glucose DMEM medium to minimize ATP production through glycolysis and compared. Under this condition, ATP levels were then markedly higher (20-29%) in both MA-10:*Tspo*Δ/Δ clones compared to intact MA-10:*Tspo*+/+ cells (Figure 4.2B). When cells under this same condition (no glucose DMEM) were treated with etomoxir, an irreversible carnitine palmitoyltransferase I (CPT1A) inhibitor to block mitochondrial FAO, ATP in MA-10:*Tspo*Δ/Δ clones decreased to levels almost identical to MA-10:*Tspo*+/+ cells (Figure 4.2B). This provided confirmation that the increase in ATP was associated with higher FAO in MA-10:*Tspo*Δ/Δ clones.

Expression levels of crucial genes involved in fatty acid metabolism indicated that MA-10:*Tspo*Δ/Δ clones had increased fatty acid uptake and utilization. Expression of the cluster of differentiation 36 (*Cd36*), also known as fatty acid translocase, was upregulated in MA-10:*Tspo*Δ/Δ clones compared to MA-10:*Tspo*+/+ cells indicating higher fatty acid uptake in these cells (Figure 4.2C). Expressions of *Cpt1a*, acyl-CoA dehydrogenase medium chain (*Acadm*), acyl-CoA dehydrogenase long chain (*Acadl*) and hydroxyacyl-CoA dehydrogenase (*Hadha*), the key genes in mitochondrial FAO, were also significantly higher in MA-10:*Tspo*Δ/Δ cells compared to MA-10:*Tspo*+/+ cells (Figure 4.2C). However, peroxisome proliferator-activated receptor alpha (*Ppara*) and the key peroxisomal FAO enzyme acyl-CoA oxidase 1 (*Acox1*) were not altered as a result of TSPO deletion (Figure 4.2C). Moreover, we observed that the upregulation of mitochondrial FAO is not attributed to higher lipogenesis, because expression of enzymes involved in the lipogenic pathway like fatty acid synthase

(*Fasn*), acetyl-CoA carboxylase alpha (*Acaca*) were not different in MA-10:*Tspo*Δ/Δ clones compared to compared to MA-10:*Tspo*+/+ cells (Figure 4.2C). The sterol regulatory element-binding protein 1c (*Srebf1c*) was observed to be downregulated in clone MA-10:*Tspo*Δ/Δ1 but not in clone MA-10:*Tspo*Δ/Δ2 (Figure 4.2C).

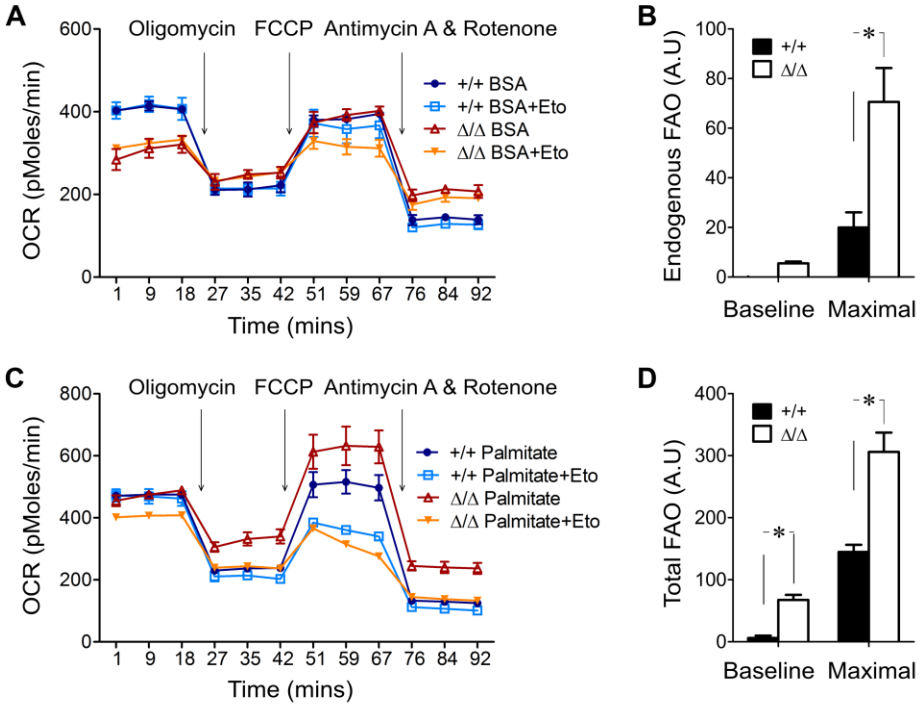

Figure 4.3. TSPO deficiency increases fatty acid oxidation in MA-10 cells. (A) MA-10:*Tspo*+/+ and MA-10:*Tspo*Δ/Δ cells were starved and given only BSA in FAO assay media. Etomoxir (Eto) was added to some wells 20 minutes before the assay. OCR was measured to indicate oxidation of endogenous fatty acids. **(B)** Quantification of endogenous FAO as the difference between conditions with or without Etomoxir treatment during starvation showed significantly higher maximal FAO in MA-10:*Tspo*Δ/Δ cells compared to intact MA-10 cells. **(C)** MA-10:*Tspo*+/+ and MA-10:*Tspo*Δ/Δ cells were starved and given BSA-palmitate. Etomoxir (Eto) was added to some wells 20 minutes before the assay. OCR was measured to indicate total FAO. **(D)** Quantification of total FAO as the difference between conditions with or without Etomoxir treatment, both containing BSA-palmitate showed higher baseline and maximal FAO in MA-10:*Tspo*Δ/Δ cells. (For all panels: n=3/group; replicated 2 times, *p<0.05).

Functional measurement of β-oxidation using substrate restricted media showed significantly higher endogenous β-oxidation rates in MA-10:*Tspo*Δ/Δ1 cells compared to MA-10:*Tspo*+/+ cells (Figure 4.3 A-B). When provided with an exogenous substrate in the form of palmitate, total mitochondrial β-

oxidation (both endogenous and exogenous) of MA-10:*Tspo*Δ/Δ1 cells were significantly higher at both baseline and maximal rates than MA-10:*Tspo*+/+ cells (Figure 4.3 C-D). These data confirmed that TSPO deletion increased mitochondrial FAO in MA-10 cells.

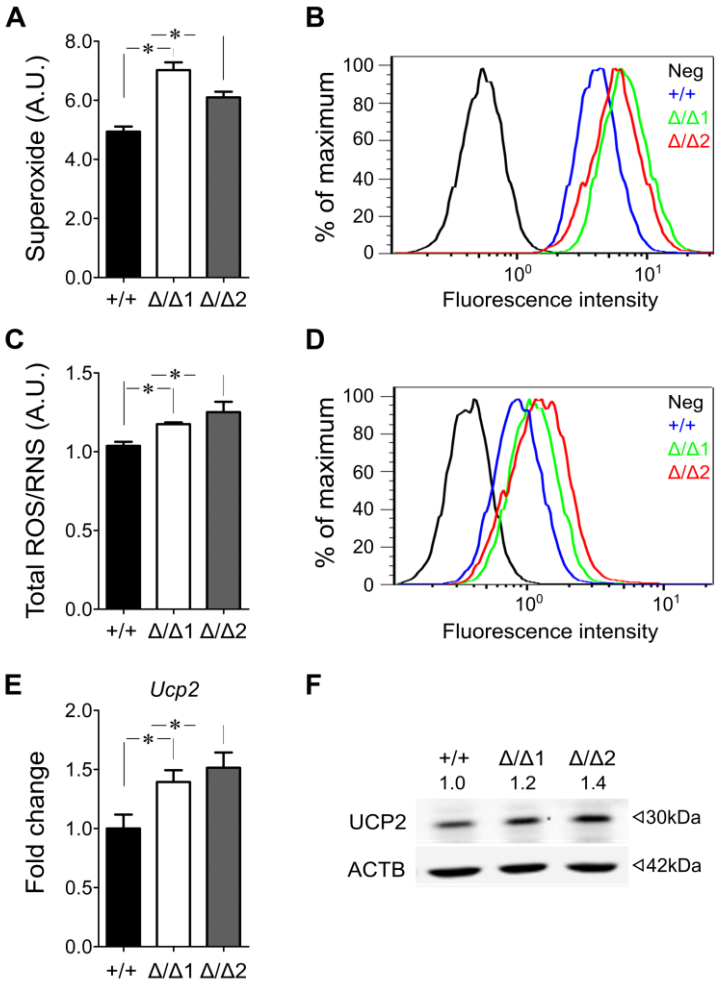

Figure 4.4. TSPO deficiency increases ROS and UCP2 levels in MA-10 cells. (A) Superoxide production in both MA-10:*Tspo*Δ/Δ cell clones was significantly higher compared to MA-10:*Tspo*+/+ cells (n=5-6/group). **(B)** Overlay plot showing higher fluorescence intensity for superoxide-responsive dye in MA-10:*Tspo*Δ/Δ clones compared to MA-10:*Tspo*+/+ cells. **(C)** Total reactive oxygen species and reactive nitrogen species (ROS/RNS) in both MA-10:*Tspo*Δ/Δ cells were significantly higher compared to MA-10:*Tspo*+/+ cells (n=5-6/group). **(D)** Overlay plot showing higher fluorescence intensity of ROS/RNS-responsive dye in MA-10:*Tspo*Δ/Δ clones compared to MA-10:*Tspo*+/+ cells. **(E)** Gene expression of *Ucp2* was upregulated in MA-10:*Tspo*Δ/Δ clones compared to MA-10:*Tspo*+/+ cells (n=3/group). **(F)** Representative Western blot for UCP2 showing increased expression in MA-10:*Tspo*Δ/Δ clones compared to MA-10:*Tspo*+/+ cells (normalized numerical intensities to ACTB are indicated).

ROS and uncoupling protein 2 are upregulated in MA-10:*Tspo*Δ/Δ cells

As we observed an increase in FAO in MA-10:*Tspo*Δ/Δ clones, we investigated if production of ROS was also increased in these cells compared to MA-10:*Tspo*+/+ cells. We detected that superoxide levels were significantly elevated in MA-10:*Tspo*Δ/Δ clones compared to MA-10:*Tspo*+/+ cells (Figure 4.4 A-B). Total ROS/RNS levels, including hydrogen peroxide, peroxynitrite and hydroxyl radicals, were also significantly higher in MA-10:*Tspo*Δ/Δ clones compared to MA-10:*Tspo*+/+ cells (Figure 4.4 C-D). Changes in mitochondrial metabolism and ROS are known to affect expression of uncoupling proteins (UCPs). We observed that *Ucp2* gene expression and UCP2 protein levels were significantly upregulated in MA-10:*Tspo*Δ/Δ clones compared to MA-10:*Tspo*+/+ cells (Figure 4.4 E-F). *Ucp1* expression was not detected in MA-10 cells (not shown).

TSPO overexpression decreases expression of FAO genes in MA-10 cells

To examine if the effects of TSPO deficiency can be reversed by reintroducing TSPO expression in MA-10:*Tspo*Δ/Δ cells, we infected cells with *Tspo* lentiviruses for stable expression. In the resulting cells, we observed strong TSPO overexpression after 5 days (Figure 4.5A). This TSPO overexpression did not perturb expression of VDAC1 in the OMM (Figure 4.5A). By examining the effect of TSPO overexpression on genes involved in FAO, we found that expression levels of *Cpt1a* and *Hadha* were significantly reduced (Figure 4.5B), indicating a reverse response to the TSPO deficient phenotype. However, expression of *Cd36, Acadl* and *Acadm* remained unchanged in TSPO overexpressing cells (not shown).

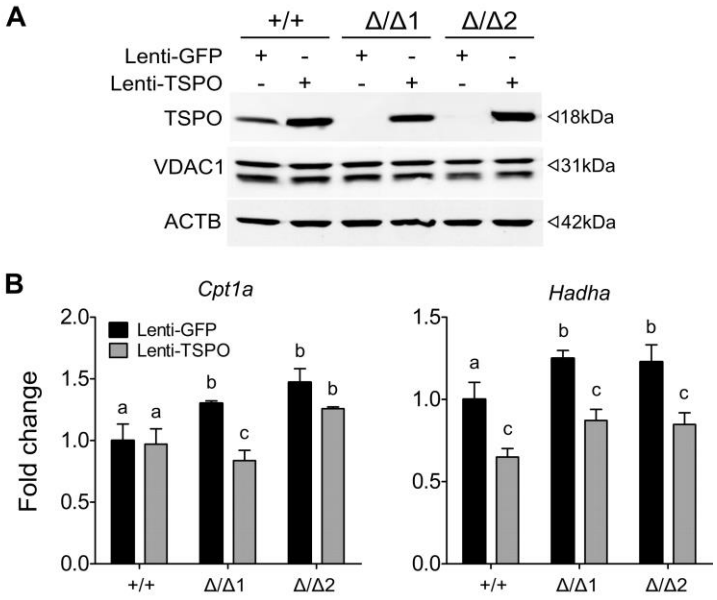

Figure 4.5. TSPO overexpression in TSPO deficient MA-10 cells downregulates genes involved in FAO. (A) Representative western blots of MA-10:*Tspo*+/+ cells and the two MA-10:*Tspo*Δ/Δ clones showing TSPO, VDAC1 and ACTB expression after infection with *Tspo* lentivirus or GFP lentivirus (control). TSPO was overexpressed in intact MA-10:*Tspo*+/+ cells and the two MA-10: *Tspo*Δ/Δ clones; expression of VDAC1 was not affected after TSPO overexpression. **(B)** Expression of *Cpt1a* and *Hadha* was significantly downregulated in TSPO-overexpressing MA-10:*Tspo*Δ/Δ cells (n=3/group; a, b, c indicate significant differences between groups, $p<0.05$).

Mitochondrial FAO genes are upregulated in *Tspo*$^{-/-}$ adrenal glands

To investigate if *in vitro* effects of TSPO deficiency on FAO were discernible *in vivo*, we examined the adrenal glands of global *Tspo*$^{-/-}$ mice for expression of genes involved in FAO compared to the *Tspo*$^{fl/fl}$ controls (Figure 4.6). We found that adrenal glands from *Tspo*$^{-/-}$ mice significantly upregulated expression of *Cd36*, suggesting higher fatty acid uptake in *Tspo*$^{-/-}$ adrenals compared to *Tspo*$^{fl/fl}$ cohorts. Expressions of mitochondrial FAO genes *Cpt1a* and *Acadl* were also significantly upregulated in *Tspo*$^{-/-}$ adrenals compared to *Tspo*$^{fl/fl}$ cohorts. Although *Acadm* and *Hadha* were found upregulated in *Tspo*$^{-/-}$ adrenals, the difference did not reach statistical significance.

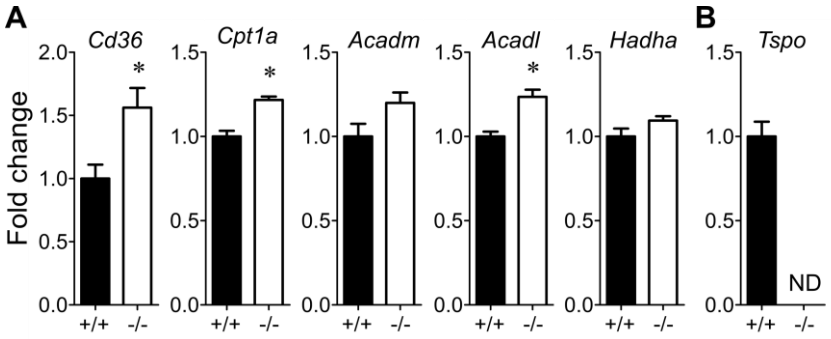

Figure 4.6. Adrenals from *Tspo*$^{-/-}$ mice show upregulation of genes involved in FAO. (A) Expression of *Cd36, Cpt1a* and *Acadl* was significantly upregulated in adrenal glands from *Tspo*$^{-/-}$ mice compared to *Tspo*$^{fl/fl}$ cohorts. Expression of *Acadm* and *Hadha* were also elevated in *Tspo*$^{-/-}$ adrenal glands but values did not reach statistical significance. **(B)** Expression of *Tspo* was confirmed to be absent in *Tspo*$^{-/-}$ adrenal glands. (For both panels: n=4/group, *p<0.05).

TSPO is highly expressed in tissues active in lipid storage/metabolism

In order to examine TSPO expression levels in different tissues, we examined a wider panel of 14 murine tissues including brown adipose tissue (BAT) and epididymal white adipose tissue (WAT), in addition to brain, thymus, heart, lung, liver, spleen, adrenal, kidney, testis and ovary that we also studied previously (Tu et al., 2014). When 75 µg protein from each tissue separated by SDS-PAGE was used in Western blots, the results showed that TSPO could be detected in almost all tissues, albeit at different levels (Figure 4.7A). Note: Loading controls like ACTB showed significant variability in expression between tissues [as seen previously (Tu et al., 2014)]; use of a mitochondrial protein like IDH2 was also not applicable due to dramatic changes to functional characteristics of mitochondria in these tissues (not shown). Based on equal protein loading, TSPO expression was the highest in adrenal glands, followed by BAT and WAT. Expression levels were at the average in lung, kidney and spleen, and weaker in other tissues, with extremely low expression in the brain (Figure 4.7A). Testis showed relatively weak expression of TSPO because only a small population of cells in the testis, that comprise of Leydig and Sertoli cells express TSPO (Morohaku et al., 2013). TSPO expression in the ovary, a major steroidogenic tissue, was at similar levels to that seen in the liver. Adrenal glands, BAT and WAT had much higher

TSPO expression that was approximately 7-, 5- and 2.5-fold respectively compared to expression seen in the liver (Figure 4.7B). These results demonstrated that TSPO expression is not enriched specifically in steroid producing tissues, but rather in tissues that are active in lipid storage or metabolism as indicated by high lipid content.

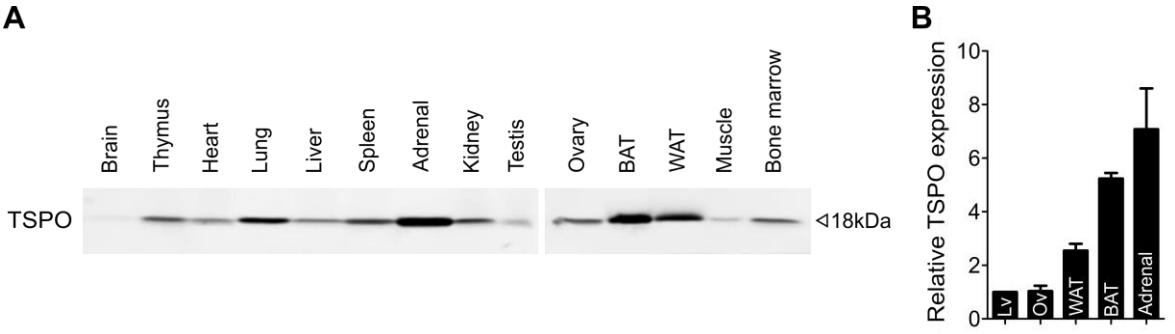

Figure 4.7. TSPO is highly expressed in tissues active in lipid metabolism. (A) Representative Western blot showing TSPO expression in 14 different tissues (75 µg protein/sample). TSPO was highly expressed in adrenal glands, followed by BAT, WAT, lung and kidney. TSPO expression was weaker in other tissues and extremely low in the brain. **(B)** Compared to liver (Lv), TSPO expression was similar, 2.5-, 5- and 7- folds higher in ovary (Ov), WAT, BAT and adrenals (Ad) respectively. (n=4 animals/group).

DISCUSSION

Several recent studies indicating that there is no physiological function for TSPO in steroidogenesis (Banati et al., 2014; Morohaku et al., 2014; Tu et al., 2014; Tu et al., 2015), have raised critical questions regarding the reason for its high levels of expression observed in steroidogenic mitochondria. By investigating different mitochondrial properties in TSPO-deficient steroidogenic MA-10 cells, we identify that TSPO expression inversely affects mitochondrial FAO. Consistent with this finding, we observed upregulation of genes involved in mitochondrial FAO in the adrenal glands of *Tspo*$^{-/-}$ mice. These findings indicate a novel TSPO function in modulating FAO that is broadly relevant for cell types that are active in lipid storage/metabolism.

In an early study that examined autoradiographic localization of TSPO in whole-body sections of neonatal rats, expression of TSPO was correlated to tissues that derive their metabolic energy primarily from oxidative phosphorylation (Anholt et al., 1985). Moreover, with the recent significant increase in obesity research and associated mouse models, use of quantitative trait loci analysis between inbred mouse strains identified *Tspo* as one of the six candidate genes that could influence triglyceride metabolism in mice (Leduc et al., 2011). Experimentally, we provide the first evidence linking TSPO and FAO by demonstrating that TSPO deletion induces a shift in substrate utilization from glucose to fatty acids for energy production in cells. Both endogenous and total mitochondrial FAO were significantly upregulated in MA-10:*Tspo*Δ/Δ clones compared to MA-10:*Tspo*+/+ cells.

Another study that explored novel transcripts associated with adipogenesis using differential display RT-PCR identified TSPO as one of the five candidate genes that showed a robust positive correlation with adipocyte differentiation (Wade et al., 2005), suggesting a direct involvement in this metabolic transition of pre-adipocytes. This was also consistent with observation that the TSPO-binding drugs PK11195 and Ro5-4864 could promote lipid deposition and adipocyte differentiation of mesenchymal stem cells (Lee et al., 2004). In a recent *in vivo* study, it was shown that TSPO-drug binding sites significantly decreased in both white and brown fat during diet-induced obesity in mice (Thompson et al., 2013). Moreover, significant downregulation of TSPO to almost half the baseline levels was also observed in the liver when animals were fed a high fat, high cholesterol diet (Dimitrova-Shumkovska et al., 2010), a condition that is known to overload fatty acid metabolism (Buettner et al., 2006). In conjunction with these observations, our detection of prominent TSPO expression in the WAT and BAT indicate that mitochondrial FAO regulation by TSPO might be of general relevance to lipid storage and/or metabolism in cells.

On investigating MA-10:*Tspo*Δ/Δ cells, we observed upregulation of genes involved in mitochondrial FAO, functional increase in OCR associated with FAO, and increased contribution of FAO to ATP production. For the genes analyzed for FAO, CPT1A is an integral OMM protein that converts

fatty acyl-CoA molecules to acylcarnitine and regulates its entry into the mitochondria (Fritz and Yue, 1963), which is considered the rate-limiting step for long-chain fatty acids β-oxidation in mammalian cells. Upregulation of *Cpt1a* in MA-10:*Tspo*Δ/Δ cells and reciprocal downregulation with TSPO overexpression indicates a correlation of TSPO and mitochondrial FAO. Inconsistency between the two MA-10:*Tspo*Δ/Δ clones in *Acadl* and *Srebf1c* expressions, without effects on *Cd36*, *Cpt1a*, *Acadm*, *Hadha*, *Ppara*, *Fasn* and *Acaca* suggest that this is unconnected to TSPO. Regardless, complexities of interactions that regulate overall fatty acid metabolic homeostasis make such aberrances difficult to interpret.

Although maximal total mitochondrial FAO in MA-10:*Tspo*Δ/Δ cells increases more than 2-fold, the observation that this was a shift in cellular metabolic homeostasis without affecting overall ATP production suggests that the function mediated by TSPO could be compensated under physiological conditions, and perhaps regulation at multiple levels. This notion is supported by the fact that a phenotypic change in global *Tspo*$^{-/-}$ mice associated with this observation was not readily detected in recent studies (Banati et al., 2014; Tu et al., 2014). The observation that genes involved in FAO are consistently upregulated albeit modest in the adrenal glands of *Tspo*$^{-/-}$ mice suggests that further characterization and response to metabolic stress need to be investigated in the *Tspo*$^{-/-}$ mouse model. These results also suggest that contexts of TSPO overexpression in pathologies may indicate metabolic reprogramming as seen in innate immune cell activation (Shriver and Manchester, 2011; Vats et al., 2006), and its overexpression in most cancer cells may also mark a response to the metabolic shift that occurs in these cells [(Pike et al., 2011; Samudio et al., 2010) and reviewed in (Carracedo et al., 2013)].

On investigating oxidative phosphorylation, TSPO deficient mitochondria did not show any deficits in OCR, coupling efficiency or proton leak. There was a modest decrease in calculated spare respiratory capacity in MA-10:*Tspo*Δ/Δ1, but not in MA-10:*Tspo*Δ/Δ2; similarly, there was a decrease in calculated ATP production in MA-10:*Tspo*Δ/Δ2, but not in MA-10:*Tspo*Δ/Δ1. These endpoints are calculated from measured OCR values that were not different between the two clones on direct

comparison; such inconsistency between the clones also indicates that these observations are not a result of TSPO deficiency. It should be noted that directly measured ATP production was not different between the two MA-10:*Tspo*Δ/Δ clones and MA-10:*Tspo*+/+ cells, indicating that an absolute interpretation of the above calculated values may not have physiological implications. This explanation is also supported by results showing that Δψm was not different between MA-10:*Tspo*Δ/Δ clones and MA-10:*Tspo*+/+ cells. This result on Δψm was consistent with a previous study assessing mitochondrial respiration and Δψm in mitochondria from primary hepatocytes of liver-specific TSPO conditional knockout mice (Sileikyte et al., 2014). However, other studies examining primary microglia (Banati et al., 2014), and fibroblasts (Zhao et al., 2015) isolated from global TSPO knockout (*Tspo*$^{-/-}$) mice reported a significantly lower OCR (and a decrease in calculated ATP production). This dissimilarity that is based on cell type could be due to integral differences in mitochondrial and cellular properties; steroidogenic cells and hepatocytes are both active in lipid metabolism, whereas lipid metabolism is not prominent in microglia. It is possible that upregulation of FAO could be providing more substrates for oxidative phosphorylation, maintaining OCR after TSPO deletion in cells inherently capable of active lipid metabolism.

Such metabolic effects mediated by TSPO might also explain the frequently made link between TSPO and oxidative stress. Although several studies indicate that high TSPO expression attenuated ROS production (Carayon et al., 1996; de Tassigny et al., 2013; Veenman et al., 2008), some studies also report the opposite effect (Gatliff et al., 2014; Klubo-Gwiezdzinska et al., 2012). We observed that cellular superoxides, as well as total ROS/RNS levels were elevated in the absence of TSPO. This could be linked to the increase in FAO, which can actively generate ROS independent of oxidative phosphorylation (Rosca et al., 2012; Schonfeld and Wojtczak, 2012). In concert, MA-10:*Tspo*Δ/Δ cells significantly upregulated expression of UCP2, a protein that has been shown to decrease ROS/superoxide (Andrews et al., 2008; Pi and Collins, 2010). Recent evidence also suggests that UCP2 facilitates export of C4 metabolites out of mitochondria (Vozza et al., 2014), and promotes mitochondrial utilization of FAO (Kukat et al., 2014), pertinent to our observation on increased FAO and suggesting a cellular response to

shift in energy homeostasis. Although the mechanism through which TSPO affects ROS production may be unclear, based on our observations in MA-10 cells, it is conceivable that TSPO affects mitochondrial ROS production via the modulation of FAO, without discounting other possible mechanisms of ROS regulation.

The basis for TSPO effect on mitochondrial FAO could be due to a few different possibilities. First, proposed association between TSPO and acyl-CoA binding protein (ACBP, also known as the diazepam binding inhibitor/DBI or acyl-CoA binding domain containing protein 1/ACBD1) might be a direct link to the regulation of fatty acid metabolism. Like TSPO, ACBP is also a highly conserved protein (Burton et al., 2005) considered the endogenous ligand for TSPO (Bovolin et al., 1990), and previously thought to be involved in steroidogenesis (Papadopoulos et al., 1991). Subsequent examination of ACBP knockout mice indicated a direct involvement in fatty acid metabolism (Lee et al., 2007; Neess et al., 2011). Expression of ACBP in tissues mirrors TSPO expression (Tong et al., 1991; Toranzo et al., 1994), and induction of ACBP during adipocyte differentiation (Mandrup et al., 1998), similar to TSPO (Wade et al., 2005), further indicates a functional relationship. Second, a functional association between TSPO and VDAC1 has been suggested (McEnery et al., 1992); VDAC1 is also known to associate with CPT1A and long chain acyl-CoA synthetase (ACSL), forming a fatty acid transfer complex at the OMM (Lee et al., 2011). It is possible that TSPO monitors or modulates activity of this transfer complex, affecting mitochondrial FAO and cellular metabolic homeostasis. Third, loss of an abundant cholesterol-binding OMM protein like TSPO may lead to changes in physical membrane properties due to cholesterol modulation, which in turn could affect mitochondrial FAO. Although we did not observe such a physical effect on core mechanisms of oxidative phosphorylation and $\Delta\Psi m$, there is evidence that CPT1A could be regulated by changes in OMM lipid composition and molecular order (Rao et al., 2011).

In conclusion, our results provide the first experimental evidence that links TSPO to mitochondrial FAO. The high correlation of TSPO levels and cells active in lipid metabolism provide a strong indication that its functional definition is not restricted to steroidogenic cells. We believe that this

discovery is the first step towards elucidating the precise physiological function of mammalian TSPO that will also advance understanding of the pathologic basis of its expression and its potential use as a diagnostic and therapeutic target in human medicine.

REFERENCES

Andrews, Z.B., Z.W. Liu, N. Walllingford, D.M. Erion, E. Borok, J.M. Friedman, M.H. Tschop, M. Shanabrough, G. Cline, G.I. Shulman, A. Coppola, X.B. Gao, T.L. Horvath, and S. Diano. 2008. UCP2 mediates ghrelin's action on NPY/AgRP neurons by lowering free radicals. *Nature*. 454:846-851.

Anholt, R.R., E.B. De Souza, M.L. Oster-Granite, and S.H. Snyder. 1985. Peripheral-type benzodiazepine receptors: autoradiographic localization in whole-body sections of neonatal rats. *J Pharmacol Exp Ther*. 233:517-526.

Anholt, R.R., P.L. Pedersen, E.B. De Souza, and S.H. Snyder. 1986. The peripheral-type benzodiazepine receptor. Localization to the mitochondrial outer membrane. *J Biol Chem*. 261:576-583.

Ascoli, M. 1981. Characterization of several clonal lines of cultured Leydig tumor cells: gonadotropin receptors and steroidogenic responses. *Endocrinology*. 108:88-95.

Banati, R.B., R.J. Middleton, R. Chan, C.R. Hatty, W. Wai-Ying Kam, C. Quin, M.B. Graeber, A. Parmar, D. Zahra, P. Callaghan, S. Fok, N.R. Howell, M. Gregoire, A. Szabo, T. Pham, E. Davis, and G.J. Liu. 2014. Positron emission tomography and functional characterization of a complete PBR/TSPO knockout. *Nature communications*. 5:5452.

Bovolin, P., J. Schlichting, M. Miyata, C. Ferrarese, A. Guidotti, and H. Alho. 1990. Distribution and characterization of diazepam binding inhibitor (DBI) in peripheral tissues of rat. *Regul Pept*. 29:267-281.

Braestrup, C., and R.F. Squires. 1977. Specific benzodiazepine receptors in rat brain characterized by high-affinity (3H)diazepam binding. *Proc Natl Acad Sci U S A*. 74:3805-3809.

Bribes, E., D. Carriere, C. Goubet, S. Galiegue, P. Casellas, and J. Simony-Lafontaine. 2004. Immunohistochemical assessment of the peripheral benzodiazepine receptor in human tissues. *J Histochem Cytochem*. 52:19-28.

Buettner, R., K.G. Parhofer, M. Woenckhaus, C.E. Wrede, L.A. Kunz-Schughart, J. Scholmerich, and L.C. Bollheimer. 2006. Defining high-fat-diet rat models: metabolic and molecular effects of different fat types. *J Mol Endocrinol*. 36:485-501.

Burton, M., T.M. Rose, N.J. Faergeman, and J. Knudsen. 2005. Evolution of the acyl-CoA binding protein (ACBP). *Biochem J*. 392:299-307.

Campanella, M., G. Szabadkai, and R. Rizzuto. 2008. Modulation of intracellular Ca2+ signalling in HeLa cells by the apoptotic cell death enhancer PK11195. *Biochem Pharmacol*. 76:1628-1636.

Campeau, E., V.E. Ruhl, F. Rodier, C.L. Smith, B.L. Rahmberg, J.O. Fuss, J. Campisi, P. Yaswen, P.K. Cooper, and P.D. Kaufman. 2009. A versatile viral system for expression and depletion of proteins in mammalian cells. *PLoS One*. 4:e6529.

Carayon, P., M. Portier, D. Dussossoy, A. Bord, G. Petitpretre, X. Canat, G. Le Fur, and P. Casellas. 1996. Involvement of peripheral benzodiazepine receptors in the protection of hematopoietic cells against oxygen radical damage. *Blood*. 87:3170-3178.

Carracedo, A., L.C. Cantley, and P.P. Pandolfi. 2013. Cancer metabolism: fatty acid oxidation in the limelight. *Nat Rev Cancer*. 13:227-232.

De Souza, E.B., R.R. Anholt, K.M. Murphy, S.H. Snyder, and M.J. Kuhar. 1985. Peripheral-type benzodiazepine receptors in endocrine organs: autoradiographic localization in rat pituitary, adrenal, and testis. *Endocrinology*. 116:567-573.

de Tassigny, A., R. Assaly, S. Schaller, R.M. Pruss, A. Berdeaux, and D. Morin. 2013. Mitochondrial translocator protein (TSPO) ligands prevent doxorubicin-induced mechanical dysfunction and cell death in isolated cardiomyocytes. *Mitochondrion*. 13:688-697.

Dimitrova-Shumkovska, J., L. Veenman, T. Ristoski, S. Leschiner, and M. Gavish. 2010. Chronic high fat, high cholesterol supplementation decreases 18 kDa Translocator Protein binding capacity in association with increased oxidative stress in rat liver and aorta. *Food and chemical toxicology : an*

international journal published for the British Industrial Biological Research Association. 48:910-921.

Fan, J., E. Campioli, A. Midzak, M. Culty, and V. Papadopoulos. 2015. Conditional steroidogenic cell-targeted deletion of TSPO unveils a crucial role in viability and hormone-dependent steroid formation. *Proc Natl Acad Sci U S A*. 112:7261-7266.

Fennell, D.A., M. Corbo, A. Pallaska, and F.E. Cotter. 2001. Bcl-2 resistant mitochondrial toxicity mediated by the isoquinoline carboxamide PK11195 involves de novo generation of reactive oxygen species. *Br J Cancer*. 84:1397-1404.

Fritz, I.B., and K.T. Yue. 1963. Long-Chain Carnitine Acyltransferase and the Role of Acylcarnitine Derivatives in the Catalytic Increase of Fatty Acid Oxidation Induced by Carnitine. *Journal of lipid research*. 4:279-288.

Furre, I.E., S. Shahzidi, Z. Luksiene, M.T. Moller, E. Borgen, J. Morgan, K. Tkacz-Stachowska, J.M. Nesland, and Q. Peng. 2005. Targeting PBR by hexaminolevulinate-mediated photodynamic therapy induces apoptosis through translocation of apoptosis-inducing factor in human leukemia cells. *Cancer Res*. 65:11051-11060.

Gatliff, J., and M. Campanella. 2012. The 18 kDa translocator protein (TSPO): a new perspective in mitochondrial biology. *Curr Mol Med*. 12:356-368.

Gatliff, J., D. East, J. Crosby, R. Abeti, R. Harvey, W. Craigen, P. Parker, and M. Campanella. 2014. TSPO interacts with VDAC1 and triggers a ROS-mediated inhibition of mitochondrial quality control. *Autophagy*. 10:2279-2296.

Gavish, M., I. Bachman, R. Shoukrun, Y. Katz, L. Veenman, G. Weisinger, and A. Weizman. 1999. Enigma of the peripheral benzodiazepine receptor. *Pharmacol Rev*. 51:629-650.

Hatty, C.R., A.P. Le Brun, V. Lake, L.A. Clifton, G.J. Liu, M. James, and R.B. Banati. 2014. Investigating the interactions of the 18kDa translocator protein and its ligand PK11195 in planar lipid bilayers. *Biochim Biophys Acta*. 1838:1019-1030.

Hirsch, J.D., C.F. Beyer, L. Malkowitz, B. Beer, and A.J. Blume. 1989. Mitochondrial benzodiazepine receptors mediate inhibition of mitochondrial respiratory control. *Mol Pharmacol*. 35:157-163.

Hong, S.H., H.B. Choi, S.U. Kim, and J.G. McLarnon. 2006. Mitochondrial ligand inhibits store-operated calcium influx and COX-2 production in human microglia. *J Neurosci Res*. 83:1293-1298.

Kinnally, K.W., D.B. Zorov, Y.N. Antonenko, S.H. Snyder, M.W. McEnery, and H. Tedeschi. 1993. Mitochondrial benzodiazepine receptor linked to inner membrane ion channels by nanomolar actions of ligands. *Proc Natl Acad Sci U S A*. 90:1374-1378.

Klubo-Gwiezdzinska, J., K. Jensen, A. Bauer, A. Patel, J. Costello, Jr., K.D. Burman, L. Wartofsky, M.J. Hardwick, and V.V. Vasko. 2012. The expression of translocator protein in human thyroid cancer and its role in the response of thyroid cancer cells to oxidative stress. *J Endocrinol*. 214:207-216.

Kukat, A., S.A. Dogan, D. Edgar, A. Mourier, C. Jacoby, P. Maiti, J. Mauer, C. Becker, K. Senft, R. Wibom, A.P. Kudin, K. Hultenby, U. Flogel, S. Rosenkranz, D. Ricquier, W.S. Kunz, and A. Trifunovic. 2014. Loss of UCP2 attenuates mitochondrial dysfunction without altering ROS production and uncoupling activity. *PLoS Genet*. 10:e1004385.

Larcher, J.C., J.L. Vayssiere, F.J. Le Marquer, L.R. Cordeau, P.E. Keane, A. Bachy, F. Gros, and B.P. Croizat. 1989. Effects of peripheral benzodiazepines upon the O2 consumption of neuroblastoma cells. *European journal of pharmacology*. 161:197-202.

Leduc, M.S., R.S. Hageman, R.A. Verdugo, S.W. Tsaih, K. Walsh, G.A. Churchill, and B. Paigen. 2011. Integration of QTL and bioinformatic tools to identify candidate genes for triglycerides in mice. *Journal of lipid research*. 52:1672-1682.

Lee, D.H., S.K. Kang, R.H. Lee, J.M. Ryu, H.Y. Park, H.S. Choi, Y.C. Bae, K.T. Suh, Y.K. Kim, and J.S. Jung. 2004. Effects of peripheral benzodiazepine receptor ligands on proliferation and differentiation of human mesenchymal stem cells. *J Cell Physiol*. 198:91-99.

Lee, K., J. Kerner, and C.L. Hoppel. 2011. Mitochondrial carnitine palmitoyltransferase 1a (CPT1a) is part of an outer membrane fatty acid transfer complex. *J Biol Chem*. 286:25655-25662.

Lee, L., C.A. DeBono, D.R. Campagna, D.C. Young, D.B. Moody, and M.D. Fleming. 2007. Loss of the acyl-CoA binding protein (Acbp) results in fatty acid metabolism abnormalities in mouse hair and skin. *J Invest Dermatol*. 127:16-23.

Li, L., T. Chen, J.D. Stanton, T. Sueyoshi, M. Negishi, and H. Wang. 2008. The peripheral benzodiazepine receptor ligand 1-(2-chlorophenyl-methylpropyl)-3-isoquinoline-carboxamide is a novel antagonist of human constitutive androstane receptor. *Mol Pharmacol*. 74:443-453.

Livak, K.J., and T.D. Schmittgen. 2001. Analysis of relative gene expression data using real-time quantitative PCR and the 2(-Delta Delta C(T)) Method. *Methods*. 25:402-408.

Maaser, K., A.P. Sutter, and H. Scherubl. 2005. Mechanisms of mitochondrial apoptosis induced by peripheral benzodiazepine receptor ligands in human colorectal cancer cells. *Biochem Biophys Res Commun*. 332:646-652.

Mandrup, S., R.V. Sorensen, T. Helledie, J. Nohr, T. Baldursson, C. Gram, J. Knudsen, and K. Kristiansen. 1998. Inhibition of 3T3-L1 adipocyte differentiation by expression of acyl-CoA-binding protein antisense RNA. *J Biol Chem*. 273:23897-23903.

McEnery, M.W., A.M. Snowman, R.R. Trifiletti, and S.H. Snyder. 1992. Isolation of the mitochondrial benzodiazepine receptor: association with the voltage-dependent anion channel and the adenine nucleotide carrier. *Proc Natl Acad Sci U S A*. 89:3170-3174.

Morohaku, K., S.H. Pelton, D.J. Daugherty, W.R. Butler, W. Deng, and V. Selvaraj. 2014. Translocator protein/peripheral benzodiazepine receptor is not required for steroid hormone biosynthesis. *Endocrinology*. 155:89-97.

Morohaku, K., N.S. Phuong, and V. Selvaraj. 2013. Developmental expression of translocator protein/peripheral benzodiazepine receptor in reproductive tissues. *PLoS One*. 8:e74509.

Mukhin, A.G., V. Papadopoulos, E. Costa, and K.E. Krueger. 1989. Mitochondrial benzodiazepine receptors regulate steroid biosynthesis. *Proc Natl Acad Sci U S A*. 86:9813-9816.

Neess, D., M. Bloksgaard, S. Bek, A.B. Marcher, I.C. Elle, T. Helledie, M. Due, V. Pagmantidis, B. Finsen, J. Wilbertz, M. Kruhoffer, N. Faergeman, and S. Mandrup. 2011. Disruption of the acyl-CoA-binding protein gene delays hepatic adaptation to metabolic changes at weaning. *J Biol Chem*. 286:3460-3472.

Papadopoulos, V., H. Amri, N. Boujrad, C. Cascio, M. Culty, M. Garnier, M. Hardwick, H. Li, B. Vidic, A.S. Brown, J.L. Reversa, J.M. Bernassau, and K. Drieu. 1997. Peripheral benzodiazepine receptor in cholesterol transport and steroidogenesis. *Steroids*. 62:21-28.

Papadopoulos, V., A. Berkovich, K.E. Krueger, E. Costa, and A. Guidotti. 1991. Diazepam binding inhibitor and its processing products stimulate mitochondrial steroid biosynthesis via an interaction with mitochondrial benzodiazepine receptors. *Endocrinology*. 129:1481-1488.

Papadopoulos, V., and W.L. Miller. 2012. Role of mitochondria in steroidogenesis. *Best Pract Res Clin Endocrinol Metab*. 26:771-790.

Pi, J., and S. Collins. 2010. Reactive oxygen species and uncoupling protein 2 in pancreatic beta-cell function. *Diabetes, obesity & metabolism*. 12 Suppl 2:141-148.

Pike, L.S., A.L. Smift, N.J. Croteau, D.A. Ferrick, and M. Wu. 2011. Inhibition of fatty acid oxidation by etomoxir impairs NADPH production and increases reactive oxygen species resulting in ATP depletion and cell death in human glioblastoma cells. *Biochim Biophys Acta*. 1807:726-734.

Rao, J.N., G.Z. Warren, S. Estolt-Povedano, V.A. Zammit, and T.S. Ulmer. 2011. An environment-dependent structural switch underlies the regulation of carnitine palmitoyltransferase 1A. *J Biol Chem*. 286:42545-42554.

Rosca, M.G., E.J. Vazquez, Q. Chen, J. Kerner, T.S. Kern, and C.L. Hoppel. 2012. Oxidation of fatty acids is the source of increased mitochondrial reactive oxygen species production in kidney cortical tubules in early diabetes. *Diabetes*. 61:2074-2083.

Samudio, I., R. Harmancey, M. Fiegl, H. Kantarjian, M. Konopleva, B. Korchin, K. Kaluarachchi, W. Bornmann, S. Duvvuri, H. Taegtmeyer, and M. Andreeff. 2010. Pharmacologic inhibition of fatty acid oxidation sensitizes human leukemia cells to apoptosis induction. *J Clin Invest*. 120:142-156.

Scarf, A.M., K.M. Auman, and M. Kassiou. 2012. Is there any correlation between binding and functional effects at the translocator protein (TSPO) (18 kDa)? *Curr Mol Med*. 12:387-397.

Schonfeld, P., and L. Wojtczak. 2012. Brown adipose tissue mitochondria oxidizing fatty acids generate high levels of reactive oxygen species irrespective of the uncoupling protein-1 activity state. *Biochim Biophys Acta*. 1817:410-418.

Selvaraj, V., and D.M. Stocco. 2015. The changing landscape in translocator protein (TSPO) function. *Trends Endocrinol Metab*. 26:341-348.

Selvaraj, V., D.M. Stocco, and L.N. Tu. 2015. Minireview: translocator protein (TSPO) and steroidogenesis: a reappraisal. *Mol Endocrinol*. 29:490-501.

Seneviratne, M.S., D. Faccenda, V. De Biase, and M. Campanella. 2012. PK11195 inhibits mitophagy targeting the F1Fo-ATPsynthase in Bcl-2 knock-down cells. *Curr Mol Med*. 12:476-482.

Shriver, L.P., and M. Manchester. 2011. Inhibition of fatty acid metabolism ameliorates disease activity in an animal model of multiple sclerosis. *Sci Rep*. 1:79.

Sileikyte, J., E. Blachly-Dyson, R. Sewell, A. Carpi, R. Menabo, F. Di Lisa, F. Ricchelli, P. Bernardi, and M. Forte. 2014. Regulation of the Mitochondrial Permeability Transition Pore by the Outer Membrane does not Involve the Peripheral Benzodiazepine Receptor (TSPO). *J Biol Chem*.

Spandidos, A., X. Wang, H. Wang, and B. Seed. 2010. PrimerBank: a resource of human and mouse PCR primer pairs for gene expression detection and quantification. *Nucleic Acids Res*. 38:D792-799.

Thompson, M.M., H.C. Manning, and K.L. Ellacott. 2013. Translocator protein 18 kDa (TSPO) is regulated in white and brown adipose tissue by obesity. *PLoS One*. 8:e79980.

Tong, Y., E. Rheaume, J. Simard, and G. Pelletier. 1991. Localization of peripheral benzodiazepine binding sites and diazepam-binding inhibitor (DBI) mRNA in mammary glands and dimethylbenz(a)antracene (DMBA)-induced mammary tumors in the rat. *Regul Pept*. 33:263-273.

Toranzo, D., Y. Tong, M.C. Tonon, H. Vaudry, and G. Pelletier. 1994. Localization of diazepam-binding inhibitor and peripheral type benzodiazepine binding sites in the rat ovary. *Anat Embryol (Berl)*. 190:383-388.

Tu, L.N., K. Morohaku, P.R. Manna, S.H. Pelton, W.R. Butler, D.M. Stocco, and V. Selvaraj. 2014. Peripheral Benzodiazepine Receptor/Translocator Protein Global Knock-out Mice Are Viable with No Effects on Steroid Hormone Biosynthesis. *J Biol Chem*. 289:27444-27454.

Tu, L.N., A.H. Zhao, D.M. Stocco, and V. Selvaraj. 2015. PK11195 effect on steroidogenesis is not mediated through the translocator protein (TSPO). *Endocrinology*. 156:1033-1039.

Vats, D., L. Mukundan, J.I. Odegaard, L. Zhang, K.L. Smith, C.R. Morel, R.A. Wagner, D.R. Greaves, P.J. Murray, and A. Chawla. 2006. Oxidative metabolism and PGC-1beta attenuate macrophage-mediated inflammation. *Cell Metab*. 4:13-24.

Veenman, L., Y. Shandalov, and M. Gavish. 2008. VDAC activation by the 18 kDa translocator protein (TSPO), implications for apoptosis. *J Bioenerg Biomembr*. 40:199-205.

Vozza, A., G. Parisi, F. De Leonardis, F.M. Lasorsa, A. Castegna, D. Amorese, R. Marmo, V.M. Calcagnile, L. Palmieri, D. Ricquier, E. Paradies, P. Scarcia, F. Palmieri, F. Bouillaud, and G. Fiermonte. 2014. UCP2 transports C4 metabolites out of mitochondria, regulating glucose and glutamine oxidation. *Proc Natl Acad Sci U S A*. 111:960-965.

Wade, F.M., C. Wakade, V.B. Mahesh, and D.W. Brann. 2005. Differential expression of the peripheral benzodiazepine receptor and gremlin during adipogenesis. *Obes Res*. 13:818-822.

Yeliseev, A.A., and S. Kaplan. 1995. A sensory transducer homologous to the mammalian peripheral-type benzodiazepine receptor regulates photosynthetic membrane complex formation in Rhodobacter sphaeroides 2.4.1. *J Biol Chem*. 270:21167-21175.

Zeno, S., L. Veenman, Y. Katz, J. Bode, M. Gavish, and M. Zaaroor. 2012. The 18 kDa mitochondrial translocator protein (TSPO) prevents accumulation of protoporphyrin IX. Involvement of reactive oxygen species (ROS). *Curr Mol Med*. 12:494-501.

Zhao, A.H., L.N. Tu, C. Mukai, M.P. Sirivelu, V.V. Pillai, K. Morohaku, R. Cohen, and V. Selvaraj. 2015. Mitochondrial translocator protein (TSPO) function is not essential for heme biosynthesis. *J Biol Chem*.

CHAPTER 5

Mammalian TSPO Is a Tetrapyrrole Sequestering Protein

ABSTRACT

Translocator protein (TSPO) is a highly conserved protein from bacteria to humans, suggesting a conserved evolutionary function beneficial for overall fitness. In mammals, TSPO is localized to the outer mitochondrial membrane and its expression has been dysregulated in many diseases. Since the model of TSPO and steroidogenesis was invalidated, many studies have proposed different functions for TSPO using different biological systems or tissue types but the exact molecular function of TSPO remains unclear. Our previous study provided the first evidence that high expression of mammalian TSPO is not restricted to steroidogenic tissues but in those that are rich in lipid droplets including white and brown adipose tissues. Using the MA-10 Leydig tumor cell line as an *in vitro* model, we demonstrated that TSPO suppresses fatty acid oxidation (FAO) and TSPO deletion induces a shift in substrate utilization from glucose to fatty acids for energy production. In this study, we examined metabolism in global TSPO knockout ($Tspo^{-/-}$) mice. From studying their basal metabolic rate, performing metabolomics, and comparing gene expression changes, we discovered that $Tspo^{-/-}$ mice had overloaded FAO compared to control $Tspo^{fl/fl}$ mice, similar to the phenotype reported for our MA-10 cell model. In a quest to pinpoint the exact molecular mechanism, we uncovered the biological function of TSPO in sequestering and preventing degradation of protoporphyrin IX (PPIX), the immediate tetrapyrrole precursor of heme. Linked to this process, we present a novel biological function of PPIX in lipid metabolism, which forms the basis for involvement of TSPO in regulating FAO.

INTRODUCTION

Translocator protein (TSPO) is a highly conserved protein from bacteria to humans, suggesting a conserved function beneficial for evolutionary fitness. Particularly in human, TSPO has been implicated in several diseases such as inflammatory disorders, cancers and neuropsychiatric diseases. Hence, TSPO binding ligands emerge as promising diagnostic and therapeutic agents being tested in clinical trials for various indications. However, the exact molecular function of TSPO remains unknown, limiting its application in human medicine.

In mammalian cells, TSPO is a transmembrane protein localized to the outer mitochondrial membrane (OMM). TSPO was linked to cholesterol translocation from cytosol into mitochondria, the rate limiting step for steroidogenesis. However, this model has been refuted by both recent genetic and pharmacological evidence, reproducible by at least 3 different laboratories, showing that complete absence of TSPO in mice and cells do not affect viability and steroid hormone production (Banati et al., 2014; Morohaku et al., 2014; Tu et al., 2014; Tu et al., 2015; Wang et al., 2016). The modest stimulating effect of some TSPO ligands on steroidogenesis, often used as the basis for the association of TSPO and steroidogenesis, was found to be non-specific and not mediated by TSPO (Tu et al., 2015). A structural study using high resolution NMR also found no evidence of potential side chains in mammalian TSPO to bind and translocate cholesterol (Jaremko et al., 2014). Moreover, this model had always failed to explain the conservation of TSPO throughout different kingdoms as cholesterol is not found in bacteria, and binding of TSPO to bacterial hopanoids, the functional analogue of cholesterol, was shown highly unlikely (Busch et al., 2017).

Since the model of TSPO and steroidogenesis was invalidated, the exact molecular function of TSPO remains controversial. Many studies have proposed different functions for TSPO using different biological systems or tissue types. In bacteria, TSPO negatively regulated activity of coproporphyrinogen III oxidase in *Rhodobacter sphaeroides* (Yeliseev and Kaplan, 1995; Yeliseev and Kaplan, 1999); degraded protoporphyrin IX (PPIX) in a light and oxygen-dependent manner in *Bacillus cereus* (Guo et al., 2015)

and *Chlorobium tepidum* (Ginter et al., 2013). In plant, TSPO was a stress-induced porphyrin scavenger via an autophagy-dependent mechanism (Vanhee et al., 2011). In Drosophila, TSPO was an essential mediator of apoptosis and played a central role in controlling longevity (Lin et al., 2014). In zebrafish, TSPO played a key role in erythropoiesis (Rampon et al., 2009). In mammals, TSPO was implicated in regulation of adipose metabolism (Dimitrova-Shumkovska et al., 2010; Thompson et al., 2013); inhibited HIV-1 envelope protein synthesis in human CD4(+) T cell line (Zhou et al., 2014); and interacted with NADPH oxidase to maintain redox homeostasis in microglia (Guilarte et al., 2016). It is obvious that all the conclusions are restricted to an isolated system or model being studied and unable to provide a satisfactory explanation for the involvement of TSPO in another system. Although the ultimate biological effect in each system could be cell type-dependent, the function of a protein at the molecular level should be unified and yet undefined for TSPO.

Our previous study provided the first evidence that high expression of mammalian TSPO is not restricted to steroidogenic tissues as previously claimed, but also in those that are rich in lipid droplets including white and brown adipose tissues (Tu et al., 2016), indicating a potential role of TSPO in lipid metabolism. Indeed, an unbiased quantitative trait loci analysis between inbred mouse strains identified *Tspo* as one of the 6 candidate genes that could influence triglyceride metabolism (Leduc et al., 2011). Another study using differential display RT-PCR identified TSPO as one of the 5 novel genes associated with adipogenesis (Wade et al., 2005). TSPO level was also significantly reduced in mouse liver and adipose tissues in different obesity models (Dimitrova-Shumkovska et al., 2010; Thompson et al., 2013), suggesting a direct regulation of TSPO in lipid homeostasis. In our previous study, we used MA-10 Leydig tumor cells as an *in vitro* model and demonstrated for the first time that TSPO supresses fatty acid oxidation (FAO) and TSPO deletion induces a shift in substrate utilization from glucose to fatty acids for energy production (Tu et al., 2016). In this study, we examined metabolic changes in global TSPO knockout ($Tspo^{-/-}$) mice. Our result showed that $Tspo^{-/-}$ mice had overloaded FAO compared to control $Tspo^{fl/fl}$ mice, similar to the phenotype we reported for our MA-10 cell model. Investigation of the mechanism uncovered a novel

function for TSPO in sequestering PPIX and regulating its levels. PPIX has long been reproducibly demonstrated as the only endogenous ligand of TSPO throughout different kingdoms (Veenman et al., 2016; Verma et al., 1987) but the significance of this interaction has not yet been characterized. Examination of the TSPO-PPIX relationship also led to the discovery of a novel biological function for PPIX in lipid metabolism, which unravels the basis for the involvement of TSPO in regulating FAO.

MATERIALS AND METHODS

Generation of mice, cells and bacteria

Tspo$^{fl/fl}$ and *Tspo*$^{-/-}$ mice in the C57BL/6 background previously generated (Tu et al., 2014), were sampled at 8-12 weeks of age for all experiments. Animals were maintained in accordance with the National Institute of Health Guide for the Care and Use of Laboratory Animals. The Institutional Animal Care and Use Committee of Cornell University approved the experiments described.

MA-10 Leydig cancer cells were grown at 37˚C under 5% CO_2 in Dulbecco's modified eagle medium/DMEM high glucose (25 mM glucose, 1 mM pyruvate) containing 10% FBS and 1% penicillin-streptomycin. TSPO knockout MA-10 cells (MA-10:*Tspo*Δ/Δ) were generated by CRISPR/Cas9-mediated targeting of exon 2 of the *Tspo* gene (Tu et al., 2015). MA-10:*Tspo*Δ/Δ cells were then transduced with *Tspo* lentiviruses to re-express TSPO (MA-10:*Tspo*Δ/Δ+TSPO) as previously described (Tu et al., 2016). To generate MA-10 cells that express TSPO with HA and Flag tags, each tag was cloned at the C-terminal of *Tspo* gene in the same lentiviral vector (pLenti CMV GFP Puro) (Campeau et al., 2009). TSPO-HA and TSPO-Flag lentiviruses were packaged and MA-10:*Tspo*Δ/Δ were transduced with both viruses to generate a cell line expressing both TSPO-HA and TSPO-Flag (MA-10:*Tspo*Δ/Δ+TSPO-HA+TSPO-Flag).

BL21 (DE3) competent *E.coli* bacteria (Thermo Fisher) were transformed with pET-21b(+) vector (Novagen) containing *Tspo* gene. Bacteria transformed with empty pET-21b(+) vector were used as the control. 3 colonies were picked for each group and plasmids were extracted and sequenced to confirm

successful transformation. Bacteria were then shaken at 37^0C in Luria-Bertani (LB) broth supplemented with 100 μg/mL Ampicillin until the optical density reached 0.6-0.8, indicating the log phase of growth. 0.5 mM Isopropyl β-D-1-thiogalactopyranoside (IPTG) was added to LB broth and bacteria were shaken for another 4 hrs to induce TSPO expression. Bacteria expressing TSPO (BL21-TSPO) and control bacteria (BL21-CTRL) were used for subsequent analysis.

Metabolic cages

Activity, VO_2, VCO_2, heat production, and respiratory exchange ratio (RER) were measured for mice using the Oxymax Lab Animal Monitoring System CLAMS (Columbus Instruments). Mice were housed individually in metabolic cages in a room with constant temperature (22˚C) and a 14h: light-dark cycle (lights on from 0500-1900 hours). They were acclimatized to the cage environment for 24 hrs before data collection for the following 24 hrs. Analysis for 60 data points/hour for activity and 3 data points/hour recorded for other parameters was carried out using the Oxymax software (Columbus Instruments).

Transmission electron microscopy

Mice in the unfed state were euthanized and perfused with Karnovsky's fixative (2.5% glutaraldehyde, 2% paraformaldehyde in 0.08 M phosphate buffer). Livers were dissected and fixed in the same fixative overnight at room temperature (RT). After fixation, tissues were processed for transmission electron microscopy as previously described (Tu et al., 2014). Stained sections were examined in a Tecnai™ T12 Spirit electron microscope (FEI), at 120 kV. High magnification images were acquired using a high-resolution CCD camera Megaview III (Olympus Soft Imaging System).

Glycogen quantification

Mice were euthanized during both fed or unfed states and liver glycogen was determined as previously described (Passonneau and Lauderdale, 1974; Zhang, 2012). In brief, one set of 15-25 mg livers was minced and boiled in 0.5 mL of 2 M HCl for 1 h. Samples were cooled to RT and neutralized with 0.5 mL of 2 M NaOH, and vortexed at 20,000 g for 10 mins. Total glucose in the supernatants was measured

using the glucose HK assay reagent (Sigma) according to manufacturer's protocol. The second set of 15-25 mg matching livers was minced and boiled in 0.5 mL of 2 M NaOH; in this condition, no glycogenolysis occurs. Samples were cooled to RT and neutralized with 0.5 mL of 2 M HCl, and vortexed at 20,000 g for 10 mins. Free glucose in the supernatants was measured as mentioned above. The difference between total glucose and free glucose in the livers corresponds to the glycogen content, which was normalized to the liver weight.

Metabolomics

Mice were euthanized during the unfed state; livers and plasma were collected and stored at -80C until analysis. Lipid extracted phase from liver homogenates (6mg) and plasma (20uL) were processed for reverse-phase lipid chromatography–quadrupole/time-of-flight mass spectrometry (CSH–QTOF MS) analysis as previously described (Tu et al., 2017). In brief, lipids were detected and quantified using an Agilent 6550 iFunnel accurate mass quadrupole/time-of-flight (QTOF) mass spectrometer with a jet stream ESI source (Agilent). Method blanks and human pooled plasma samples were used as QC controls. MS-DIAL software (Tsugawa et al., 2015) was used to process the raw data and annotations were made based on an in-house accurate mass and retention time lipid library created using LipidBlast, as described previously (Kind et al., 2013). Statistical analyses for all metabolites between *Tspo*$^{fl/fl}$ and *Tspo*$^{-/-}$ mice were performed as previously described (Tu et al., 2017). False discovery rate-adjusted p values less than 0.05 were considered significant.

PPIX and heme quantification

Tissues, cells and bacteria were lysed in 1% Triton X-100 in Tris-buffered saline. Samples were centrifuged at 5,000 g for 5 mins and the supernatant homogenates were collected. For PPIX quantification, 1:1 methanol:1N perchloric acid (MeOH-PCA) was added to the homogenates in the volume ratio of 2:1. Samples were centrifuged at 10,000 g for 5 mins and the supernatants were ready for PPIX fluorescent measurement. For heme quantification, 2-5 μl of the homogenates was added to 500 μl of saturated (2 M) oxalic acid and boiled for 30 mins to produce PPIX from heme. Samples were then centrifuged at 10,000 g

for 10 mins at 4°C. PPIX fluorescence in the supernatant was measured as previously described (Zhao et al., 2016). Heme and PPIX values were normalized to protein content in each sample.

Gene expression

Total RNA was extracted from tissues of 8-12 week old *Tspo*$^{fl/fl}$ and *Tspo*$^{-/-}$ mice using Trizol (Life Technologies). Reverse transcription was carried out using Multiscribe™ reverse transcriptase (Life Technologies). Gene expressions were quantified using a SYBR® Green detection method with validated primer sequences obtained from PrimerBank database (Spandidos et al., 2010). Primer specificity and amplification efficiency were confirmed and sequences are provided in Supplemental Table 1. All expression data were normalized to internal control gene, TATA box-binding protein (*Tbp*). Relative quantification of fold-change was performed using the $2^{-\Delta/\Delta Ct}$ method (Livak and Schmittgen, 2001).

Immunoblots

Proteins were separated by SDS-PAGE and immunoblotted using rabbit monoclonal primary antibodies against TSPO (Abcam), isocitrate dehydrogenase 2 (IDH2) (Abcam), mouse monoclonal antibodies against voltage-dependent anion channel 1 (VDAC1) (Abcam), Flag tag (Sigma), rabbit polyclonal antibody against Hemagglutini (HA) tag (Thermo Fisher). Each primary antibody was multiplexed with the loading control β-actin (Li-Cor). Simultaneous detection was performed using IRDye 700 and 800 labeled secondary antibodies under a laser fluorescence scanner (Li-Cor) and quantified using ImageJ as described previously (Tu et al., 2014).

Crosslinking and co-immunoprecipitation

L-photo-leucine (Thermo Fisher) was dissolved to final concentration of 1 mM in DMEM-limiting medium (Thermo Fisher) supplemented with 10% dialyzed FBS (Thermo Fisher), 30 mg/L L-Methionine and 1% penicillin-streptomycin. MA-10 cells were grown to 70% confluence, washed twice with PBS and incubated with L-photo-leucine containing medium for 24 hrs. The medium was then removed and replaced with PBS. Cells were irradiated with UV light at 345 nm for 10 mins to induce permanent crosslinking. For

all other crosslinkers, MA-10 cells were grown to 80% confluence and medium was replaced with PBS. Glutaraldehyde (GA) was added to final concentration of 2.5%, incubated for 6 mins at RT and quenched with 1 M glycine for 3 mins. Dithiobis(succinimidyl propionate) (DSP) (Thermo Fisher) 2 mM or Dimethyl 3,3'-dithiobispropionimidate (DTBP) (Thermo Fisher) 5 mM was incubated with the cells for 30 mins at RT and quenched with 50 mM glycine for 15 mins. After crosslinking, cells were then lysed in NP-40 lysis buffer, and kept on ice for 15 mins. Samples were centrifuged at 1,000g for 5 mins to remove nuclei and debris. SDS was added to 0.8% final concentration to completely disrupt all membranes and denature proteins. Cell lysates were diluted 1:10 using PBS with 0.02% Tween-20 before being used for immunoprecipitation.

Immunoprecipitation was done using Dynabeads Protein G (Thermo Fisher) for TSPO antibody or Dynabeads protein A (Thermo Fisher) for Flag antibody according to manufacturer's protocol. In brief, 8 ug of antibodies was incubated with every 50 mg of beads for 2 hrs at 4^0C. The bead-antibody complex was then washed using PBS with 0.02% Tween-20 to remove unbound antibodies. Diluted cell lysates mentioned above was added to the bead-antibody complex, and rotated overnight at 4^0C. The bead-antibody-antigen complex was washed 3 times with PBS and the antigen was eluted from the beads using 50 mM glycine pH 2.8 supplemented with 1% SDS.

Statistics

Numeric differences between groups were compared using a Student's t-test; comparisons for more than two groups were performed using ANOVA and *post hoc* Tukey's test ($p<0.05$ was considered significant). All analyses were performed using Prism 5 (GraphPad).

RESULTS

Deletion of TSPO increases mitochondrial FAO

To examine if absence of TSPO caused any metabolic disturbances, we assessed *Tspo*$^{fl/fl}$ and *Tspo*$^{-/-}$ mice in metabolic cages for continuous 24 hr monitoring. *Tspo*$^{-/-}$ mice showed significantly lower oxygen consumption rate (OCR) than the control group, during both light and dark cycles which correspond to unfed and fed states in mice respectively (Figure 5.1A). The respiratory exchange ratio (RER), an indicator of which fuel source is being metabolized by the body, was significantly lower in *Tspo*$^{-/-}$ mice than in *Tspo*$^{fl/fl}$ mice during the light cycle or unfed state (Figure 5.1B). A lower RER indicates more active utilization of fatty acids rather than glucose for energy production in *Tspo*$^{-/-}$ mice in the unfed state. RER in the dark cycle or fed state was similar between *Tspo*$^{fl/fl}$ and *Tspo*$^{-/-}$ mice (Figure 5.1B). There was no difference in the ambulatory and total activities between the two genotypes in both light and dark cycles (not shown).

Since our *Tspo*$^{-/-}$ mice are a global knockout model, the metabolic phenotype observed could be the result of many altered inputs from different metabolic tissues where TSPO is expressed. Therefore, to confirm that absence of TSPO indeed causes more active utilization of fatty acids to produce energy through FAO, we decided to examine liver, the chief metabolic organ that reflects the changes to whole body metabolism. Gene expression analysis every 6 h showed that critical genes involved in fatty acid synthesis: sterol regulatory element-binding protein 1c (*Srebp1c*), fatty acid synthase (*Fasn*), acetyl-coA carboxylase α (*Acaca*) and genes involved in mitochondrial FAO: carnitine palmitoyltransferase 1a (*Cpt1a*), trifunctional enzyme subunit α (*Hadha*) were highly elevated in *Tspo*$^{-/-}$ liver compared to the control group at various time points (Figure 5.1C). This indicates that *Tspo*$^{-/-}$ liver synthesize and utilize more fatty acids for energy production than *Tspo*$^{fl/fl}$ liver. The magnitude of the difference was particularly prominent late in the light cycle or unfed state. The difference in gene expression in the dark cycle was not as consistent and noticeable among different genes as compared to those in the light cycle. This result agrees with our metabolic cage data where *Tspo*$^{-/-}$ mice displayed significantly lower RER only in the unfed state, particularly towards the end of the light cycle.

Transmission electron microscopy of livers in the unfed state revealed noticeably more glycogen granules deposited in the *Tspo*$^{-/-}$ hepatocytes than the control group (Figure 5.1D). In the physiological unfed state, fatty acids are not the primary source of fuel as mice preferentially deplete glycogen store in the liver first before mobilizing fat. We then quantified the liver glycogen content and found that in the fed state (dark cycle) when glycogen is mainly synthesized and stored, there was no difference in the glycogen content between *Tspo*$^{fl/fl}$ and *Tspo*$^{-/-}$ liver (Figure 5.1E). However, in the unfed state (light cycle) when glycogen is broken down for energy, *Tspo*$^{-/-}$ mice utilized significantly less glycogen and therefore had significantly more glycogen stored in the liver compared to the *Tspo*$^{fl/fl}$ mice (Figure 5.1E). These results again support our conclusion that *Tspo*$^{-/-}$ mice indeed spared glucose and utilized more lipids for energy production compared to *Tspo*$^{fl/fl}$ mice.

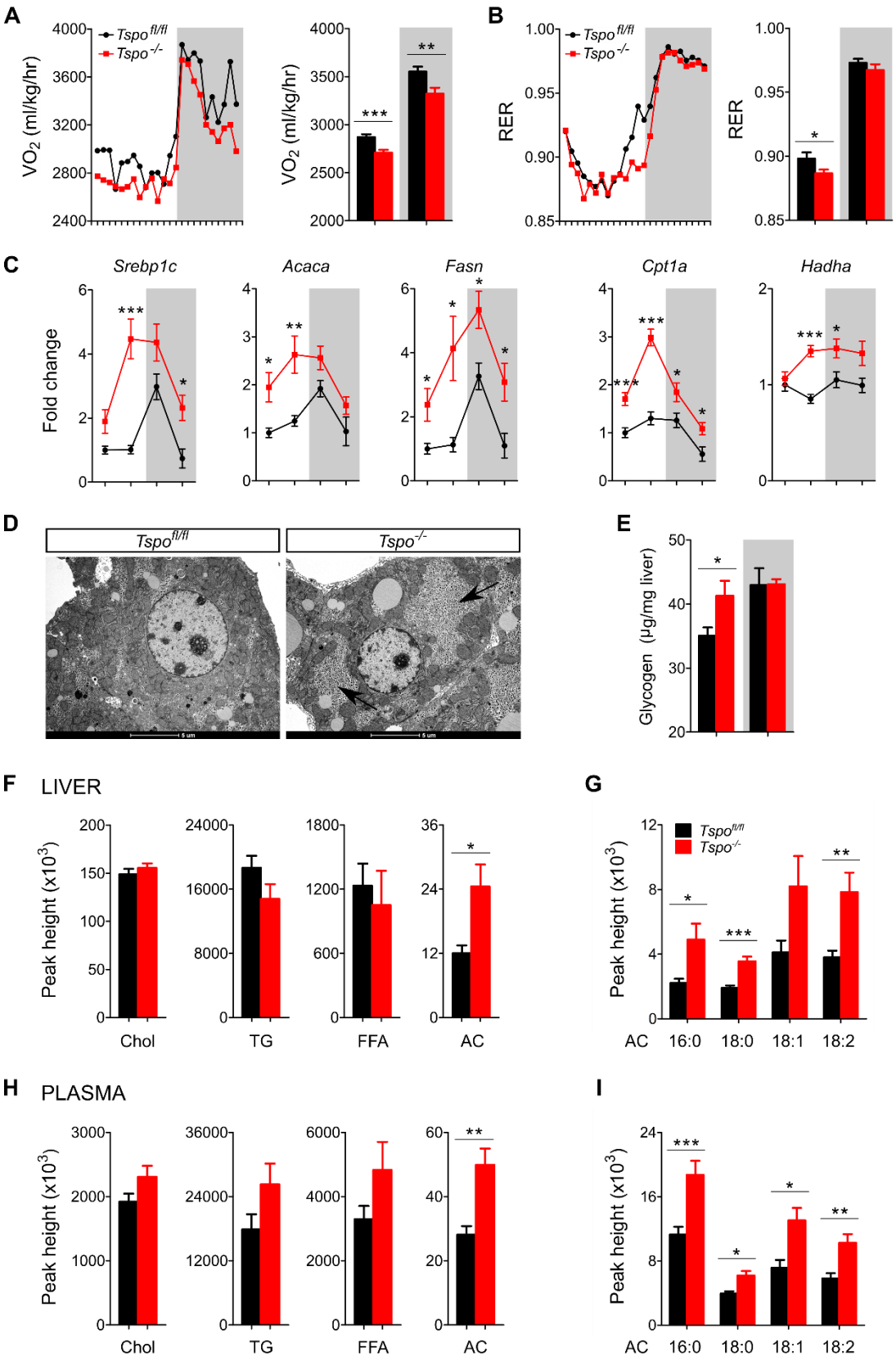
A
B
C
D
E
F
G
H
I
Tspo fl/fl
Tspo -/-
VO2 (ml/kg/hr)
RER
Srebp1c
Acaca
Fasn
Cpt1a
Hadha
Fold change
Glycogen (µg/mg liver)
LIVER
PLASMA
Peak height (x10^3)
Chol
TG
FFA
AC
16:0
18:0
18:1
18:2

Figure 5.1. Deletion of TSPO increases mitochondrial FAO. (A) Monitoring oxygen consumption (VO_2) over a 24-hour period in *Tspo*$^{fl/fl}$ and *Tspo*$^{-/-}$ mice showed that VO_2 was significantly decreased in both light and dark cycles in *Tspo*$^{-/-}$ mice compared to *Tspo*$^{fl/fl}$ cohorts. **(B)** Monitoring respiratory exchange ratio (RER) over a 24-hour period in *Tspo*$^{fl/fl}$ and *Tspo*$^{-/-}$ mice showed that RER was significantly decreased in the light cycle, and remained the same in the dark cycle in *Tspo*$^{-/-}$ mice compared to *Tspo*$^{fl/fl}$ cohorts (n=12/group). **(C)** Gene expression analysis every 6 h showed that critical genes involved in fatty acid synthesis: sterol regulatory element-binding protein 1c (*Srebp1c*), fatty acid synthase (*Fasn*), acetyl-coA carboxylase α (*Acaca*) and genes involved in mitochondrial FAO: carnitine palmitoyltransferase 1a (*Cpt1a*), trifunctional enzyme subunit α (*Hadha*) were highly elevated in *Tspo*$^{-/-}$ liver compared to the control group (n=5-6 mice/group/time point). **(D)** Transmission electron micrographs of the livers in unfed state showed significantly more glycogen granules (arrow) in *Tspo*$^{-/-}$ mice compared to *Tspo*$^{fl/fl}$ cohorts. **(E)** Quantification of glycogen content confirmed significantly more glycogen in livers of *Tspo*$^{-/-}$ mice compared to *Tspo*$^{fl/fl}$ cohorts in the unfed state (light cycle). Level of glycogen was similar between the two genotypes in the fed state (dark cycle) (n=5-9 mice/group). **(F)** Lipidomic analysis of the livers in the unfed state showed no difference in the total levels of cholesterol (Chol), triglycerides (TG) and free fatty acids (FFA) between the two genotypes. Total level of acylcarnitines (AC) was almost doubled in *Tspo*$^{-/-}$ livers compared to *Tspo*$^{fl/fl}$ group (n=8/group). **(G)** Levels of all long-chain ACs, except AC(18:1), were significantly elevated in *Tspo*$^{-/-}$ livers compared to *Tspo*$^{fl/fl}$ group (n=8/group). **(H)** Lipidomic analysis of the plasma in the unfed state showed no difference in the total levels of Chol, TG and FFA between the two genotypes. Total level of AC was significantly higher in *Tspo*$^{-/-}$ plasma compared to *Tspo*$^{fl/fl}$ group (n=8/group). **(I)** Levels of all long-chain ACs examined were elevated in *Tspo*$^{-/-}$ plasma compared to *Tspo*$^{fl/fl}$ group (n=8/group).

To further characterize metabolic changes as a result of TSPO deletion, liquid chromatograph/mass spectrometry-based profiling of the liver and plasma metabolomes were performed in mice at the unfed state. No significant changes were observed in total cholesterol (Chol), triglycerides (TG) and free fatty acids (FFA) levels between the livers of *Tspo*$^{fl/fl}$ and *Tspo*$^{-/-}$ mice (Figure 5.1F). However, the total level of acylcarnitines (AC), the committed form of fatty acids for FAO, was almost doubled in *Tspo*$^{-/-}$ livers compared to *Tspo*$^{fl/fl}$ group (Figure 5.1F). Analysis of long-chain ACs revealed marked increase in ACs of palmitic acid (16:0), stearic acid (18:0) and linoleic acid (18:2) in *Tspo*$^{-/-}$ livers compared to *Tspo*$^{fl/fl}$ group (Figure 5.1G). AC of oleic acid (18:1) was also elevated in *Tspo*$^{-/-}$ livers but the value did not reach statistical significance. In the plasma, similar to the liver, there were no significant changes in the total levels of Chol, TG, FFA between *Tspo*$^{fl/fl}$ and *Tspo*$^{-/-}$ mice (Figure 5.1H). Levels of all examined long-chain ACs were significantly elevated in *Tspo*$^{-/-}$ plasma compared to *Tspo*$^{fl/fl}$ group (Figure 5.1I). Such accumulation of ACs often indicates highly active or overloaded mitochondrial FAO, causing the excessive secretion of ACs into plasma. This supports our conclusion that *Tspo*$^{-/-}$ mice indeed have increased FAO. In addition to liver and

plasma, we also found no changes in total cholesterol level, both free cholesterol and cholesterol esters, in the adrenal glands and brown adipose tissues of *Tspo*$^{-/-}$ mice (not shown). These are tissues where TSPO is the most highly expressed, and such similarity between the two genotypes rules out the possibility of any involvement of TSPO in cholesterol homeostasis, including translocation.

Taken together, our results suggest that TSPO has an inhibitory effect on mitochondrial FAO, and loss of TSPO causes the flux of fatty acids in the form of ACs into mitochondria for β-oxidation.

TSPO dimerization is induced by protoporphyrin IX (PPIX)

It has not been documented in the literature whether TSPO could bind FFA or interact with any proteins directly involved in FAO. In the previous study (Tu et al., 2016), we proposed 3 possible mechanisms for how TSPO could affect FAO: 1/ binding to acyl-coA-binding protein (ACBP) (Bovolin et al., 1990), which has been shown to be directly involved in fatty acid metabolism (Lee et al., 2007; Neess et al., 2011); 2/ binding to VDAC1 (McEnery et al., 1992), which forms FFA transfer complex with CPT1a at the OMM (Lee et al., 2011); 3/ changing physical membrane properties or lipid compositions of the OMM. Now we find the third option unlikely as our lipidomics comparing *Tspo*$^{fl/fl}$ and *Tspo*$^{-/-}$ livers did not detect any shifts in compositions of membrane phospholipids including all classes of sphingophospholipids and glycerophospholipids (not shown). In order to examine the other two possibilities, we performed co-immunoprecipitation to identify interacting partners of TSPO. TSPO is a transmembrane protein; and traditional co-immunoprecipitation using a weak- or non- denaturing condition to lyse cells is very prone to false positives as micelle-like vesicles formed under this condition entrap nonspecific membrane proteins nearby. Hence, we used crosslinkers to covalently link interacting proteins and then disrupted membranes completely under a strong denaturing condition with SDS. Crosslinkers with different chemistry (L-photo-leucine linking Leu to Leu; GA, DSP, DTBP linking primary amines), different spacer arm lengths, different reactivity and hydrophobicity were used to avoid artifacts. Western blot result showed only one consistent band of a TSPO complex at 30-32 kDa across all the crosslinkers used (Figure 5.2A). However, immunoprecipitation using a monoclonal TSPO antibody followed by proteomics did not detect any other

protein at 14-16 kDa in this complex (not shown), suggesting the complex to be a homodimer of TSPO. We then expressed TSPO-HA and TSPO-Flag proteins in MA-10:*Tspo*Δ/Δ cells. TSPO-HA protein was readily detected in the complex pulled down by a monoclonal anti-Flag antibody, confirming the dimerization of TSPO (Figure 5.2B).

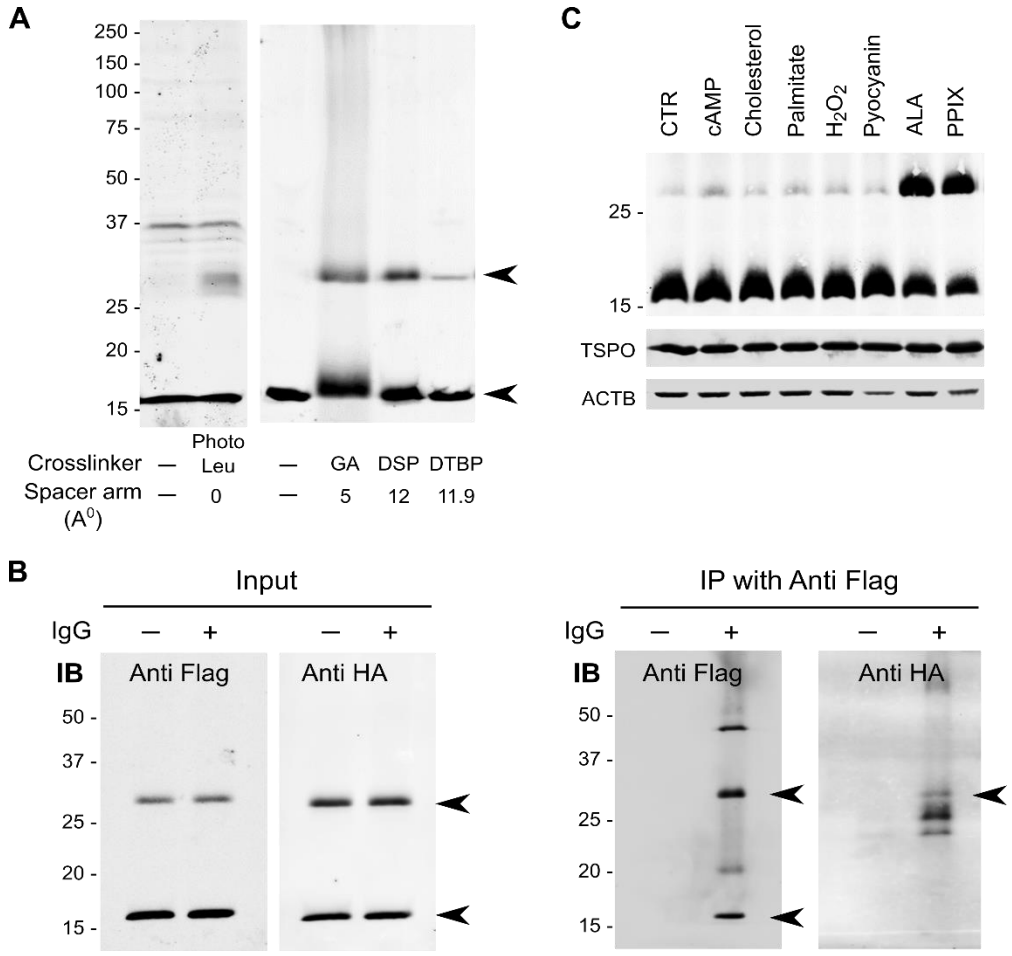

Figure 5.2. TSPO dimerization is induced by PPIX. (A) Western blot result showed one consistent band of a TSPO complex at 30-32 kDa across all the crosslinkers used in MA-10 cells. **(B)** Co-immunoprecipitation was carried out with lysates prepared from MA-10:*Tspo*Δ/Δ cells expressing TSPO-Flag and TSPO-HA. Cells were incubated with DSP to crosslink interacting proteins. Immunoblots (IB) of the input using anti-Flag and anti-HA antibodies detected both monomer and dimer bands at 16 and 30kDa respectively. Cell lysates were then immunoprecipitated (IP) with anti-Flag antibody and then blotted using anti-HA antibody. The presence of TSPO-HA in the complex pulled down by anti-Flag antibody confirmed the formation of a homodimer. **(C)** MA-10 cells were treated with different chemicals and TSPO dimer formation was evaluated. cAMP, cholesterol, palmitic acid, H_2O_2 and pyocyanin did not affect dimer formation. ALA and PPIX strikingly increased TSPO dimer formation.

To investigate whether the dimerization of TSPO is a random physical association or of significant biological relevance, several conditions were applied to MA-10 cells to identify any changes in the dimer formation. Interestingly, only 5-aminolevulinic acid (ALA) and protoporphyrin IX (PPIX) strikingly increased the dimerization of TSPO (Figure 5.2C). ALA is the precursor of PPIX while PPIX is the immediate precursor of heme. PPIX is the only endogenous ligand of TSPO that has been reproducible across different studies and systems. All other tested stimuli including cAMP, different forms of lipids (cholesterol, palmitic acid) and reactive oxygen species (H_2O_2, pyocyanin) failed to alter the dimerization of TSPO (Figure 5.2C). Other conditions such as starvation, serum supplementation and hypoxia also did not have any effect on TSPO dimer formation (not shown). Specificity of PPIX in inducing dimerization of TSPO was compared with other porphyrin derivatives. PPIX was found to be the strongest inducer while iron-containing porphyrins including heme were either much weaker or had no effect at all (not shown).

TSPO regulates the level of PPIX in cells and tissues

The effect of TSPO deletion and overexpression on PPIX and heme levels was examined in three different systems: mouse tissues, MA-10 cells and BL21 *E.coli*. First, total levels of PPIX and heme were quantified in various mouse tissues. As demonstrated in our previous study (Tu et al., 2016), tissues rich in lipid droplets such as Harderian glands, adrenal glands and brown adipose tissues (BAT) have the highest TSPO expression (Figure 5.3A). Expression of VDAC1, another protein in the OMM, does not correlate with the lipid content of tissues like TSPO (Figure 5.3A). Strikingly, we noticed the same strong correlation that these lipid-rich tissues also had a very high level of free PPIX compared to other tissues (Figure 5.3A). This trend was not observed with the total level of heme (not shown). Comparing level of free PPIX between $Tspo^{fl/fl}$ and $Tspo^{-/-}$ mice, no differences between the two genotypes were found in tissues with low-moderate level of TSPO expression such as brain, spleen, liver, and bone marrow, agreeing with our previous findings (Zhao et al., 2016). However, in tissues with very high level of TSPO expressions, absence of TSPO significantly reduced the level of PPIX (Figure 5.3A), but not heme (not shown). These data suggest that

binding of TSPO to PPIX increases the availability of PPIX in tissues, potentially by protecting it from degradation or bioconversion.

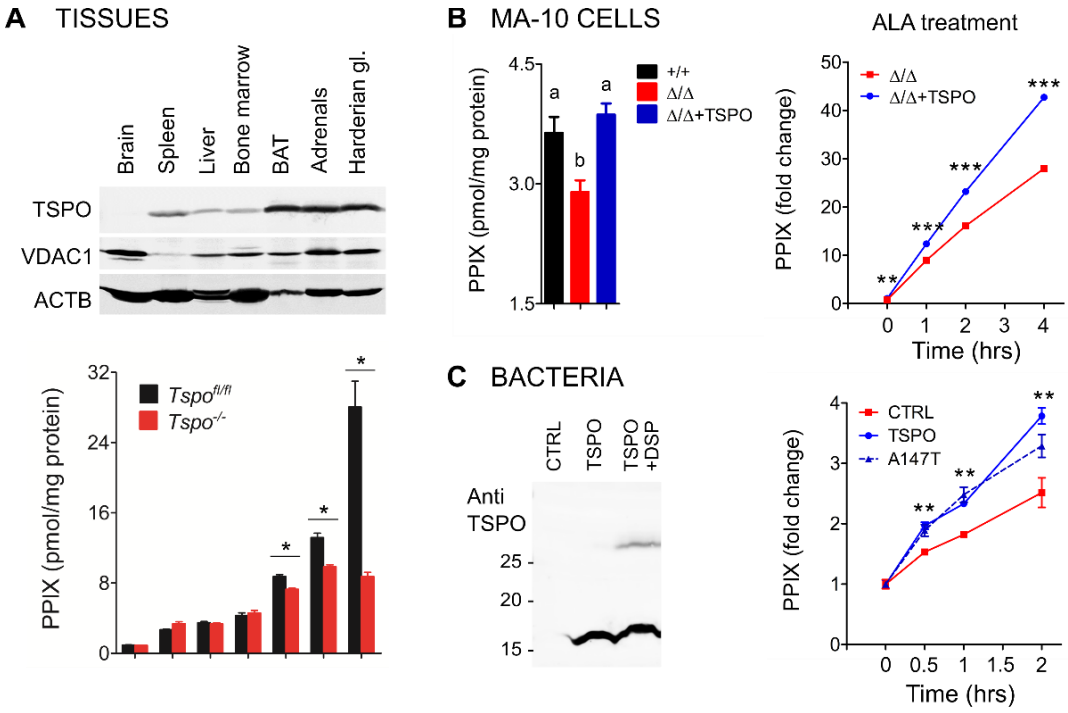

Figure 5.3. TSPO regulates the level of PPIX in cells and tissues. (A) Various mouse tissues were examined for TSPO expression and PPIX content. Tissues low in TSPO expression such as brain, spleen, liver and bone marrow had low level of PPIX. Tissues high in TSPO expression such as brown adipose tissue (BAT), adrenal glands, Harderian glands had high level of PPIX. In tissues high in PPIX and TSPO expression, *Tspo*$^{-/-}$ have significantly lower level of PPIX compared to *Tspo*$^{fl/fl}$ group (n=6-8/group). **(B)** MA-10:*Tspo*Δ/Δ cells had significantly lower level of PPIX at baseline compared to control MA-10 cells. Re-expressing TSPO in MA-10:*Tspo*Δ/Δ cells rescued level of PPIX to the similar level in MA-10 cells (n=3/group). Treatment with ALA increased intracellular PPIX level in all cells wover time. MA-10:*Tspo*Δ/Δ+TSPO cells accumulated much more PPIX at 1, 2, 4 hr time points compared to MA-10:*Tspo*Δ/Δ cells (n=3/group). **(C)** BL21 bacteria was induced to express mammalian TSPO and the expression was confirmed by the 16kDa band in western blot. Crosslinking with DSP showed the same band of TSPO dimer at 30kDa. Treatment with ALA increased intracellular PPIX level in the bacteria over time. Bacteria expressing TSPO accumulated significantly more PPIX at 0.5, 1, 2 hr time points compared to control bacteria. Bacteria expressing TSPO with A147T polymorphism accumulated the same level of PPIX as bacteria expressing wild type TSPO (n=3/group).

In MA-10 cells, TSPO knockout MA-10:*Tspo*Δ/Δ cells showed significantly lower baseline PPIX level than the wild type MA-10 cells (Figure 5.3B). When the knockout clone was re-expressed TSPO, the level of PPIX was rescued in these cells and became comparable to that in the control MA-10 cells (Figure

5.3B). To avoid misinterpretation as the result of any clonal effect when comparing the knockout clone and the wild type heterogeneous MA-10 cell population, we decided to use the TSPO knockout clone and the TSPO re-expressing cells from the same clone for further analysis. When these two groups of cells were challenged with ALA for PPIX production, the difference observed in PPIX level at baseline was further exacerbated with time. Cells with TSPO (Δ/Δ+TSPO) accumulated significantly more PPIX than cells without TSPO (Δ/Δ) at all examined time points (Figure 5.3B), substantiating our observation in mouse tissues.

To rule out possibilities of interference or compensation from other biological systems that might mediate the changes in intracellular PPIX level, we introduced mammalian TSPO into BL21 *E.coli* bacteria that do not have any other mammalian machinery. Western blot result confirmed successful IPTG induction of mammalian TSPO expression in the bacteria (Figure 5.3C). Crosslinking with DSP showed the same TSPO dimer band at 30 kDa (Figure 5.3C), suggesting proper folding of the protein in bacteria. When the bacteria were challenged with ALA, we observed the exact same trend that bacteria expressing mammalian TSPO accumulated significantly more PPIX over time compared to the control bacteria (Figure 5.3B). Bacteria expressing mammalian TSPO with A147T polymorphism performed the same as those expressing wild type TSPO (Figure 5.3C), indicating that this polymorphism did not affect the function of TSPO. The above experiment was performed in the dark condition, simulating the dark environment in mammalian tissues.

TSPO binding protects PPIX from degradation or bioconversion

TSPO synthetic ligands: PK11195, Ro5-4864 and Etifoxine were added to MA-10 cells to displace bound PPIX from TSPO. Levels of PPIX in wild type MA-10 cells treated with PK11195 and Ro5-4864 significantly reduced and reached similar levels to *Tspo*Δ/Δ cells (Figure 5.4A). Etifoxine did not have any effect on the level of PPIX, most probably due to the inability to displace PPIX from its binding to TSPO. The effects of PK1115 and Ro5-4864 were specific and mediated by TSPO as no changes in PPIX level were observed when these ligands were added to *Tspo*Δ/Δ cells (Figure 5.4A). PPIX displaced from TSPO

by the ligands was likely to be degraded or converted into an unknown metabolite as total level of heme remained constant after all treatments (not shown). Interestingly, when bound PPIX was displaced by PK1115 and Ro5-4864, baseline TSPO dimers also dissociated as shown in the western blot (Figure 5.4B), substantiating our conclusion that TSPO dimerization was indeed only triggered by PPIX binding to TSPO.

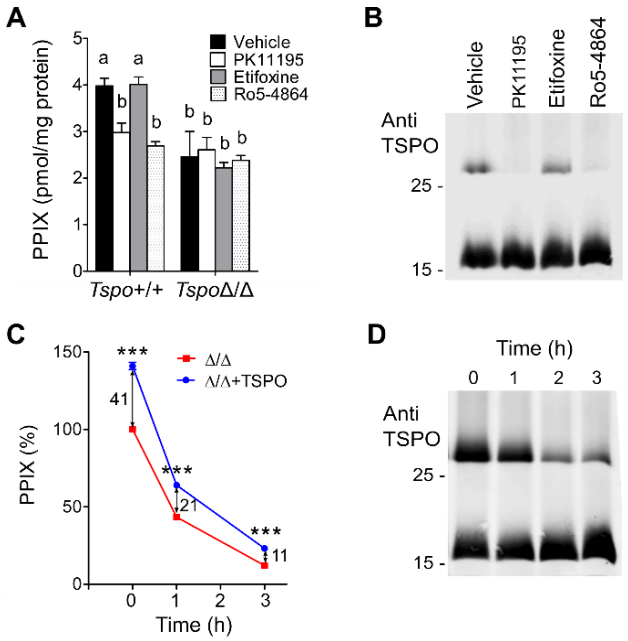

Figure 5.4. TSPO binding protects PPIX from degradation. (A) MA-10 cells were treated with TSPO ligands PK11195, Etifoxine and Ro5-4864. Levels of PPIX in MA-10 cells treated with PK11195 and Ro5-4864 significantly reduced and reached similar level of PPIX in *Tspo*Δ/Δ cells. Etifoxine did not have any effect on the level of PPIX in MA-10 cells (n=4/group). **(B)** MA-10 cells were treated with TSPO ligands and crosslinked with GA. No dimer form was detected in western blot after PK11195 and Ro5-4864 treatment while Etifoxine did not affect dimer formation. **(C)** *Tspo*Δ/Δ and *Tspo*Δ/Δ+TSPO cells were treated with ALA to accumulate PPIX for 6 hr. ALA was removed and level of PPIX quickly went down over time. At time 0, *Tspo*Δ/Δ+TSPO cells accumulated 41% more PPIX than *Tspo*Δ/Δ cells. The difference reduced to 21% and 11% after 1 and 3 hr respectively. **(D)** MA-10 cells were treated with ALA for 6 h to accumulate PPIX. ALA was then removed and cell lysates were crosslinked with GA to examine dimer formation at 1, 2, 3 hr time points. Western blot showed diminishing presence of TSPO dimer over time.

To examine whether the binding and protection of TSPO to PPIX is permanent, we treated MA-10 cells with ALA for 6 h to induce non-physiologically high level of PPIX accumulation in the cells. ALA was then removed to stop further PPIX synthesis and PPIX levels were measured over time in *Tspo*Δ/Δ and *Tspo*Δ/Δ+TSPO cells. At time 0 when ALA was just removed, *Tspo*Δ/Δ+TSPO cells accumulated 41%

more PPIX than *Tspo*Δ/Δ cells (Figure 5.4C). However, after 1 h of ALA removal, total level of PPIX dropped drastically in both groups, indicating that PPIX is actively and quickly removed from cells. The difference in PPIX level between the 2 genotypes reduced by half to only 21% after 1 h and to 11% after 3 h of ALA removal (Figure 5.4C), which is attributed to the release of bound PPIX from TSPO over time for degradation. The reduction in PPIX binding also corresponded to the dissociation of TSPO dimers over time (Figure 5.4D). Together, this data show that binding of PPIX to TSPO is a reversible, dynamic process and under regulation of cellular demand.

First evidence of biological effect of PPIX on lipid metabolism

We reported for the first time that PPIX, not heme is highly enriched in lipid-rich tissues, suggesting a potential role of PPIX in lipid homeostasis. However, very limited research has been done to examine if PPIX could have any independent physiological effects besides being converted to heme. In this experiment, mice were injected with 25 mg/kg ALA to transiently and acutely increase PPIX levels in all the tissues. After 4 hrs, lipid metabolism was examined in the livers of both $Tspo^{fl/fl}$ and $Tspo^{-/-}$ mice to determine whether such global surge in PPIX level has any biological effect and whether the effect is TSPO-dependent. Oil Red O (ORO) staining showed that $Tspo^{fl/fl}$ livers had neutral lipid deposits while these were much less noticeable and mostly absent in $Tspo^{-/-}$ livers (Figure 5.5A). Quantification of the ORO staining confirmed significantly smaller liver areas in $Tspo^{-/-}$ mice having lipid deposits compared to the $Tspo^{fl/fl}$ group (Figure 5.5B). Gene expression analysis showed that *Acaca*, the gene catalyzing the rate-limiting step in fatty acid synthesis was significantly downregulated only in $Tspo^{fl/fl}$ mice after ALA injection (Figure 5.5C). Other genes involved in lipid synthesis: *Srebp1c* and *Fasn* were not affected in both genotypes. Most intriguingly, genes involved in FAO: *Cpt1a* and *Hadha* were both severely downregulated after ALA injection in both genotypes (Figure 5.5C), indicating that a surge in PPIX level in the body could markedly inhibit FAO. The inhibitory effect was much more prominent in the presence of TSPO due to higher PPIX level: *Cpt1a* and *Hadha* were downregulated by 80% and 55% respectively in $Tspo^{fl/fl}$ mice while they were downregulated only by 40% and 25% respectively in $Tspo^{-/-}$ mice. This explains why unmetabolized lipids

started to accumulate more in *Tspo*$^{fl/fl}$ livers compared to the *Tspo*$^{-/-}$ mice as shown in ORO staining. To extrapolate further, this also explains why our *Tspo*$^{-/-}$ mice having lower PPIX level at baseline would upregulate the FAO machinery compared to *Tspo*$^{fl/fl}$ mice.

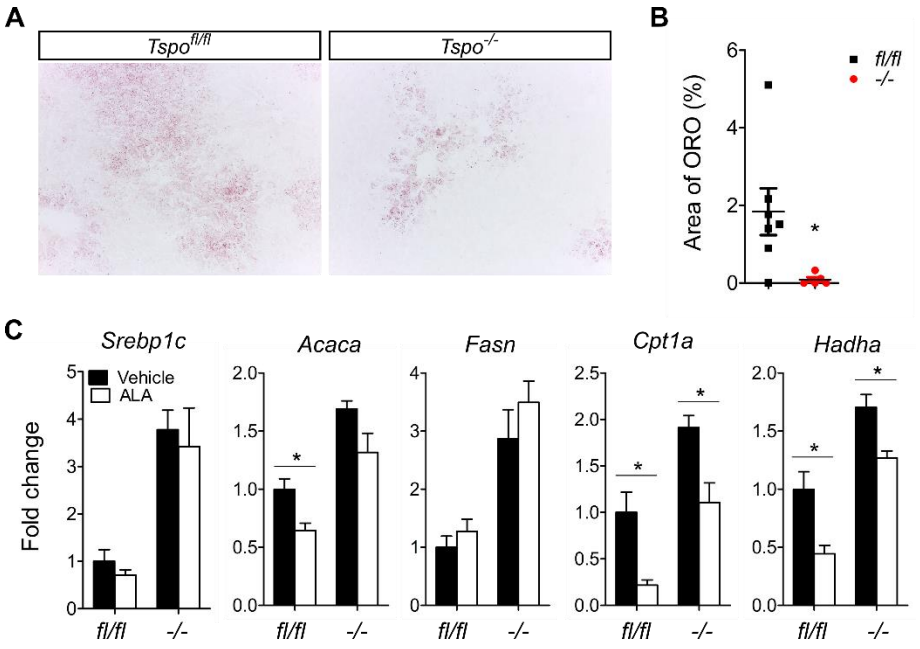

Figure 5.5. PPIX inhibits liver FAO. Mice were injected ALA 25mg/kg and livers were examined after 4 hrs. **(A)** Oil Red O (ORO) staining showed that *Tspo*$^{fl/fl}$ livers had neutral lipid deposits (red color), while these were mild or mostly absent in *Tspo*$^{-/-}$ livers. **(B)** Quantification of the ORO stained area confirmed significantly smaller liver areas in *Tspo*$^{-/-}$ mice having lipid deposits compared to the *Tspo*$^{fl/fl}$ group (n=5-7 mice/group). **(C)** Gene expression analysis showed that after ALA injection, *Srebp1c* and *Fasn* were not affected in both genotypes while *Acaca* was significantly downregulated only in *Tspo*$^{fl/fl}$ livers. After ALA injection, *Cpt1a* and *Hadha* were strikingly downregulated by 80% and 55% respectively in *Tspo*$^{fl/fl}$ livers while they were downregulated only by 40% and 25% respectively in *Tspo*$^{-/-}$ livers (n=4 mice/group).

DISCUSSION

PPIX and tetrapyrroles are the only endogenous ligands of TSPO that have been demonstrated in almost all kingdoms (Veenman et al., 2016). Functional characterization of TSPO binding to PPIX has been reported in several studies in bacteria and plants but extremely limited in mammals, possibly due to the daunting old model of TSPO in steroidogenesis. Our study concludes that mammalian TSPO binds reversibly to sequester PPIX in the form of a dimer and prevents PPIX from quick degradation or

bioconversion in cells. Hence, cells expressing high level of TSPO have a larger reservoir of PPIX, which can be released for biological actions on demand. We propose that this mechanism is also conserved for TSPO in other species. Indeed, the most systematic and extensive functional characterization of TSPO and PPIX interaction was done in *Rhodobacter sphaeroides* (Yeliseev and Kaplan, 1995; Yeliseev and Kaplan, 1999) and shared many similar findings with ours. When TSPO was absent, bacteria accumulated significantly less PPIX compared to wild type bacteria (Yeliseev and Kaplan, 1999); instead they produced more Mg-protoporphyrins (Yeliseev and Kaplan, 1999) and bacteriochlorophylls (Yeliseev and Kaplan, 1995), the downstream enzymatic products of PPIX in photosynthetic bacteria. In Arabidopsis thaliana, TSPO was found to be a scavenger for porphyrins including heme and PPIX although the binding affinity for PPIX was weaker than heme (Vanhee et al., 2011). When treated with ALA to induce porphyrins accumulation, transgenic plant cells overexpressing TSPO could sequester markedly more porphyrins compared to wild type plant cells. High level of TSPO protected cells from porphyrin-induced phototoxicity and when TSPO was degraded by autophagy, excess porphyrins were also removed (Vanhee et al., 2011). From these studies, it seems that the ultimate effects of TSPO-PPIX interaction vary in different biological systems, but sequestering and shielding PPIX or tetrapyrroles is the conserved biological function of TSPO. A recent structural study in *Bacillus cereus* by Guo *et al*, however, concluded that TSPO actively degraded PPIX but only when UV light and oxygen were present (Guo et al., 2015). Although it is arguable that this is the unique function of TSPO in bacteria, it is hard to comprehend such important enzymatic activity is lost during evolution of a small protein like TSPO. This result also contradicts the study in *Rhodobacter sphaeroides* where no TSPO corresponded to a low level of PPIX (Yeliseev and Kaplan, 1999). We speculate that the use of albumin protein as the negative control for TSPO in the Guo *et al* study was not adequate. Bacterial TSPO is particularly rich in tryptophan residues, which are highly photoexcitable and the emission wavelength spectrum of tryptophan significantly overlaps with the absorption spectrum of PPIX (Shaw and Pal, 2008). That could explain why TSPO altered PPIX absorption spectrum only in the presence of UV light. A tryptophan-rich protein would serve as a better negative control than albumin to determine if the effect is indeed mediated by bacterial TSPO.

TSPO has been found to interact with several proteins and hence placed in different unrelated functional models (Gatliff et al., 2014; Guilarte et al., 2016; Rone et al., 2012). These interactions were concluded from experiments performed under a non- or weak- denaturing condition that is prone to produce false positives for transmembrane proteins due to incomplete disruption of lipid membranes. In our study, we used different crosslinkers to covalently link interacting proteins and preserve the interactions when cells are lysed in a strong denaturing condition. We only observed a single band of TSPO dimer at 30-32kDa, and no other band up to 250kDa. This agreed with the glutaraldehyde crosslinking result of TSPO in *Rhodobacter sphaeroides* (Yeliseev and Kaplan, 2000). Although TSPO dimerization has been reported in literature, it is often not based on definitive experimental evidence. For instance, TSPO was reported to exist in several forms of oligomers since multiple bands were detected in a western blot using TSPO polyclonal antisera (Delavoie et al., 2003). These extra bands are likely nonspecific as they have not been reported in studies using TSPO monoclonal antibodies (Morohaku et al., 2014; Tu et al., 2014). Crystallographic studies of bacterial TSPO concluded that purified TSPO formed a highly stable dimer (Guo et al., 2015; Li et al., 2015) while the NMR structure of mouse TSPO was found to be a monomer (Jaremko et al., 2014). Moreover, the dimerization interface was completely different between *Bacillus cereus* and *Rhodobacter sphaeroides* TSPO (Guo et al., 2015; Li et al., 2015), raising questions why the dimerization sites are not conserved and whether the dimerization itself is an artifact due to hydrophobic aggregation of TSPO during purification and/or crystallization. Our study not only confirmed TSPO dimerization but also demonstrated that the dimer form is likely to have biological significance. TSPO dimerization is greatly induced or stabilized only by porphyrins, particularly PPIX, suggesting that shielding PPIX from degradation or bioconversion requires TSPO in the dimer form. However, the exact dimerization interface remains to be investigated.

Level of free PPIX in cells and tissues is directly regulated by TSPO and correlates with the level of TSPO expression. Therefore, we speculate that cell type-dependent biological effects of TSPO reported in literature are mediated by biological actions of PPIX, rather than directly by TSPO. PPIX is believed to

be committed to heme synthesis and has no other function in cells. However, early reports showed that level of free PPIX is readily detectable in many tissues at varying degrees under different pathological conditions. In neoplastic diseases and chronic circulatory disorders, free PPIX was abundant in many tissues but highest in adrenal glands, with values up to 100 and 200 times higher than in normal adrenals respectively (Zawirska, 1978). In adrenal tumorous diseases without hyperplastic lesions, level of PPIX was even 4 times higher than adrenals of patients with porphyria (Zawirska, 1977), a disorder that causes severe build-up of porphyrins in the body. Interestingly, this marked elevation only applied to PPIX, not copro- or uro-porphyrins, suggesting a specific regulation for PPIX in the tissues. When rats were starved for 24 hrs, activity of ALA synthase, the rate-limiting enzyme to synthesize porphyrins, doubled in the adrenal glands but stayed the same in the liver. This led to accumulation of PPIX in adrenals that was surprisingly not accompanied by any changes in the heme content of the tissue (Condie et al., 1976). These data clearly indicate unknown biological functions of PPIX that are tightly regulated under physiological and pathological conditions. Our study reports for the first time a strong correlation between PPIX level and lipid-rich tissues. When mice were injected with ALA to induce PPIX production in the whole body, mitochondrial FAO was strikingly inhibited in the liver and the effect was more prominent when PPIX was preserved in the presence of TSPO. This also explains why TSPO, by binding and maintaining high level of PPIX in the OMM, has an inhibitory effect on FAO and deletion of TSPO in the mice and MA-10 cells lifts up this inhibitory mechanism, causing a surge in mitochondrial FAO as observed in both systems.

Although evidence for biological functions of PPIX is extremely limited, there has been direct evidence that PPIX could bind to several proteins such as soluble guanylate cyclase (Ignarro et al., 1982), transferases (Smith et al., 1985), beta lactoglobulin (Dufour et al., 1990), hemoglobin and myoglobin (Sil et al., 2004). The binding site could be the same as heme due to their similarity in structure, or distinct. Some of these bindings have been characterized to have biological significance as they modify protein functions. PPIX, but not other structural analogs, is a strong activator of soluble guanylate cyclase (Ignarro et al., 1982), hence significantly increased cGMP-mediated relaxation of bovine pulmonary arteries

(Mingone et al., 2006). Furthermore, among all naturally occurring porphyrins, PPIX was found to be the strongest inhibitor of glutathione S-transferase isozymes (Smith et al., 1985), the key detoxifying enzymes important for cellular metabolism. Other biological effects reported for PPIX with unknown molecular mechanism include inhibition of HIV virus replication, not due to inhibition of viral enzyme reverse transcriptase (Asanaka et al., 1989); and induction of Heme-binding protein 23kDa (HBP23) mRNA expression to a similar level elicited by heme (Immenschuh et al., 1997). Interestingly, the inhibitory effect of PPIX on HIV virus replication could underlie the inhibitory effect of TSPO on HIV-1 replication in human CD4(+) T cell line (Zhou et al., 2014). From these studies, we speculate that PPIX could have diverse biological functions, including inhibition of FAO, but the molecular mechanism of action is a brand-new area to investigate. A few possible mechanisms are: 1/ PPIX inserts into different lipid membranes due to its high hydrophobicity and alters functions of membrane proteins; 2/ similar to heme, PPIX directly binds to proteins, changes protein conformation and functions; 3/ PPIX is converted to some other metabolites that have bioactivities.

Our study concludes that TSPO sequesters PPIX, protects it from degradation or bioconversion, and therefore directly regulates level of free PPIX in cells. Similar to TSPO, PPIX is enriched in tissues rich in lipid droplets and has an inhibitory effect on mitochondrial FAO. Although the range of biological functions for PPIX remain elucidated, reported effects of TSPO in various systems needs careful interpretation as they could be mediated through PPIX. TSPO, therefore, maybe better known as a the Tetrapyrrole Sequestering PrOtein.

REFERENCES

Asanaka, M., T. Kurimura, H. Toya, J. Ogaki, and Y. Kato. 1989. Anti-HIV activity of protoporphyrin. *AIDS (London, England)*. 3:403-404.

Banati, R.B., R.J. Middleton, R. Chan, C.R. Hatty, W.W. Kam, C. Quin, M.B. Graeber, A. Parmar, D. Zahra, P. Callaghan, S. Fok, N.R. Howell, M. Gregoire, A. Szabo, T. Pham, E. Davis, and G.J. Liu. 2014. Positron emission tomography and functional characterization of a complete PBR/TSPO knockout. *Nature communications*. 5:5452.

Bovolin, P., J. Schlichting, M. Miyata, C. Ferrarese, A. Guidotti, and H. Alho. 1990. Distribution and characterization of diazepam binding inhibitor (DBI) in peripheral tissues of rat. *Regulatory peptides*. 29:267-281.

Busch, A.W., Z. WareJoncas, and B.L. Montgomery. 2017. Tryptophan-Rich Sensory Protein/Translocator Protein (TSPO) from Cyanobacterium Fremyella diplosiphon Binds a Broad Range of Functionally Relevant Tetrapyrroles. *Biochemistry*. 56:73-84.

Campeau, E., V.E. Ruhl, F. Rodier, C.L. Smith, B.L. Rahmberg, J.O. Fuss, J. Campisi, P. Yaswen, P.K. Cooper, and P.D. Kaufman. 2009. A versatile viral system for expression and depletion of proteins in mammalian cells. *PloS one*. 4:e6529.

Condie, L.W., T.R. Tephly, and J. Barbon. 1976. Studies on heme synthesis in the rat adrenal. *Ann Clin Res*. 8 Suppl 17:83-88.

Delavoie, F., H. Li, M. Hardwick, J.C. Robert, C. Giatzakis, G. Peranzi, Z.X. Yao, J. Maccario, J.J. Lacapere, and V. Papadopoulos. 2003. In vivo and in vitro peripheral-type benzodiazepine receptor polymerization: functional significance in drug ligand and cholesterol binding. *Biochemistry*. 42:4506-4519.

Dimitrova-Shumkovska, J., L. Veenman, T. Ristoski, S. Leschiner, and M. Gavish. 2010. Chronic high fat, high cholesterol supplementation decreases 18 kDa Translocator Protein binding capacity in association with increased oxidative stress in rat liver and aorta. *Food and chemical toxicology : an international journal published for the British Industrial Biological Research Association*. 48:910-921.

Dufour, E., M.C. Marden, and T. Haertle. 1990. Beta-lactoglobulin binds retinol and protoporphyrin IX at two different binding sites. *FEBS letters*. 277:223-226.

Gatliff, J., D. East, J. Crosby, R. Abeti, R. Harvey, W. Craigen, P. Parker, and M. Campanella. 2014. TSPO interacts with VDAC1 and triggers a ROS-mediated inhibition of mitochondrial quality control. *Autophagy*. 10:2279-2296.

Ginter, C., I. Kiburu, and O. Boudker. 2013. Chemical catalysis by the translocator protein (18 kDa). *Biochemistry*. 52:3609-3611.

Guilarte, T.R., M.K. Loth, and S.R. Guariglia. 2016. TSPO Finds NOX2 in Microglia for Redox Homeostasis. *Trends in pharmacological sciences*.

Guo, Y., R.C. Kalathur, Q. Liu, B. Kloss, R. Bruni, C. Ginter, E. Kloppmann, B. Rost, and W.A. Hendrickson. 2015. Protein structure. Structure and activity of tryptophan-rich TSPO proteins. *Science (New York, N.Y.)*. 347:551-555.

Ignarro, L.J., K.S. Wood, and M.S. Wolin. 1982. Activation of purified soluble guanylate cyclase by protoporphyrin IX. *Proceedings of the National Academy of Sciences of the United States of America*. 79:2870-2873.

Immenschuh, S., C. Nell, S. Iwahara, N. Katz, and U. Muller-Eberhard. 1997. Gene regulation of HBP 23 by metalloporphyrins and protoporphyrin IX in liver and hepatocyte cultures. *Biochem Biophys Res Commun*. 231:667-670.

Jaremko, L., M. Jaremko, K. Giller, S. Becker, and M. Zweckstetter. 2014. Structure of the mitochondrial translocator protein in complex with a diagnostic ligand. *Science (New York, N.Y.)*. 343:1363-1366.

Kind, T., K.H. Liu, Y. Lee do, B. DeFelice, J.K. Meissen, and O. Fiehn. 2013. LipidBlast in silico tandem mass spectrometry database for lipid identification. *Nature methods*. 10:755-758.

Leduc, M.S., R.S. Hageman, R.A. Verdugo, S.W. Tsaih, K. Walsh, G.A. Churchill, and B. Paigen. 2011. Integration of QTL and bioinformatic tools to identify candidate genes for triglycerides in mice. *Journal of lipid research*. 52:1672-1682.

Lee, K., J. Kerner, and C.L. Hoppel. 2011. Mitochondrial carnitine palmitoyltransferase 1a (CPT1a) is part of an outer membrane fatty acid transfer complex. *The Journal of biological chemistry*. 286:25655-25662.

Lee, L., C.A. DeBono, D.R. Campagna, D.C. Young, D.B. Moody, and M.D. Fleming. 2007. Loss of the acyl-CoA binding protein (Acbp) results in fatty acid metabolism abnormalities in mouse hair and skin. *The Journal of investigative dermatology*. 127:16-23.

Li, F., J. Liu, Y. Zheng, R.M. Garavito, and S. Ferguson-Miller. 2015. Protein structure. Crystal structures of translocator protein (TSPO) and mutant mimic of a human polymorphism. *Science (New York, N.Y.)*. 347:555-558.

Lin, R., A. Angelin, F. Da Settimo, C. Martini, S. Taliani, S. Zhu, and D.C. Wallace. 2014. Genetic analysis of dTSPO, an outer mitochondrial membrane protein, reveals its functions in apoptosis, longevity, and Ab42-induced neurodegeneration. *Aging cell*. 13:507-518.

Livak, K.J., and T.D. Schmittgen. 2001. Analysis of relative gene expression data using real-time quantitative PCR and the 2(-Delta Delta C(T)) Method. *Methods (San Diego, Calif.)*. 25:402-408.

McEnery, M.W., A.M. Snowman, R.R. Trifiletti, and S.H. Snyder. 1992. Isolation of the mitochondrial benzodiazepine receptor: association with the voltage-dependent anion channel and the adenine nucleotide carrier. *Proceedings of the National Academy of Sciences of the United States of America*. 89:3170-3174.

Mingone, C.J., S.A. Gupte, J.L. Chow, M. Ahmad, N.G. Abraham, and M.S. Wolin. 2006. Protoporphyrin IX generation from delta-aminolevulinic acid elicits pulmonary artery relaxation and soluble guanylate cyclase activation. *Am J Physiol Lung Cell Mol Physiol*. 291:L337-344.

Morohaku, K., S.H. Pelton, D.J. Daugherty, W.R. Butler, W. Deng, and V. Selvaraj. 2014. Translocator protein/peripheral benzodiazepine receptor is not required for steroid hormone biosynthesis. *Endocrinology*. 155:89-97.

Neess, D., M. Bloksgaard, S. Bek, A.B. Marcher, I.C. Elle, T. Helledie, M. Due, V. Pagmantidis, B. Finsen, J. Wilbertz, M. Kruhoffer, N. Faergeman, and S. Mandrup. 2011. Disruption of the acyl-CoA-binding protein gene delays hepatic adaptation to metabolic changes at weaning. *The Journal of biological chemistry*. 286:3460-3472.

Passonneau, J.V., and V.R. Lauderdale. 1974. A comparison of three methods of glycogen measurement in tissues. *Analytical biochemistry*. 60:405-412.

Rampon, C., M. Bouzaffour, M.A. Ostuni, P. Dufourcq, C. Girard, J.M. Freyssinet, J.J. Lacapere, G. Schweizer-Groyer, and S. Vriz. 2009. Translocator protein (18 kDa) is involved in primitive erythropoiesis in zebrafish. *FASEB journal : official publication of the Federation of American Societies for Experimental Biology*. 23:4181-4192.

Rone, M.B., A.S. Midzak, L. Issop, G. Rammouz, S. Jagannathan, J. Fan, X. Ye, J. Blonder, T. Veenstra, and V. Papadopoulos. 2012. Identification of a dynamic mitochondrial protein complex driving cholesterol import, trafficking, and metabolism to steroid hormones. *Mol Endocrinol*. 26:1868-1882.

Shaw, A.K., and S.K. Pal. 2008. Resonance energy transfer and ligand binding studies on pH-induced folded states of human serum albumin. *J Photochem Photobiol B*. 90:187-197.

Sil, S., T. Bose, D. Roy, and A.S. Chakraborti. 2004. Protoporphyrin IX-induced structural and functional changes in human red blood cells, haemoglobin and myoglobin. *J Biosci*. 29:281-291.

Smith, A., I. Nuiry, and Y.C. Awasthi. 1985. Interactions with glutathione S-transferases of porphyrins used in photodynamic therapy and naturally occurring porphyrins. *Biochem J*. 229:823-831.

Spandidos, A., X. Wang, H. Wang, and B. Seed. 2010. PrimerBank: a resource of human and mouse PCR primer pairs for gene expression detection and quantification. *Nucleic acids research*. 38:D792-799.

Thompson, M.M., H.C. Manning, and K.L. Ellacott. 2013. Translocator protein 18 kDa (TSPO) is regulated in white and brown adipose tissue by obesity. *PloS one*. 8:e79980.

Tsugawa, H., T. Cajka, T. Kind, Y. Ma, B. Higgins, K. Ikeda, M. Kanazawa, J. VanderGheynst, O. Fiehn, and M. Arita. 2015. MS-DIAL: data-independent MS/MS deconvolution for comprehensive metabolome analysis. *Nature methods*. 12:523-526.

Tu, L.N., K. Morohaku, P.R. Manna, S.H. Pelton, W.R. Butler, D.M. Stocco, and V. Selvaraj. 2014. Peripheral benzodiazepine receptor/translocator protein global knock-out mice are viable with no effects on steroid hormone biosynthesis. *The Journal of biological chemistry*. 289:27444-27454.

Tu, L.N., M.R. Showalter, T. Cajka, S. Fan, V.V. Pillai, O. Fiehn, and V. Selvaraj. 2017. Metabolomic characteristics of cholesterol-induced non-obese nonalcoholic fatty liver disease in mice. *Sci Rep*. 7:6120.

Tu, L.N., A.H. Zhao, M. Hussein, D.M. Stocco, and V. Selvaraj. 2016. Translocator Protein (TSPO) Affects Mitochondrial Fatty Acid Oxidation in Steroidogenic Cells. *Endocrinology*. 157:1110-1121.

Tu, L.N., A.H. Zhao, D.M. Stocco, and V. Selvaraj. 2015. PK11195 effect on steroidogenesis is not mediated through the translocator protein (TSPO). *Endocrinology*. 156:1033-1039.

Vanhee, C., G. Zapotoczny, D. Masquelier, M. Ghislain, and H. Batoko. 2011. The Arabidopsis multistress regulator TSPO is a heme binding membrane protein and a potential scavenger of porphyrins via an autophagy-dependent degradation mechanism. *The Plant cell*. 23:785-805.

Veenman, L., A. Vainshtein, N. Yasin, M. Azrad, and M. Gavish. 2016. Tetrapyrroles as Endogenous TSPO Ligands in Eukaryotes and Prokaryotes: Comparisons with Synthetic Ligands. *International journal of molecular sciences*. 17.

Verma, A., J.S. Nye, and S.H. Snyder. 1987. Porphyrins are endogenous ligands for the mitochondrial (peripheral-type) benzodiazepine receptor. *Proceedings of the National Academy of Sciences of the United States of America*. 84:2256-2260.

Wade, F.M., C. Wakade, V.B. Mahesh, and D.W. Brann. 2005. Differential expression of the peripheral benzodiazepine receptor and gremlin during adipogenesis. *Obesity research*. 13:818-822.

Wang, H., K. Zhai, Y. Xue, J. Yang, Q. Yang, Y. Fu, Y. Hu, F. Liu, W. Wang, L. Cui, H. Chen, J. Zhang, and W. He. 2016. Global Deletion of TSPO Does Not Affect the Viability and Gene Expression Profile. *PloS one*. 11:e0167307.

Yeliseev, A.A., and S. Kaplan. 1995. A sensory transducer homologous to the mammalian peripheral-type benzodiazepine receptor regulates photosynthetic membrane complex formation in Rhodobacter sphaeroides 2.4.1. *The Journal of biological chemistry*. 270:21167-21175.

Yeliseev, A.A., and S. Kaplan. 1999. A novel mechanism for the regulation of photosynthesis gene expression by the TspO outer membrane protein of Rhodobacter sphaeroides 2.4.1. *The Journal of biological chemistry*. 274:21234-21243.

Yeliseev, A.A., and S. Kaplan. 2000. TspO of rhodobacter sphaeroides. A structural and functional model for the mammalian peripheral benzodiazepine receptor. *The Journal of biological chemistry*. 275:5657-5667.

Zawirska, B. 1977. Porphyrins and morphology of the adrenals in some endocrinologic syndromes and other diseases. *Mater Med Pol*. 9:26-33.

Zawirska, B. 1978. Organ Porphyrins in Human Circulatory Disorders and Neoplastic Disease. Diagnosis and Therapy of Porphyrias and Lead Intoxication. *Diagnosis and Therapy of Porphyrias and Lead Intoxication*.

Zhang, P. 2012. Analysis of Mouse Liver Glycogen Content. *Bio-protocol*. 2:e186.

Zhao, A.H., L.N. Tu, C. Mukai, M.P. Sirivelu, V.V. Pillai, K. Morohaku, R. Cohen, and V. Selvaraj. 2016. Mitochondrial Translocator Protein (TSPO) Function Is Not Essential for Heme Biosynthesis. *The Journal of biological chemistry*. 291:1591-1603.

Zhou, T., Y. Dang, and Y.H. Zheng. 2014. The mitochondrial translocator protein, TSPO, inhibits HIV-1 envelope glycoprotein biosynthesis via the endoplasmic reticulum-associated protein degradation pathway. *Journal of virology*. 88:3474-3484.

CHAPTER 6

Final Conclusions and Future Directions

My studies and 25 years of TSPO research

The highly prevalent model linking TSPO to steroidogenesis was presumptively built on extensive pharmacological and genetic studies. Although it is not our intention to criticize, we are under obligation to point out that almost all mechanistic studies emanated from a single research group led by Papadopoulos and their collaborators. This model has apparently misled the field of TSPO research for the past 25 years, and acceptance of these results prevented the search for the true function of TSPO. Their early reports claiming that deletion of TSPO caused embryonic lethality in mice (Papadopoulos et al., 1997a) and severely decreased viability in cells (Papadopoulos et al., 1997b) discouraged further attempts to generate genetic tools to rigorously evaluate TSPO as a pharmacological target and its precise function. Our careful reappraisal of 25-year TSPO literature revealed serious inconsistencies and limitations in these studies that led to the inaccurate association of TSPO and steroidogenesis (Selvaraj et al., 2015). Our lab also generated the first global *Tspo*$^{-/-}$ mice and showed that TSPO is not required for survival and development as the *Tspo*$^{-/-}$ mice were healthy with no apparent abnormalities (Tu et al., 2014). Both knocking-down and knocking-out of TSPO in different steroidogenic cell lines did not affect cell viability (Tu et al., 2014; Tu et al., 2015). Furthermore, steroid hormone production was not affected in *Tspo*$^{-/-}$ mice as well as steroidogenic cells lacking TSPO compared to the controls (Tu et al., 2014; Tu et al., 2015). These findings, reproduced by 2 other independent laboratories (Banati et al., 2014; Wang et al., 2016), refuted the 25-year old dogma and removed TSPO as being a component of the steroid biosynthetic machinery associated with the mitochondria.

The modest stimulating effects of some TSPO binding chemicals on steroid hormone production are often cited as the early evidence linking TSPO and steroidogenesis (Krueger and Papadopoulos, 1990; Papadopoulos et al., 1990; Papadopoulos et al., 1991). The proposed therapeutic applications of these chemicals in human medicine are also based on the theory that they could stimulate *de novo* steroid hormone synthesis at the target sites (Nothdurfter et al., 2012). Since TSPO is shown not involved in steroidogenesis, the use of these chemicals becomes questionable due to unclear mechanism of action. Moreover, potential

off-target effects of TSPO binding chemicals have not been seriously examined, although there are reports in the literature of TSPO-independent actions of several chemicals, particularly PK11195 (Gonzalez-Polo et al., 2005; Hans et al., 2005; Seneviratne et al., 2012). Using the TSPO knock out MA-10 Leydig cancer cells, I performed the very first target validation demonstrating that PK11195 considered the prototypical TSPO binding drug could induce steroid hormone production to the same extent regardless of the presence or absence of TSPO (Tu et al., 2015). This indicated that the effect of PK11195 on steroidogenesis may be mediated through binding to an unidentified cellular target other than TSPO in steroid hormone producing cells. Such rigorous target validation studies were not previously possible as it was widely believed that TSPO-deleted cells would not be viable. These findings hence raise immediate concerns over the use of TSPO binding drugs in clinical trials due to the lack of a known target function and unpredictable side effects.

Although TSPO is not involved in steroidogenesis, its high expression in steroidogenic tissues such as the adrenal glands is irrefutable. Upon extensive tissue profiling, I found that TSPO is enriched in tissues rich in lipid droplets including adipose tissues, suggesting a role in lipid metabolism instead of steroidogenesis (Tu et al., 2016). Using both TSPO knockout MA-10 cells and *Tspo*$^{-/-}$ mice as the models, I demonstrated that deletion of TSPO increased mitochondrial fatty acid oxidation (FAO). In searching for a mechanism underlying this phenotype, I performed co-immunoprecipitation to identify interacting partners of TSPO that are involved in regulating FAO. Interestingly, my study demonstrated that TSPO did not have any interacting partners, but formed a dimer, which could be induced or stabilized by protoporphyrin IX (PPIX), the endogenous ligand of TSPO. Level of PPIX was found to be high in tissues rich in lipid droplets and directly regulated by TSPO. This study is the first to report such correlation between free PPIX level and lipid-rich tissues. Although TSPO-PPIX interaction has long been documented in the literature, the biological significance especially in mammalian systems has not been characterized in depth. Moreover, my findings suggest that conclusions from studies in which TSPO was placed in different models interacting with different proteins (Gatliff et al., 2014; Guilarte et al., 2016; Rone et al., 2012) or

shown to form dimers and oligomers (Delavoie et al., 2003; Guo et al., 2015; Li et al., 2015) were likely misinterpreted due to artifacts and technical limitations. TSPO indeed dimerizes to sequester PPIX but the dimerization interface remains to be examined.

TSPO has been demonstrated to have many biological effects in different systems and organisms (Gatliff et al., 2014; Guilarte et al., 2016; Rone et al., 2012) but these effects are unrelated and no studies have attempted to connect them or unify them by providing the exact molecular mechanism of TSPO. I proposed that throughout different kingdoms, sequestering PPIX and increasing its availability is the primary conserved function of TSPO, and the reported cell type-dependent biological effects for TSPO are mediated by biological actions of PPIX in cells rather than directly by TSPO. However, studies on PPIX function are extremely limited, making it challenging to provide satisfactory explanations to all biological effects reported for TSPO. My study attempted to find a mechanism how TSPO inhibits FAO in cells and mice and found that this effect could be attributed to the biological action of PPIX. The finding that high level of PPIX could severely inhibit FAO is novel and serves as very first evidence for one of PPIX functions in cells.

In conclusion, my studies help correct the current model of TSPO function in steroidogenesis and identify the true function of TSPO in sequestering and protecting PPIX from degradation, without any "translocator" function. Therefore, TSPO needs to be renamed as the Tetrapyrrole Sequestering PrOtein, so that the gene and protein nomenclature provides a relationship to function.

Future directions

Since TSPO is now removed from the steroidogenic machinery, it paves the way for active research in the field of steroidogenesis to elucidate the mechanism of how cholesterol is delivered from the cytosol or OMM to IMM. The steroidogenic acute regulatory protein (STAR) is a strong candidate as its expression in steroidogenic cells in the absence of hormone stimulation resulted in an increase in steroid biosynthesis

(Clark et al., 1994). Mutations in the *Star* gene were responsible for the potentially fatal lipoid congenital adrenal hyperplasia (lipoid CAH), a disease in which severely afflicted individuals are unable to synthesize steroids (Lin et al., 1995). Currently, STAR has been modeled to deliver cholesterol to the OMM and TSPO carried out the mitochondrial cholesterol import process. Since we now know such cooperation does not exist, re-examining the exact mode of action of STAR or identify other partners that assist STAR in this process will shed light on the mechanism of cholesterol transport for steroidogenesis.

Binding of TSPO to PPIX has long been documented but the binding site of PPIX to TSPO remains to be characterized. It is also important to determine if PPIX binding site is close to or the same as that of other TSPO binding chemicals and how interaction with the binding chemicals affects the function of TSPO in PPIX sequestering. This will help to interpret or predict the biological effects of the TSPO binding chemicals more accurately once we understand the biological actions of PPIX in cells. In addition, structural studies on TSPO dimerization are not yet conclusive. Recent crystallographic studies of bacterial TSPO presented different dimerization interfaces between *Bacillus cereus* and *Rhodobacter sphaeroides* TSPO (Guo et al., 2015; Li et al., 2015); this could be artefactual due to a forced conformation that may be needed a transmembrane protein like TSPO to crystalize. Dimerization was not found in an NMR study of murine TSPO (Jaremko et al., 2014). Perhaps examining membrane-bound TSPO structure in the presence of PPIX using high resolution NMR would provide us with more precise information on TSPO dimerization and the structural interface mediating this process.

Since TSPO directly regulates the level of PPIX in cells, the ultimate biological effects by targeting TSPO would largely depend on PPIX actions in cells. Therefore, elucidating biological functions of PPIX is critical to interpret biological effects reported for TSPO, such as its upregulation in neuroinflammation and other diseases. This would certainly be an interesting new research area in the future. And until more information about PPIX actions is uncovered, the potential of TSPO as a therapeutic target may not be realized in human medicine.

REFERENCES

Banati, R.B., R.J. Middleton, R. Chan, C.R. Hatty, W.W. Kam, C. Quin, M.B. Graeber, A. Parmar, D. Zahra, P. Callaghan, S. Fok, N.R. Howell, M. Gregoire, A. Szabo, T. Pham, E. Davis, and G.J. Liu. 2014. Positron emission tomography and functional characterization of a complete PBR/TSPO knockout. *Nature communications*. 5:5452.

Clark, B.J., J. Wells, S.R. King, and D.M. Stocco. 1994. The purification, cloning, and expression of a novel luteinizing hormone-induced mitochondrial protein in MA-10 mouse Leydig tumor cells. Characterization of the steroidogenic acute regulatory protein (StAR). *J Biol Chem*. 269:28314-28322.

Delavoie, F., H. Li, M. Hardwick, J.C. Robert, C. Giatzakis, G. Peranzi, Z.X. Yao, J. Maccario, J.J. Lacapere, and V. Papadopoulos. 2003. In vivo and in vitro peripheral-type benzodiazepine receptor polymerization: functional significance in drug ligand and cholesterol binding. *Biochemistry*. 42:4506-4519.

Gatliff, J., D. East, J. Crosby, R. Abeti, R. Harvey, W. Craigen, P. Parker, and M. Campanella. 2014. TSPO interacts with VDAC1 and triggers a ROS-mediated inhibition of mitochondrial quality control. *Autophagy*. 10:2279-2296.

Gonzalez-Polo, R.A., G. Carvalho, T. Braun, D. Decaudin, C. Fabre, N. Larochette, J.L. Perfettini, M. Djavaheri-Mergny, I. Youlyouz-Marfak, P. Codogno, M. Raphael, J. Feuillard, and G. Kroemer. 2005. PK11195 potently sensitizes to apoptosis induction independently from the peripheral benzodiazepin receptor. *Oncogene*. 24:7503-7513.

Guilarte, T.R., M.K. Loth, and S.R. Guariglia. 2016. TSPO Finds NOX2 in Microglia for Redox Homeostasis. *Trends in pharmacological sciences*.

Guo, Y., R.C. Kalathur, Q. Liu, B. Kloss, R. Bruni, C. Ginter, E. Kloppmann, B. Rost, and W.A. Hendrickson. 2015. Protein structure. Structure and activity of tryptophan-rich TSPO proteins. *Science (New York, N.Y.)*. 347:551-555.

Hans, G., S. Wislet-Gendebien, F. Lallemend, P. Robe, B. Rogister, S. Belachew, L. Nguyen, B. Malgrange, G. Moonen, and J.M. Rigo. 2005. Peripheral benzodiazepine receptor (PBR) ligand cytotoxicity unrelated to PBR expression. *Biochem Pharmacol*. 69:819-830.

Jaremko, L., M. Jaremko, K. Giller, S. Becker, and M. Zweckstetter. 2014. Structure of the mitochondrial translocator protein in complex with a diagnostic ligand. *Science (New York, N.Y.)*. 343:1363-1366.

Krueger, K.E., and V. Papadopoulos. 1990. Peripheral-type benzodiazepine receptors mediate translocation of cholesterol from outer to inner mitochondrial membranes in adrenocortical cells. *J Biol Chem*. 265:15015-15022.

Li, F., J. Liu, Y. Zheng, R.M. Garavito, and S. Ferguson-Miller. 2015. Protein structure. Crystal structures of translocator protein (TSPO) and mutant mimic of a human polymorphism. *Science (New York, N.Y.)*. 347:555-558.

Lin, D., T. Sugawara, J.F. Strauss, 3rd, B.J. Clark, D.M. Stocco, P. Saenger, A. Rogol, and W.L. Miller. 1995. Role of steroidogenic acute regulatory protein in adrenal and gonadal steroidogenesis. *Science*. 267:1828-1831.

Nothdurfter, C., T.C. Baghai, C. Schule, and R. Rupprecht. 2012. Translocator protein (18 kDa) (TSPO) as a therapeutic target for anxiety and neurologic disorders. *Eur Arch Psychiatry Clin Neurosci*. 262 Suppl 2:S107-112.

Papadopoulos, V., H. Amri, N. Boujrad, C. Cascio, M. Culty, M. Garnier, M. Hardwick, H. Li, B. Vidic, A.S. Brown, J.L. Reversa, J.M. Bernassau, and K. Drieu. 1997a. Peripheral benzodiazepine receptor in cholesterol transport and steroidogenesis. *Steroids*. 62:21-28.

Papadopoulos, V., H. Amri, H. Li, N. Boujrad, B. Vidic, and M. Garnier. 1997b. Targeted disruption of the peripheral-type benzodiazepine receptor gene inhibits steroidogenesis in the R2C Leydig tumor cell line. *J Biol Chem*. 272:32129-32135.

Papadopoulos, V., A.G. Mukhin, E. Costa, and K.E. Krueger. 1990. The peripheral-type benzodiazepine receptor is functionally linked to Leydig cell steroidogenesis. *J Biol Chem*. 265:3772-3779.

Papadopoulos, V., F.B. Nowzari, and K.E. Krueger. 1991. Hormone-stimulated steroidogenesis is coupled to mitochondrial benzodiazepine receptors. Tropic hormone action on steroid biosynthesis is inhibited by flunitrazepam. *J Biol Chem*. 266:3682-3687.

Rone, M.B., A.S. Midzak, L. Issop, G. Rammouz, S. Jagannathan, J. Fan, X. Ye, J. Blonder, T. Veenstra, and V. Papadopoulos. 2012. Identification of a dynamic mitochondrial protein complex driving cholesterol import, trafficking, and metabolism to steroid hormones. *Mol Endocrinol*. 26:1868-1882.

Selvaraj, V., D.M. Stocco, and L.N. Tu. 2015. Minireview: translocator protein (TSPO) and steroidogenesis: a reappraisal. *Molecular endocrinology*. 29:490-501.

Seneviratne, M.S., D. Faccenda, V. De Biase, and M. Campanella. 2012. PK11195 inhibits mitophagy targeting the F1Fo-ATPsynthase in Bcl-2 knock-down cells. *Curr Mol Med*. 12:476-482.

Tu, L.N., K. Morohaku, P.R. Manna, S.H. Pelton, W.R. Butler, D.M. Stocco, and V. Selvaraj. 2014. Peripheral Benzodiazepine Receptor/Translocator Protein Global Knockout Mice are Viable with no Effects on Steroid Hormone Biosynthesis. *J Biol Chem*.

Tu, L.N., A.H. Zhao, M. Hussein, D.M. Stocco, and V. Selvaraj. 2016. Translocator Protein (TSPO) Affects Mitochondrial Fatty Acid Oxidation in Steroidogenic Cells. *Endocrinology*. 157:1110-1121.

Tu, L.N., A.H. Zhao, D.M. Stocco, and V. Selvaraj. 2015. PK11195 effect on steroidogenesis is not mediated through the translocator protein (TSPO). *Endocrinology*. 156:1033-1039.

Wang, H., K. Zhai, Y. Xue, J. Yang, Q. Yang, Y. Fu, Y. Hu, F. Liu, W. Wang, L. Cui, H. Chen, J. Zhang, and W. He. 2016. Global Deletion of TSPO Does Not Affect the Viability and Gene Expression Profile. *PloS one*. 11:e0167307.